8-2013

Optimization of sample preparation in Matrix-Assisted Laser Desorption/Ionization (MALDI) Mass Spectrometry of macromolecules

Evgenia Akhmetova
University of Arkansas, Fayetteville

OPTIMIZATION OF SAMPLE PREPARATION IN MATRIX-ASSISTED LASER DESORPTION/IONIZATION (MALDI) MASS SPECTROMETRY OF MACROMOLECULES

OPTIMIZATION OF SAMPLE PREPARATION IN MATRIX-ASSISTED LASER DESORPTION/IONIZATION (MALDI) MASS SPECTROMETRY OF MACROMOLECULES

A dissertation submitted in partial fulfillment
of the requirements for the degree of
Doctor of Philosophy in Chemistry

by

Evgenia Akhmetova
Moscow State University
Specialist in Chemistry, 2006

August 2013
University of Arkansas

This dissertation is approved for recommendation to the Graduate Counsil

_____
Dr. Charles L. Wilkins
Dissertation Director

_____
Dr. David Paul
Committee Member

_____
Dr. Ingrid Fritsch
Committee Member

_____
Dr. Bill Durham
Committee Member

ABSTRACT

New method for the matrix-assisted laser desorption ionization time-of-flight (MALDI-TOF) and Fourier transform mass spectrometry (MALDI-FTMS) analysis of low molecular weight polyvinyl acetate (PVAc) was developed and then applied to the characterization of commercially available chewing gum. The optimization of MALDI analysis of PVAc was achieved by investigating the influence of sample preparation variables such as the choice of solvent and choice of matrix-analyte ratio. It was demonstrated that the use of ethyl acetate as a solvent and 2,5-Dihydroxybenzoic acid as a matrix yielded the highest signal intensity for the pure polymer sample. The application of TOF technique did not produce accurate molecular structure of PVAc, and so FTMS method was employed as well and allowed to accurately establish the identity of the end groups of the polymer.

A sample preparation protocol for the successful MALDI analysis of [6,6]-phenyl-C61-butyric acid methyl ester (PCBM) was developed by investigating the influence of the matrix, solvent, deposition method and matrix-to-analyte ratio. It was found that the application of dithranol as a matrix, lowest molar matrix:analyte ratio of 250:1, toluene as a solvent for both matrix and analyte and aerospray sample deposition technique for MALDI analysis produced spectra with the highest intensity of PCBM signal, the smallest amount of fragments, the fewest products of gas phase reactions and the best reproducibility. Gas-phase reactions of PCBM in the high vacuum conditions of the FTMS and TOF mass spectrometry experiments were also investigated and a possible mechanism for these reactions was proposed. It was suggested that during or after desorption/ionization step of MALDI process, several kinds of oxidized and reduced PCBM derivatives are formed.

The influence of the sample preparation parameters (the choice of the matrix, matrix:analyte ratio, salt:analyte ratio) was investigated and optimal conditions were established for the MALDI time-of-flight mass spectrometry analysis of the poly(styrene-co-pentafluorostyrene) copolymers. These were synthesized by atom transfer radical polymerization. Use of 2,5-Dihydroxybenzoic acid as matrix resulted in spectra with consistently high ion yields for all matrix:analyte:salt ratios tested. The optimized MALDI procedure was successfully applied to the characterization of three copolymers obtained by varying the conditions of polymerization reaction. It was possible to establish the nature of the end groups, calculate molecular weight distributions, and determine the individual length distributions for styrene and

pentafluorostyrene monomers, contained in the resulting copolymers. Based on the data obtained, it was concluded that individual styrene chain length distributions are more sensitive to the change in the composition of the catalyst (the addition of small amount of $CuBr_2$) than is the pentafluorostyrene component distribution.

ACKNOWLEDGEMENTS

I would like to express deep gratitude to my advisor Dr. Charles L. Wilkins for his guidance and help throughout my time in graduate school. His mentoring helped me to grow as a scientist and learn how to be an independent researcher, thus making the time I've spent at the University of Arkansas the most important time of my life.

I also would like to thank Dr. Ingrid Fritsch, Dr. Bill Durham and Dr. David Paul for their help and input during my graduate career – their comments and recommendations improved my understanding of the subject of this dissertation and were very helpful to me.

I would like to acknowledge the Chemistry and Biochemistry Department of the University of Arkansas for providing financial support for my research. In addition, I want to thank the undergraduate students whom I was privileged to mentor and who contributed to the research described in this dissertation.

I'm thankful to the friends I made during my stay in graduate school, and especially past members of Wilkins group for their support, friendship and productive conversations about mass spectrometry. I'm very grateful to my wonderful new American family and my parents for their love and support, and to my husband Lucian who is always there for me when things get rough.

TABLE OF CONTENTS

I. MATRIX-ASSISTED LASER DESORPTION IONIZATION MASS SPECTROMETRY AS APPLIED TO THE ANALYSIS OF SYNTHETIC POLYMERS – AN OVERVIEW

A. *Introduction*

Since its introduction by Karas and co-workers[1] and by Tanaka et al.[2] in the late 1980s, Matrix-Assisted Laser Desorption/Ionization (MALDI) has became a powerful analytical tool for the investigation of important properties of industrial polymer materials, such as the identity of polymer chain repeat units, end groups[3, 4,] absolute molecular weights, molecular weight distributions[5-8], and the presence and nature of any additives. The key aspects of the typical MALDI experiment are the generation of intact singly charged ions and an absence of fragmentation. These features of MALDI ionization technique made possible the analysis of such complex mixtures as synthetic polymers and allowed the quantitative determination of average molecular weights. Other characteristics of MALDI important for the analysis of chemically and physically heterogeneous samples are exceptionally high sensitivity of this method (with modern instrumentation the attomole level is achievable)[9]. However, as applied to the analysis of industrial polymers, MALDI ionization has one significant drawback – due to the diverse chemical nature of polymers no standard sample preparation protocol or universal matrix has been developed and therefore the success of the analysis often depends on a trial and error approach used to find the optimal matrix, solvent and matrix-to-analyte ratio.

MALDI time-of-flight (TOF) mass spectrometry is the usual choice for characterization of polymer weight distribution due to its relatively low cost of equipment, theoretically unlimited mass range and simplicity of analysis[10]. However, MALDI Fourier Transform Ion-Cyclotron Resonance mass spectrometry (FT-ICR MS or FTMS) offers high resolution and extremely high mass accuracy unreachable with TOF mass analyzers. Thus, FTMS is well suited for the analysis of complex polymer-based materials and allows not only determination of the molecular weight distribution but also identification of the end-groups of different oligomeric chains, chemical composition distributions, block-length distributions for block copolymers and the architecture of polymer molecules.

In this chapter, the fundamentals of the conventional solvent-based MALDI method and parameters of experimental design important for the success of polymer analysis will be discussed and an overview of the main principles of TOF and FT-ICR mass spectrometry will be provided.

B. *Fundamental aspects of Matrix-Assisted Laser Desorption/Ionization*

The introduction of MALDI in 1988 was arguably the most important breakthrough in the field of mass spectrometry of polymers and in a few short years along with another soft ionization technique – electrospray ionization (ESI) has replaced other desorption/ionization methods utilized in mass spectrometry of polymers. Previous methods include fast atom bombardment (FAB), desorption chemical ionization (DCI), laser desorption ionization (LDI), plasma desorption (PD) and field desorption (FD). The first examples of polymer characterization by MALDI were presented by Tanaka et. al[2] in 1988. The polymers analyzed were 4kDa poly(propylene glycol) (PPG) and 20 kDa poly(ethylene glycol) using a slurry of ultra fine cobalt powder in glycerol as the matrix. The first application of small organic molecules as matrices for MALDI analysis can be traced back to the pioneering paper by Karas and Hillenkamp[11] where they used nicotinic acid as a matrix to analyze proteins with high molecular weights (up to 67 kDa). However, the first example of analysis of synthetic polymers with organic molecules as matrices was demonstrated by Castoro, Koster and Wilkins[12] in the early 1992. They successfully applied 3,5-dimethoxy-4-hydroxycinnamic acid (sinapinic acid) to the FTMS analysis of series of polyethylene glycols, with molecular weights ranging from 1000 Da to 10kDa. Another early example of application of organic matrices to the analysis of polymers was described in a paper by Danis et. al.[13] published later in the same year. They also used sinapinic acid as a matrix (probably inspired by the results obtained by Castoro et al) in the analysis of water soluble 200 kDa poly(styrene sulfonic acid) and 3 kDa poly(acrylic acid).

The MALDI experiment is a complex, multi-step event, accomplished by co-crystallizing the analyte with a chosen matrix, which strongly absorbs light at the wavelength of the laser, consequent excitation of the matrix, followed by ionization of analyte and detection of the formed ions in the mass spectrometer. The co-crystallization happens after a small amount of the analyte and matrix mixture is deposited on the target plate, and the solvent is evaporated. The homogeneity of the surface of the deposited sample is of utmost importance, because it directly affects the quality of MALDI spectra with respect to the reproducibility and signal intensity (this will be discussed in greater detail in subsequent sections). After sample preparation is complete, the target plate is placed into a mass spectrometer and the sample-matrix crystals are subjected to a short pulse of UV or IR laser (typically no more than a few

microseconds). During this time, the matrix molecules absorb the energy of the laser and begin to eject off the sample surface, carrying with them analyte molecules into the gas phase forming a gas plume. It has been shown that this gas plume forms as an explosive transition from solid to the gaseous phase either due to desorption or ablation at higher laser fluences[14]. The current opinion on the mechanism of MALDI is that during this first step in a very dense initial plume of excited matrix and analyte molecules, primary ionization reactions take place[15]. The nature of these reactions and the source of ions formed is still a topic of a debate, mostly because radical, protonated, cationized and de-protonated species all can be observed in a single MALDI experiment, clearly indicating the complexity of underlying processes.

Two different models were suggested to describe primary ionization reactions that take place during MALDI event – the cluster and photoexitation/energy pooling models. The first model was proposed by Karas et al[16] in order to explain the main feature of MALDI – abundance of singly charged ions. Their model suggested that singly and multiply charged analyte ions are formed in the solution with the matrix and retain their charge when co-crystallized with it on the target plate. After the desorption stage, the large clusters containing the matrix and analyte ions are ejected from the surface and undergo secondary neutralization reactions with free electrons that are always present in the primary plume. The outcome of these reactions is that multiply charged analyte ions interact with electrons until they are singly charged or neutral (hence the name – "lucky survivors"). The second model[17] suggests that the ionization occurs due to energy "pooling" (re-distribution) of two or more matrix molecules in different excited states to give matrix radical cations or products of excited state proton-transfer reactions as demonstrated on eq. 1, 2 and 3 as well as multi-photon ionization of neutral matrix molecules (eq.3)[15]:

$$M + M + 2h\nu \rightarrow [M^* + M^*] \rightarrow M + M^{+\bullet} + e^- \quad (1)$$

$$M + M + nh\nu \rightarrow [M^* + M] \rightarrow [M\text{-}H]^- + [M+H]^+ \quad (2)$$

$$M + nh\nu \rightarrow M^{+\bullet} + e^- \quad (3)$$

Reactions of highly excited matrix molecules with neutral analyte are also possible (eq. 4, 5):

$$[M^* + M^*] + A \rightarrow M + M + A^{+\bullet} + e^- \quad (4)$$

$$M + h\nu \rightarrow M^* + A \rightarrow [M\text{-}H]^- + [A+H]^+ \quad (5)$$

The mechanisms of secondary ionization reactions, which happen after the initial dense plume expansion further into the vacuum, are much better understood. It is also generally believed that the

analyte ions are formed mostly due to the bimolecular collisions with the excess of matrix ions in this expanding plume. The products of secondary ionization reactions make up a significant portion of the overall ion yield of MALDI process and are observed in the spectra. The most important secondary ionization reactions that lead to the ionization of analyte include proton transfer from the matrix to analyte (eq. 6), electron transfer (eq. 7) and cationization, if the salts of metals are present (eq. 8).

$$[M+H]^+ + A \rightarrow M + [A+H]^+ \quad (6)$$

$$M^{+\bullet} + A \rightarrow M + A^{+\bullet} \quad (7)$$

$$A + Cat^+ \rightarrow [A+Cat]^+ \quad (8)$$

Products of these reactions are mainly responsible for ions observed in MALDI spectra. Shortly after these ionization reactions take place, an ion cloud of mostly singly charged analyte ions is formed and is directed towards the mass analyzer (usually by using various ion optics) and then detected. The general diagram of the overall MALDI process is presented on the Fig. 1.1.

C. *Important parameters in sample preparation for MALDI analysis of polymers*

1. **Selection of the matrix**

Although the mechanism of MALDI is still a topic of debate, it is widely known that the choice of proper sample preparation conditions plays a crucial role in the success of any MALDI analysis. However, due to the diverse chemical nature of synthetic polymers, no standard sample preparation protocol has been established for their analysis. Over the years, multiple attempts have been made to optimize and rationalize the choice of such important parameters as the nature of the matrix[18, 19] , its concentration[20, 21], solvent[22] and cationizing agent[23].

The choice of an appropriate matrix is the central point in designing MALDI a sample preparation protocol. As it is mentioned in several sources[9, 10, 24], the main properties that a good candidate for a matrix compound must fulfill are as follows:

- High absorption ability at the employed laser wavelength
- Good vacuum stability
- Good solubility in the solvents that can also dissolve analyte
- Good miscibility with analyte in the solid state
- Capability of efficient desorption

Aside from these more obvious requirements, it is vital that matrix must be able to strongly interact with the polymer – only then it can efficiently transfer energy absorbed from the laser and promote ionization. Therefore, close contact between matrix and analyte molecules is required. Some sources describe this type of interaction as formation of "solid solution" in which polymer molecules are evenly distributed within matrix crystals. If the polymer is segregated from the matrix in any way, the analysis will most likely fail. As fundamentals of MALDI sample preparation for polymers were investigated over the years, it was established that several factors influence whether or not close contact between matrix and analyte can be established. Most significant factors contributing to the formation of "solid solution" are 1) chemical nature of the matrix, 2) deposition method and 3) choice of solvent[25].

Hanton and Owens investigated the influence of chemical nature of matrix and determined that formation of a "solid solutions" when the polymer molecules are evenly dispersed in the matrix is observed when the polarity of the matrix matches the polarity of the polymer, which in turn leads to superior quality mass spectra[26]. The results of their experiments lead to the formulation of the mutual compatibility guide to selecting the matrix for polymers analysis, which is based on their relative hydrophilicity/hydrophobicity (Fig.1.2). To use the guide to narrow down the choice of a matrix for a MALDI analysis of a new polymer, one must consider its solubility properties and structure and match them to those of one of the common polymers from the right side on the chart. Knowing that, a matrix with similar polarity can be selected from the left side.

The same authors also suggested the general guideline for the MALDI sample preparation of new samples, which included 1) choosing the solvent able to obtain clear solution of the polymer; 2) choosing the matrix, based on the hydrophobicity/hydrophilicity of both matrix and the polymer; 3) preparing solution of the selected matrix in the chosen solvent[27]. Unfortunately, the situation is not as straightforward as it seems. It will be shown in chapter V on the example of fluorinated (co)polystyrenes, that sometimes the matrices that *should* work based on the reasoning and experimental observations described above, do not. This once more proves that there are still discoveries to be made about exact nature of interaction between the matrix and polymer and its importance in MALDI analysis.

2. Influence of the solvent

The choice of the suitable solvent is also essential for the success of any solvent-based polymer MALDI analysis. First of all, if the sample doesn't completely dissolve in the solvent of choice, it will lead to severe mass discrimination – only the soluble portion of the sample will be detected in the spectra. For example, it was demonstrated[28] that by varying the solvent used for MALDI sample preparation, drastically different molecular weight values were obtained for the same unfractionated sample of poly(3-hexylthiophene). When acetone and hexane were used, only low molecular weight fractions that are soluble in these solvents were observed, whereas when methylene chloride, THF and chloroform were employed, it was possible to detect gradually higher and higher molecular weight oligomers. This work demonstrated one of the options available to prepare "problematic" polymers with high polydispersity for MALDI analysis without involving GPC separation – simple Soxhlet extraction with a suitable solvent can give a narrow fraction, perfectly suitable for further mass spectrometry analysis. Second, the other important issue that must be considered when selecting a solvent for polymer MALDI analysis is the risk of sample segregation during the crystallization process. Multiple examples[22, 29-32] confirm that when even a very small amount of polymer's non-solvent soluble portion is present, it leads to severe mass discrimination and therefore errors in molecular weight calculations and very poor spot-to-spot signal reproducibility due to the inhomogeneity of the surface of the samples. When a mixture of solvents is used to prepare a MALDI sample, as the solvent evaporates, its composition changes due to the loss of more volatile component of the mix, and therefore the solubility of the polymer changes as well. If the non-volatile component of the solvent mixture is a non-solvent for the polymer (such as water for polystyrene), it will start to precipitate before incorporation into the matrix crystals. This segregation of the sample has been observed by various techniques, such as time-of-flight secondary ion mass spectrometry,[26] optical microscopy,[32] MALDI imaging[33]. To minimize these complications, it is advisable to avoid mixtures of solvents and use the same solvent to make all solutions throughout sample preparation process. In this way, preliminary segregation of the polymer from the matrix during crystallization of the MALDI sample could be minimized[9, 10, 22, 25]. Segregation of the matrix and analyte produces a non-homogeneous surface of the sample with clusters of analyte and matrix crystals of various sizes, and ultimately leads to very poor spot-to-spot and shot-to-shot reproducibility of analysis

and can also lead to severe mass discrimination and errors in MWD calculations[29]. In order to improve homogeneity and reduce segregation of the sample, it was also suggested that the use of fast drying solvents (such as acetone) is beneficial, since when evaporation of the solvent happens quickly the sample will have less time to segregate[25, 26, 34]. It should be noted though, that the use of fast drying solvent does not guarantee superior quality spectra every time, as it was demonstrated in a recent comprehensive study of solvent effect on MALDI analysis of several different polymers[35] – it was concluded that as long as the all components of the sample are soluble in the solvent, reliable good quality data can be obtained regardless of the evaporation rate.

3. **Choice of cationizing agent**

Most synthetic polymers are neutral in solutions and don't form ions easily by themselves. Therefore, in order to perform their mass spectrometry analysis successfully, ionization aid is required. Typically, salts of various metals are added to the matrix during the sample preparation to enhance the analyte signal. The choice of the cationization agent is determined only by the nature of the polymer – it should have high affinity to the chosen cation. For example, it is well known that oxygen-containing polymers such as polyethers and polyesters[36, 37, 38, 39] readily cationize with ions of alkali metals whereas unsaturated hydrocarbon polymers such as polystyrene most efficiently form adducts with transition metals (Ag^+, Cu^+).[40-43] Therefore, It is clear that the polarity of macromolecules is very important when considering a choice of cationizing agent. Interestingly, it has been proposed that the Lewis acid and base theory can be used as a guide for selection of a suitable ionization aid. Llenes and O'Malley[44] suggested that most polymers could be considered as bases that share an electron with a cation, which can be considered as acid in this case. Non-polar polymers, especially those containing conjugated systems, such as polystyrene or polybutadiene can act as donors of electrons, are easily polarizable and can be considered as soft bases. On the other hand, polymers containing electronegative atoms like oxygen or nitrogen do not have excess electron density to donate and can be considered hard bases. Following the Lewis acid/base concept, soft acids form stable pairs with soft bases whereas hard acids bind most strongly to hard bases. When considering the cations commonly used to promote ionization in MALDI analysis, it can be noted that the large cations of transitional metals, such as Ag^+ and Cu^+ carry extra electrons on their d-orbitals and can be polarized easily, and thus can be considered soft acids.

Small alkali metal cations like Na^+ or Li^+ have high positive charge density and do not carry any non-binding electrons in their valence shells, making them hard acids. Therefore, based on the concept described above, it can be predicted that soft bases like non-polar hydrocarbon polymers would most successfully bind with soft acids like cations of transition metals, whereas hard bases like polyethers and polyesters will be cationized most efficiently by hard acids like alkali cations. This reasoning explains experimental data very well and allows simplifying the choice of efficient cationizing agent when developing sample preparation protocols for new polymers.

4. Importance of a sample deposition method

Several sample deposition methods have been developed over the years. The simplest and still very popular method is the dried droplet method, introduced by Karas and Hillenkamp.[11] This method involves dissolving matrix and analyte along with an appropriate cationizing agent in a solvent (common or otherwise) and mixing solutions together in an empirically determined ratio. Then a small volume of the mixture is deposited onto a target plate and allowed to dry at room temperature and in air. Despite the obvious benefits (simple, fast), the serious drawback of this method lies in the fact that the solvent is allowed to evaporate from the deposited sample mixture slowly. During this evaporation process, the polymer segregates from the matrix and starts to precipitate from the solution, thus producing a very inhomogeneous surface of the sample with crystals of varying sizes, where polymer chains are excluded from the matrix crystals to the significant degree. Because of this segregation of the sample, the close contact between the matrix and analyte molecules, which is required for efficient ionization, can't be achieved uniformly throughout the sample surface. This, in turn, leads to the poor signal intensities, poor spot-to-spot reproducibility and in worst cases, mass discrimination. The latter was clearly demonstrated by Weidner et al[33] with the imaging MALDI-TOF mass spectrometry[10, 25, 45, 46]. They observed that the variation in number average molecular weight of polystyrene calculated from two different positions within the same spot prepared by dried-droplet method could be more than 15%. To improve the situation, either a fast drying solvent, or deposition methods that produce small droplets of the sample mixture should be used. Both of these approaches allow for significant enhancement in spot-to-spot reproducibility and better ion signal of the analyte. The reason for these improvements lies in the reduction of the drying time, which leads to lesser degree of segregation between the polymer and the

matrix – there is simply not enough time for thermodynamically driven precipitation of the analyte. Also, both of these approaches yield smaller and much more uniform matrix crystals, which also helps to achieve a very close contact between the matrix and a polymer chains. Even if segregation does occur, the matrix and polymer molecules on the surface are located very close to each other due to the small size of the matrix crystals and can be desorbed with the same laser shot. The two most popular and widely used small droplet deposition methods are electrospray[47, 48] and aerospray[41, 49]. Both these methods were successfully applied to the analysis of macromolecules and demonstrated that formation of a very homogeneous surface of the sample with uniform matrix microcrystals, generates much more consistent MALDI results with respect to the reproducibility and in case of electrospray deposition, gives up to 3 times higher signals of the analyte when compared to the dried droplet method[25]. In the electrospray method, very small droplets of solution are ejected from an electrospray needle and are deposited onto a target plate, which is held at a very short distance from the needle tip. Because of the extremely small size of the droplets produced, they reach the plate almost dry, which again, prevents the segregation of the sample. The only drawbacks of the electrospray deposition method are the relative complexity of the process and possibility of a fragmentation of fragile analyte molecules. In aerospray deposition, the sample mixture is being sprayed onto a target plate through a very thin capillary with nitrogen gas. This method also produces a very homogeneous surface of the sample, with uniform microcrystals of the matrix. The process is very simple, fast, and does not require a serious financial investment needed to purchase an electrospray deposition device.

D. *Time-of-flight mass spectrometry: an overview*

The main attraction of time-of-flight (TOF) mass spectrometry for analysis of synthetic polymers lies in comparatively low cost of the instrument, simplicity of its maintenance and operation and possible molecular weight range up to 10^6 Da[50]. In addition, modern TOF mass analyzers offer high sensitivity and mass accuracy 5-50 ppm[25], which is sufficient for routine characterization of polymers. In this section, a brief overview of the principles of TOF mass spectrometry will be provided, since various excellent sources of more detailed information can be found elsewhere in the literature.[9, 10, 25, 50, 51]

The simplest TOF mass spectrometer (linear TOF) consists of a high vacuum small source region, a longer field free region (drift length D) and a detector. A simplified diagram of a linear TOF mass

spectrometer is shown in Fig. 1.3 to illustrate a general principle of time-of-flight mass spectrometry. Ions are formed in an electric field in the source by any ionization technique applicable, such as electron ionization, chemical ionization, laser desorption ionization, matrix-assisted laser desorption/ionization and electrospray ionization.[50]

Then, produced ions of all masses (m) are simultaneously accelerated by application of a high voltage extraction potential (V) as they exit the source. Ions with different masses will leave the ion source region with the same final kinetic energy (K.E.) but will be moving with different velocities (v) as it is follows from the equation for kinetic energy (eq. 9):

$$K.E. = zeV = \frac{mv^2}{2} \qquad (9),$$

where *e* is the charge of electron, z is the number of charges on the ion, and *V* is the extraction potential. After the ions leave the source region, they enter field free region (a drift tube) of known length D, where no electric field is applied. Since all ions have the same kinetic energy, from eq. 9 it follows that ions with smaller mass will travel faster than heavier ions and therefore they will separate based on their velocities. Lighter ions will reach detector faster than heavier ions, as it is demonstrated in Fig. 1.3. The time it takes for an ion with mass m and charge z to travel from the exit of the source region to the detector through a drift tube with length D, can be expressed by using eq. 9 and expression for velocity (v = D/t) (eq.10):

$$t = \sqrt{\frac{m}{2zeV}}D \qquad (10)$$

By recording the time of flight (t) for different ions, their mass-to-charge ratios can be calculated from the expression above as such (eq. 11):

$$\frac{m}{z} = 2eV\frac{t^2}{D^2} \qquad (11).$$

E. *The fundamentals of Fourier transform mass spectrometry*

Fourier transform mass spectrometry (FTMS) possesses unique features, which makes this technique one of most powerful tools for analysis of complex mixtures, such as synthetic polymers. These features are extremely high accuracy and resolving power, attainable with FTMS but not possible with other mass analyzers. The characteristics of the synthetic polymers are expressed by their molecular weight distributions, chemical composition of the monomer units, the nature of the end groups, and polydispersity index (PDI). The FTMS technique is not only able to characterize all of these aspects[4], but to detect side reactions and possible contaminants as well as to provide disambiguation of analysis when more than one compositional assignment for observed oligomers is possible. This last feature is especially valuable in the analysis of very complex samples – synthetic copolymers[52]. In this chapter, only the basic overview of FTMS will be given since there have been a number of reviews,[53-55] tutorials[56-58] and book chapters[25, 50, 59] written on the subject, as well as numerous publications, exploring the fundamentals and applications of this method.

FTMS is based on the ion cyclotron resonance (ICR) principle[55]. After ionization of the analyte is complete, produced ions are transferred and then trapped into an ICR cell at ultra-high vacuum conditions, which is situated in the homogeneous magnetic field produced by a strong superconducting magnet. To ensure the homogeneity of the field, the cell is located inside the bore of the magnet. In the cell, the ions are trapped by application of a low potential to the trapping electrodes shaped as plates that are positioned perpendicularly to the magnetic field. In addition to the oscillating motion between trapping plates, as soon as ions enter the cell, they exhibit cyclotron motion in circular orbits with the frequencies f_c given by the fundamental eq. 12 due to the influence of the Lorentz force of a magnetic filed:

$$f_c = \frac{zB}{2\pi m} \qquad (12),$$

where z is the charge of the ion with mass m (amu), B is the magnetic field strength in Tesla and f_c cyclotron frequency of the ion. The cyclotron motion is a product of the influence of Lorentz force and a centrifugal force, direction of which is perpendicular to the magnetic field. Equation 12 demonstrates that every ion has its own characteristic cyclotron frequency.

In order to detect the ions after they are trapped, they are excited by application of a broadband radio frequency signal to the second pair of opposing electrodes, which are located in parallel with magnetic field (transmitter plates). When the frequency of the applied RF signal matches f_c of the ion, a resonance condition is fulfilled and the ions with the same m/z absorb the energy and are accelerated to the orbits larger than their cyclotron radius from the center of the cell. This provides the basis for mass spectrometry, since the mass separation happens because only ions with frequencies resonant with RF are accelerated. As coherent packets of ions with the same values of m/z draws closer to the receiver plates, the ions induce an AC image current, which then can be measured. The amplitude of the image current is proportional to the number of ions in the packet. The detection of each individual packet of ions by applying a fixed frequency RF pulse and testing for the presence of that specific m/z ratio is possible but extremely time and labor consuming. Therefore, during an actual FTMS experiment, the *multichannel advantage* is used, meaning that all ions in the cell are detected simultaneously. It is done by accelerating all trapped ions in a short period of time by subjecting them to the short RF pulse ("RF chirp"), which is swept across the entire range of cyclotron frequencies of interest. After the acceleration, the image current, which is induced by the coherent ion packets of varying m/z ratios, is amplified and recorded. This cumulative image current is the superimposition of individual sinusoidal image currents from each coherent ion packet, each of which represents the cyclotron frequency of the ions versus the time during image current induction. In order to convert the data collected from time domain to frequency domain, Fourier transformation is performed on the composite transient signal and then the equation 12 is used to convert frequencies to m/z[55].

Mass resolving power (R) in FTMS is directly proportional to the time duration of acquired transient signal and the maximum mass resolution can be expressed as follows (eq. 13):

$$R = \frac{m}{\Delta m_{1/2}} = \frac{f_c T}{2} \qquad (13),$$

where m is the mass of the ion and f_c is its cyclotron frequency; $\Delta m_{1/2}$ is the full width of the peak at half height; T is the amount of time the transient is observed. The value of T is restricted by computational capabilities of the computer system used for storage and amount of time available for the analysis and by the level of vacuum in the system. It is very important to maintain an ultra-high level of vacuum in FTMS

system because the amplitude of transient signal decays with time as collisions between the ions and neutral particles in the cell disrupt the coherence of ion packets and force them to relax from their accelerated orbits too early (so called pressure induced damping)[55, 56].

FTMS produces the highest resolving power and unmatched mass accuracy when compared to any other mass analyzer. The reason why FTMS has this advantage over other mass spectrometry techniques lies in that the mass separation is based on frequency, rather than on time (like in TOF) or other parameter. The frequency can be measured more accurately than any other experimental parameter, thus giving inherently higher resolution and therefore higher mass accuracy than any other type of mass measurement.[50]

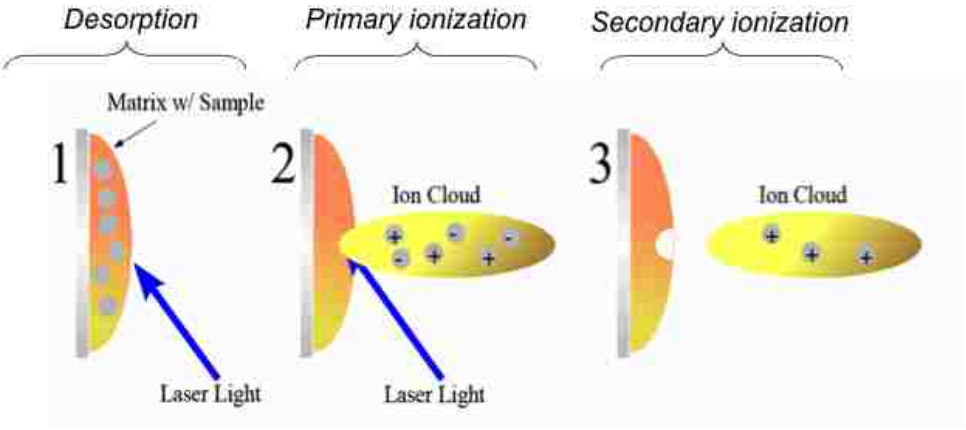

Figure 1.1 The main steps in MALDI process. Reprinted from Zenobi, R. and Knochenmuss, R.[15]

Matrices		Polymers
	Hydrophilic	
2,5-Dihydroxybenzoic acid (DHB)		Polypropylene glycol (PPG)
α-Cyano-hydroxycinnamic acid (CHCA)		Polyvinyl acetate (PVAc)
Ferulic acid (FA)		Polytetramethylene glycol
Indoleacrylic acid (IAA)		Polymethylmethacrylate (PMMA)
Dithranol		Polystyrene (PS)
all trans-Retinoic acid (RA)		Polybutadiene (PBD)
Diphenylbutadiene		Polydimethylsiloxane (PDMS)
	Hydrophobic	

Figure 1.2 Relative compatibility scale for common matrices and polymers based on their hydrophilicity/hydrophobicity. Reprinted from Hanton, S. D. and Owens, K. G.[27]

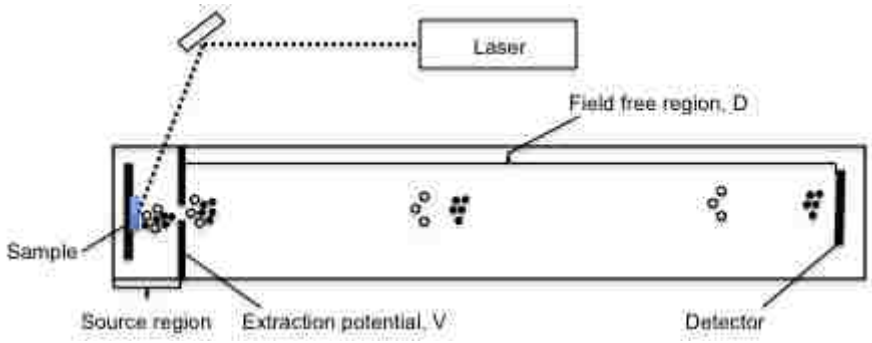

Figure 1.3 Simplified diagram of linear time-of-flight mass spectrometer. Circles represent heavy ions, dots – light ions

II. SYNTHETIC POLYMERS

A. *Introduction*

It is difficult to overestimate the importance and omnipresence of polymers, also known as macromolecules, in human society. In fact, all life as we know it depends on polymers – naturally occurring bio-macromolecules such as nucleic acids, proteins and carbohydrates are both the foundation and fuel of every known life form. These natural polymers in the form of wood, fibers such as cotton, silk and wool as well as various gums and resins also utilized by humans to satisfy various needs of everyday life from the dawn of human civilization. However, with the advancement of the technological progress, the demand for these natural polymer-based materials increased and the need of improvement of their properties as well as the need to reduce the cost of their production became evident, thus providing the ground for the development new man-made materials – synthetic polymers.

The first steps were made in the nineteenth century, starting with the discovery of vulcanization of rubber by Charles Goodyear in 1839, the synthesis of polystyrene by Simon (also in 1839) and with later discoveries of Ebonite or hard rubber (1851, Nelson Goodyear), Celluloid (1868, John Hyatt), and poly(vinyl chloride) (first discovered by accident in 1838 by Regnault and later in 1872 by Baumann)[60]. The first truly synthetic polymeric material based on the condensation reaction of phenol with formaldehyde was introduced in 1907 by Leo Bakeland with the product named Bakelite. As a consequence the 20th century can be marked as the beginning of the age of synthetic polymers[60, 61]. However, despite discovery and application of several other important synthetic polymer-based materials in the 1920's, no significant progress was made in the area of polymer chemistry up to 1930s due to the largely intuitive and empirical methods employed and lack of fundamental understanding of molecular nature and properties of polymers. This situation changed with the approach of World War II, when the research in both theoretical and applied polymer chemistry accelerated to accommodate the military demands. In a very short time remarkable developments were made: introduction of several types of synthetic rubber, Nylon 6, silicones, Teflon and other fluorocarbon resins and polyethylene to name a few[61, 62]. Most importantly, the theoretical foundations of polymer chemistry were laid due to the efforts of many organic chemists, physics, mathematicians and engineers, most notably the 'father of synthetic polymer science' – Wallace Hume Carothers. His ideas were based on the *macromolecular hypothesis*,

proposed in 1920 by Hermann Staudinger, stating that polymeric materials (such as natural rubber) are made of long-chain molecules of very high molecular weight, and are not formed due to the physical association of smaller molecules. Carothers took this concept further, suggesting the use of small organic molecules as building blocks in the construction of large polymer chains by the means of established organic chemistry reactions. He also suggested investigating how the final properties of the polymers would depend on the chemical composition[61].

All these discoveries and ideas, along with the fact that a wide variety and vast quantities of polymers can be made from inexpensive and readily available starting materials led to the explosive growth of polymer science after World War II. New materials based on synthetic polymers are developed at an accelerated rate to suit the specific needs of transportation, rubber, coatings/adhesives, electronic, military, textile, medical and food industries by providing required physical and chemical properties. As a result, it is virtually impossible to indicate any area of modern everyday life where products made from *synthetic* polymers do not play an important role. This explains why almost 90 billion pounds of synthetic polymers are consumed every year in the United States and why the polymer production is the fastest growing industry in the world[60, 61].

The term 'polymer' is derived from the two Greek words – *poly* and *meros* meaning 'many parts' and used to describe a molecule made by the repetition of a simpler unit, called a *monomer*[63]. The term 'macromolecule', meaning a large molecule of a high molecular weight is sometimes used as a synonym for a polymer. A 'monomer' is a molecule of low molecular weight, which can be converted to a polymer by combining with other monomers. A polymer molecule consists of thousands or even millions of atoms linked by covalent bonds to form a chain-like molecule, and so hundreds up to thousands monomers are joined together during the polymerization process. Because of the peculiarities of the polymerization process in general, any polymer-based material consists of a mixture of molecules with a distribution of various chemical and physical parameters. These include variations of chain length (and hence of molecular weight), stereochemistry of individual molecules, branching or interconnections, overall arrangement and nature of monomeric units, nature of end groups as well as variations in physical conformations, organization and alignment of the chains. Therefore it can easily be perceived that the final properties of a material "represent the sum total of the statistical distribution of the chemical and

physical configurations of its component molecules"[64]. It should also be noted that the physical properties usually associated with polymers greatly depend on the large size of their molecular chains. As the molecular weight and chain lengths increases during polymerization, the molecules start to twist and tangle within themselves and with the other molecules. When a high enough molecular weight is reached, the attractive intermolecular forces and entanglement of the chains leads to the increased strength and impact resistance of the material[61, 62].

B. *Classification of polymers*

Polymers can be categorized in various ways; in fact, the same material usually belongs to multiple classes at the same time. In most general terms, such classifications can be based on molecular structure of polymers, response to the environment, their physical state and chemical composition as well as commercial applications.[61]

1. **Molecular structure**

Based on the identity and arrangement of monomer units in the polymeric chains, the polymers can be classified as homopolymers and copolymers[60, 64, 65].

- *Homopolymers* – consists of identical repeating units;
- *Copolymers* – has two or more types of monomers (polymers with three different monomers in their structure are called *terpolymers*). Copolymers can be further divided into categories based on their sequencing arrangement, such as:

    1) *Random copolymers* – random distribution of different monomers along the chain, no specific pattern;

    2) *Alternating copolymers* – contains regular, alternating arrangement of different monomeric units;

    3) *Block copolymers* – the polymeric chain consists of groups of identical monomers, following one another.

2. **Molecular geometry**

Polymer molecules, due to their size and endless variability of chemical composition can possess several distinctly different geometries, based on how the monomeric units are arranged in their chains. The main variations in macromolecular geometry include[61, 62]:

- *Linear polymers* – consisting of monomeric units arranged in the simple straight chain.
- *Branched polymers* – have chain branches attached along the polymer backbone that are of the same structure as the main chain. *Graft copolymers* are also branched polymers, in which the backbone and the branches are made up of different types of monomeric units.
- *Cross-linked (network) polymers* – linear polymeric chains are bonded together by chemical linkages, thus forming three-dimensional networks. *Cycolmatrix polymers* can also be classified as cross-linked, in them ring systems are linked together to form an infinite matrix of connected units. Graphite and some silicate minerals represent examples of inorganic cyclomatrix polymers.
- *Star-shaped polymers* – has several polymeric arms propagating from the same core. *Dendrimers* are the special subcategory of star-shaped polymers with highly branched arms and with overall spherical three-dimensional structure.
- *Ladder polymers* – have two linear polymeric chains that are joined together in a regular fashion by crosslinking units.

3. **Structural isomerism**

Tacticity is a form of stereoisomerism that occurs in polymers when their constituent monomers possess a steric center in the backbone of the polymeric chain. There are three classes of stereoisomers possible for such polymers[60, 61].

- *Isotactic* – all substituent functional groups that are present in individual monomers are positioned on the same side of the polymer backbone.
- *Syndiotactic* – the substituent functional groups are arranged on alternating sides along the backbone.
- *Atactic* – the spatial distribution of the substituents down the polymer's chain is random.

Another type of stereoisomerism possible for some classes of polymers is *geometric (cis/trans) isomerism.* It occurs in polymers, which still contain double bonds in their backbone and are made from diene monomers, such as isoprene and butadiene[62].

Positional isomerism (*orienticity*) occurs in addition polymers obtained by certain types of polymerization reactions, such as free radical and some cationic and anionic polymerizations. In the polymers formed in these reactions, the attachment of every subsequent monomer to the propagating

chain can happen either head-to-tail (the substituted carbon on the monomer is defined as 'head', and the other and as 'tail') or head-to-head, although head-to-tail is always predominant due to the steric effects and influence of resonance[64, 66].

4. **Response to the environment**

The response of a material and its stability at different temperatures is critical when considering its final application. Therefore, often classification can be made based on how materials behave as a result of temperature variation. Based on the performance at high temperature, polymers can be divided into two categories – thermoplastics and thermosets.

- *Thermoplastics* – soften and flow when heated, and therefore can be remolded many times to new shapes. When cooled, they do not set or cure, but merely harden and hold their shape until subjected to heat again. These polymers consist of mostly linear chains that have no chemical bonds with adjacent molecules and so when heated, the chains can slide over one another thus allowing the polymer to flow or stretch without degrading[61, 62].

- *Thermosets* – do not flow or soften when heated, but decompose completely instead. The chains in these polymers are covalently joined by linkages, and form three-dimensional interconnected network (cross-linked polymers), which forms during curing/setting of the polymer under UV light or in the presence of heat. The presence of such a network prevents polymeric chains from being able to move as chains in thermoplastics do when the heat is applied[61, 62].

Depending on the application of the material, environmental factors other then variation in temperature and materials' response to them must be considered. Examples include among many others: barrier properties of materials and their selective permeability to certain compounds that might be present in the environment; conductivity (insulating versus conducting polymers) and surface properties when polymer is in contact with other compounds.

5. **Physical state**

Polymers can be classified as amorphous or semicrystalline based on the distinct physical state their chains can assume. As the temperature increases, both types of polymers undergo phase change comparable (but not identical) to the physical state changes of small molecules. The properties of the amorphous and semicrystalline materials within the same temperature range may be very different[60-62].

- *Amorphous polymers* – are composed of random entanglements of polymer chains that are in the constant motion and do not demonstrate a significant degree of order in their structure. At low temperatures these polymers are glasses and can crack or break just like glass. In this state, the polymer's chains are packed tightly together and do not posses considerable freedom of motion. As the temperature increases, the chains begin to move faster and start to disentangle from one another once the glass-transition temperature (T_g) is reached. At this temperature, the stiffness of the polymer drastically decreases and it transforms into a rubber. In the rubbery amorphous state polymeric chains have enough freedom of motion to be able to slide past one another and they are not as tightly packed together as in the glassy state. If the temperature increases further, the chain disentanglement speeds up, elastomeric material continues to soften and gradually turns into a viscous liquid. This process is reversible, and if the temperature drops, the polymer goes back to a rubbery state and then to glass without loosing its properties[62].

- *Crystalline (semicrystalline) polymers* – contains microscopic domains where polymeric chains are packed in ordered fashion (*crystallites* or *spherulites*) and are surrounded by material in amorphous state[65]. Polymers can't form macroscopic crystals like small molecules mostly due to the large length of their chains: they can't fully disentangle and align perfectly during the cooling time when the polymer's chains are still mobile[62, 64]. The degree of crystallinity in most polymers of this class is does not exceed 90% and is usually significantly less. Polymers can form various kinds of crystals, but they are all made of segments from numerous adjacent molecules and a single molecule can contribute chain segments to several spherulites, thus tying them together. In addition, some parts of the chain might not be involved in the formation of the crystalline regions and therefore the same molecule contributes to both amorphous and crystalline states serving as a link between two different physical states. At low temperatures, semicrystalline polymers contain crystalline and glassy domains and behave like glass. As the temperature rises, the motion in their amorphous sections increases and when T_g is reached, the material becomes flexible, but the crystalline domains will remain intact, holding the polymer chains together. The material will retain flexibility and strength until the rising temperature reaches melting point (T_m). When it happens, the polymers' chains disentangle, crystallites will melt and material will liquefy[62].

6. **Chemical composition**

Another way to classify polymers is to evaluate their overall chemical composition and more specifically which functional groups are present in the macromolecule. The elemental composition, chemical groups present (ester, nitrille, ether, hydroxyl, aromatic, etc.) and a way of synthesis all can be considered as means to classify polymers.

7. **Application**

It is often helpful to categorize polymers with their commercial applications in mind. From this standpoint, polymers can be classified as rubbers/elastomers, rigid plastics, adhesives, fibers, coatings or polymers for special use (such as conductive polymers for solar cells fabrication)[61, 62].

- *Elastomers (rubbers)* – are defined as materials that "can be elongated to at least twice its original length and which will retract forcibly to essentially its original length"[62]. The elastic properties of rubbers are mainly due to the entanglement of the polymeric chains, and so in order to achieve functional degree of elasticity, molecular weights of these polymers must be sufficiently high. Another important consideration here is that the use temperature of the rubber must be higher than T_g of the polymer, otherwise it will loose its elastic properties to the great extent.

- *Rigid plastics* – this category includes both thermosets and thermoplastics, as long as their T_g temperatures are higher than the use temperatures. It must be noted that the presence of various types of additives is a key part of the formulation of modern plastics and allows fine-tuning their performance of by enhancing desired physical and mechanical properties. Therefore, it is safe to define rigid plastics as complex systems highly customized for specific commercial applications, which contains the polymers as well as multiple additives including curing agents, stabilizers, processing aids and various performance-enhancing additives[62].

- *Adhesives* – modern adhesives are highly formulated, complex systems, in which synthetic polymers plays integral part.[67] Depending on the type of adhesive, different classes of polymers are used for their fabrication. Several broad categories of adhesives can be identified: solvent-based, latex, pressure sensitive, hot-melt and reactive adhesives[62]. Each of these classes uses different mechanism of interaction between substrate and the adhesive and therefore requires polymers with different properties. For example, pressure sensitive adhesives are highly viscous elastomers, which flow when the pressure

is applied to them and thus attach to the substrate surface, whereas hot-melt adhesives are thermoplastic materials that applied to the substrate in the molten state and develop adhesion as they solidify.

- *Fibers* – natural polymers such as cellulose in the form of cotton, as still very widely used in the manufacture of fibers, but the products made with synthetic fibers are ubiquitous and an integral part of the modern world. Synthetic fibers are usually made from various types of crystalline thermoplastics, modified with performance-enhancing additives and processed into fibers.[61, 62]

- *Coatings* – modern polymer-based coatings and surface finishes are complex mixtures that contain all or most of the following: a film-forming polymer, pigments, stabilizers and a volatile solvent.[62] They can be classified into several categories, such as lacquers, enamels, varnishes, latex and oil paints. Just as with the adhesives described above, each class of coatings interacts with the surface in a dissimilar way, has different performance requirements and therefore calls for chemically different polymers, depending on the specific application. Examples of the polymer classes used in coatings include vinyl polymers, polyacrylates, amino-, phenolic and epoxy resins, and urethane polymers among others[62].

C. *Main types of polymerization reactions*

Polymerization can be accomplished in three different ways: (1) by breaking a C-C double bond, (2) by using monomers with two functional groups and (3) by cleavage of a cyclic monomer. Therefore, it is easy to understand why there are three main categories of polymerization reactions – addition, condensation and ring opening[60, 63, 64, 66].

- *Addition polymerization* ("chain growth") – monomers containing double bonds are added to the growing end of the chain, which contains an active site[63]. Examples of monomers that can be used in this type of polymerization include vinyl chloride, styrene, ethylene and other alkenes, since the polymerization occurs by consequent additions of monomers across the double bond. The chain growth occurs rapidly by addition of one molecule at a time at the end of the chain and the initiation species continues to propagate until termination. Radical, ionic, group transfer and plasma polymerization are all examples of addition polymerization. Depending on the exact conditions of the polymerization reaction and on the nature of the monomers, the active site on the end of growing chain can be a free radical, carbocation or carboanion. All chain growth polymerization has at least three kinetic steps: initiation,

propagation and termination. *Radical polymerizations* initiated by free radicals, produced one way or another (heat, UV-radiation, atom transfer to the catalyst) from small organic molecules, called initiators. Most vinyl monomers undergo fast radical polymerization in the presence of the initiating free radicals by consequent addition of monomers onto a free radical sites during a propagation step and continue to do so until either the monomer is exhausted or until two propagating chains terminate by coupling. Radical polymerizations are difficult to control and they lead to polymers with wide distributions of molecular weight and chemical composition[60]. However, radical polymerization is a robust and simple technique, forgiving to impurities present and functional groups of monomers. Therefore, the controlled living polymerization methods, including atom-transfer radical polymerization (or ATRP) which will be discussed in the later chapter, were developed in order to improve the controllability of reaction and allowed to obtain well defined, narrow polydispersity polymers[68]. *Ionic polymerizations* are much less forgiving in terms of reaction conditions as compared with radical polymerization and specific conditions have to be met to carry out polymerization effectively. For example, cationic polymerization requires monomers with electron donating functional groups (alkoxy, phenyl) whereas anionic polymerization is restricted to the reaction of monomers with electron-withdrawing groups. These limitations are due to the requirements for successful stabilization of active anionic and cationic intermediates that are formed after the initiation step. Ionic polymerizations are initiated either by a strong acidic catalyst (cationic polymerization) or by strong carbanion agents, such as organolithium reagents (anionic polymerization) and are typically carried out in solvents with low polarity[60, 63].

- *Condensation polymerization* ("step growth") – monomers and growing polymeric chain combine through elimination of small molecules such as water or ammonia and without any initiator present. Monomers that can participate in this type of polymerizations include monomers with at least two functional groups, such as diols, diacids, diamines and others. In "step growth" reactions, the chain is formed gradually, step-wise and the molecular weight of the system increases slowly. The most common examples of polymers produced by polycondensation reactions, include polyamides, polyesters, polyurethanes and polycarbonates.[60, 63, 64]

- *Ring-opening polymerization* – takes place by cleavage of a ring with subsequent addition of the linear product to the end of the growing chain[63]

D. *Molecular weight distributions of synthetic polymers*

One of the most strikingly different properties of synthetic polymers, as compared with small molecules, is that polymeric chains do not have a precise, singular structure with the same number of atoms of each kind in each chain. Instead, due to the statistical nature of polymerization reactions, multiple chains are produced that can differ not only in number of monomeric units which compose the chain, but also in nature of the end groups, frequency and length of branching, nature of the side groups and other structural features[60, 62]. Therefore, synthetic polymers are always mixtures of individual molecules that can differ significantly from one another and are therefore *polydisperse*. As such, they can't be assigned uniform molecular weight like that of pure chemical compounds. Instead, polymers have a *heterogeneous molecular weight* and to describe it, statistically derived averages should be used[61, 62]. Essentially, these averages describe the distribution of chain lengths that are present in the polymer sample.

Although there have been several different averages derived for the characterization of molecular weights of polymers, the most widely used and generally accepted are number average M_n and weight-average M_w molecular weights. These averages can be measured by analytical methods, for example using colligative properties of polymers, light scattering and ultracentrifugation[61]. The number average molecular weight is the arithmetic mean and can be calculated as any other numerical average, by multiplying the molecular weight of each chain M_i by the number of chains of that mass N_i, then adding them and dividing by the total number of polymeric chains[69] (eq. 1):

$$M_n = \frac{(N_1M_1 + N_2M_2 + ... + N_iM_i)}{\sum_i N_i} = \frac{\sum_i N_iM_i}{\sum_i N_i} \qquad (1)$$

Since the sum SN_iM_i essentially represents total weight of the sample, number-average molecular weight can be considered an average molecular weight per molecule. M_n values are more sensitive to the presence of low molecular weight molecules and affected by high molecular weight molecules to a smaller degree. Because colligative properties of polymers are dependent on the number of molecules present[60], analytical methods such as ebulliometry, cryometry, osmometry and end-group analysis can be used to determine M_n.[60, 61, 69]

Weight-average molecular weight is a weight-average arithmetic mean and is calculated by multiplying molecular weight of each chain M_i by its weight W_i, summing them, and dividing by the total weight of the sample (eq. 2):

$$M_w = \frac{(W_1M_1 + W_2M_2 + ... + W_iM_i)}{\sum_i W_i} = \frac{\sum_i W_iM_i}{\sum_i W_i} \qquad (2)$$

By substituting $W_i = N_i M_i$, more conventional expression for M_w can be obtained (eq. 3):

$$M_w = \frac{\sum_i N_iM_i^2}{\sum_i N_iM_i} \qquad (3)$$

Weight-average molecular weight is more sensitive to the presence of heavier chains than M_n and can be derived from the experiments in which "each molecule makes a contribution to the measured result relative to its size"[60]. The method most commonly used to determine M_w is light-scattering photometry.

The width and shape of molecular weight distribution (MWD) of polymers contains information about the polymerization mechanism and kinetics[69]. To characterize the width of MWD, the ratio of two molecular weight averages can be taken (eq. 4):

$$PDI = \frac{M_w}{M_n} \qquad (4)$$

This ratio, also called the polydispersity index (PDI), describes the range of variation in molecular weight distribution. Thus, high PDI indicates that there are a significant number of chains with very different molecular weights present in the sample whereas low polydispersity indices indicate that most molecules in the sample have very similar molecular weights. As mentioned above, PDI values reflect the polymerization mechanism. For example, conventional free radical polymerization usually produces polymers with very broad molecular weight distributions with PDI from 3 to 5, due to the uncontrollable nature of this reaction. Whereas for anionic polymerization, polymers with a very narrow MWD and PDI close to 1 can be obtained because one can have much better control over the polymerization reaction[69].

III. METHOD DEVELOPMENT FOR COMPOSITIONAL ANALYSIS OF LOW MOLECULAR WEIGHT POLYVINYL ACETATE (PVAC) BY MALDI –MASS SPECTROMETRY AND ITS APPLICATION TO THE ANALYSIS OF CHEWING GUM

A. *Introduction*

Polyvinyl acetate (PVAc) is a thermoplastic polyvinyl ester prepared by the radical polymerization of the vinyl acetate monomer. Due to its good adhesion to various porous surfaces and to a certain extent, to its cold flow, polyvinyl acetate is widely used in production of water-based emulsion paints, adhesives for textile, paper and wood. Other important applications of PVAc include the manufacture of non-woven textile fibers, inks and its use in textile finishing[70]. Another particularly interesting and important use of polyvinyl acetate is in production of chewing gum bases.

As described by manufacturers and other sources[71-75], a chewing gum base is an inert and insoluble non-edible substance used as a support for the soluble portion of chewing gum fit for human consumption (various sugars, polyoils, and flavors). Regular chewing gum usually contains 20-25% of gum base and sugar-free chewing gum up to 30% base on average[76]. In general, chewing gum utilizes a combination of natural or synthetic elastomers such as polymers of limonene or other dipentenes with rosin-glycerol esters in their formulation. Properly selected base provides the chewing gum with its masticatory properties. The exact compositions of gum bases is usually a trade secret, but generally they contain the ingredients from the following categories[76]:

- Elastomers – provide elasticity or bounce, and can be natural latexes or synthetic rubbers. Natural latexes include couma macrocarpa (also called leche caspi or sorva), loquat (also called nispero), tunu, jelutong or chicle, which is still commercially produced.
- Resins – provide a cohesive body or strength, and most often include glycerol esters of gum rosin, terpene resins and polyvinyl acetate.
- Waxes – act as softening agents and are most commonly paraffin or microcrystalline wax.
- Fats – behave as plasticizers and mainly come from hydrogenated vegetable oils.
- Emulsifiers – help to hydrate the gum base,most common being lecithin or glycerol monostearate.
- Fillers – impart texture of the gum. Most commonly used fillers are calcium carbonate or talk.
- Antioxidants – protect from oxidation and extend shelf life; the most common type used is BHT.

Historically, naturally occurring elastic materials such as natural latexes with additions of gutta and various resins of natural origin were employed in the production of chewing gum bases. However, due to various economic reasons such as high cost, the difficulty of obtaining naturally occurring elastomers and the lack of a dependable supply, formulations of chewing gums bases were modified to include synthetic polymers[77, 78]. Several synthetic polymers are the usual choice as elastomers in a base, with the most popular being copolymers of styrene-butadiene and isobutylene-isoprene as well as poly(isobutylene), polyisoprene and polyethylene. They provide the gum base with elasticity and with a cohesive body. Low and medium molecular weight polyvinyl acetate and other polymers of vinyl esters are also widely used in the chewing gum base formulations. These play an important role as a hydrophilic type detackifier, by sorbing saliva and becoming slippery when the gum is chewed[79, 80]. Polyvinyl acetate (PVAc) is the most useful vinyl polyester since it is readily available in non-toxic form while having physical characteristics and masticatory properties most suitable for chewing gum base manufacture. It was also discovered that the use of a two-component blend of PVAc consisting of low and medium molecular weight oligomers, significantly improves the film formation and supports a thick bubble shape in bubble gums. This improves the quality of the final product[79]. It also should be noted that polyvinyl acetate comprises a significant portion of the gum base material: the contribution of this polymer in the overall base composition can be as high as 60%, whereas the total contribution of all other synthetic polymers is significantly less, rarely exceeding 20%.[79 81].

Based on the examples provided above, it can be concluded that the polyvinyl acetate is one of the key ingredients in a successful chewing/bubble gum base formulation. As with any synthetic polymer, its physical properties directly depend on its overall composition, namely on the molecular weight distribution, chemical composition distribution, functionality type distribution, and the architecture of the oligomeric chains. Thus, the development of an analytical method that would allow the determination of these distributions could be extremely beneficial in development of new gum base compositions.

It should be noted that information about analytical methods for chewing gums overall is very scarce. This information is usually geared towards the identification of its low molecular weight components[82] or to the studies of interaction between the base and the low molecular weight

constituents[83]. To the best of our knowledge, no open literature reports have been made on the analysis of polymers present in the commercially available chewing gum bases.

Matrix-Assisted Laser Desorption/Ionization (MALDI) mass spectrometry is a well-established and powerful analytical tool that has been successfully applied to the analysis of various classes of synthetic polymers[10]. It provides information not only about molecular weight of the oligomeric chains which comprise the polymer sample, but also gives invaluable information about a polymer's overall chemical composition, structure and functionality[25]. It has also been demonstrated that MALDI-MS can be used effectively in the analysis of very complex mixtures such as blends of polymers[84-86], synthetic lubricants[87], high boiling crude oil fractions[88], coal tar pitch[89] and soot[90]. These examples demonstrate the great versatility of the MALDI method, and its applicability to a wide array of types of samples, including extremely complex heterogeneous mixtures. It therefore seems logical to suggest that MALDI mass spectrometry would be perfectly suitable for the analysis of such multi-component polymer-based samples used as chewing gum bases.

Only a few examples of MALDI analysis of polyvinyl acetate can be found in the literature over the past several decades. The earliest example is the work by Danis et al.[91] published in 1993, in which several synthetic polymers, including PVAc, were analyzed by MALDI-TOF mass spectrometry. These researches investigated the use of different matrices, such as *trans*-3-indoleacrylic acid (IAA), 2,5-dihydroxybenzoic acid (DHB) and 2-(4-hydroxyphenylazo)benzoic acid (HABA) and the influence of a solvent chosen to prepare samples, as applied to the analysis of chemically different polymers. They suggested the use of DHB as a matrix and methanol as a solvent for the successful analysis of PVAc, although no additional details about sample preparation for this polymer were given. The work published in 1996 by the same research group[92] described application of gel permeation chromatography (GPC) coupled with MALDI-TOF mass spectrometry to the analysis of two polydisperse polymer standards, one of which was PVAc 40 kDa. In their sample preparation, the standards were first subjected to the separation by GPC and then the fractions were collected and analyzed with MALDI-TOF. By using acetone as a solvent and 0.2M solution of IAA as a matrix, it was possible to obtain mass spectrum of PVAc and derive a correlation between measured mass and elution volumes of the fractions. Finally, in the paper by Hanton and Owens[27] published in 2005, the importance of solid phase solubility in MALDI

sample preparation of polymer samples was systematically examined. The series of polymers investigated included a variety of samples with different polarities, ranging from very non-polar (polybutadiene) to very polar (polyethyleneglycol). Polyvinyl acetate with molecular weight of 1500 Da was also included in the investigation. A diverse set of matrices was chosen also based on their polarities, and it was established that for success of MALDI analysis, matrix and polymer must match in polarity. Also, a relative solubility scale which relates different polymers to matrices based on their mutual solid state solubility was developed and used to correctly predict which matrix should be used for specific type of polymers. For PVAc, hydrophilic matrices such as DHB and thiourea were recommended.

Time-of-Flight (TOF) mass spectrometry is a usual choice for characterization of polymer molecular weight distributions and compositional analysis due to the relatively low cost of equipment, simplicity of analysis and theoretically unlimited mass range. However, Fourier Transform Mass Spectrometry (FTMS) offers high resolution and extremely high mass accuracy unreachable with TOF mass analyzers. Due to these capabilities, FTMS is well suited for the accurate structural characterization of complex mixtures, such as synthetic polymers.

In this chapter, the applicability of MALDI mass spectrometry techniques to the structural characterization of a complex polymer-based sample will be demonstrated. The optimization of MALDI analysis is first achieved by investigating the influence of sample preparation variables (choice of solvent, choice of matrix-analyte ratio) on analysis of pure low molecular weight polyvinyl acetate and then the optimized protocol is applied to the characterization of commercially available chewing gum.

B. *Experimental*

1. **Materials**

Polyvinyl acetate with unknown molecular weight was received from International Chewing Gum Association (ICGA) for the characterization of low molecular weight fractions by MALDI mass spectrometry. The matrix compound 2,5-dihydroxybenzoic acid (DHB) and three different solvents (acetone, methanol, ethyl acetate, all HPLC grade) used to make solutions of polymer and matrix were purchased from Sigma Aldrich and used without further purification. A sample of chewing gum Wrigley's® "Double Mint" was purchased from a local grocery store. The calibrant compound poly(ethylene glycol) (PEG) with molecular weight of 1500 Da was also purchased from Sigma Aldrich and used as received.

2. Instrumentation and analysis

MALDI-TOF experiments were performed using a Bruker Reflex III TOF mass spectrometer (Bruker Daltonics, Billerica, MA) operating in reflectron mode. A pulsed nitrogen laser operating at l = 337 nm was employed. All spectra were recorded in positive ion mode under delayed extraction conditions (220 ns) and in reflector mode. The accelerating voltage was 20 kV. The average pressure during the analysis was ~ $1*10^{-8}$ torr. Each spectrum was obtained as a sum of 500 laser shots.

MALDI-FTMS mass spectra were acquired using the 9.4Tesla IonSpec Ultima FTMS (IonSpec/Varian Inc., Lake Forrest, CA) with an external ionization MALDI source. The mass spectrometer was equipped with a pulsed Nd:YAG laser operating at l = 355 nm. Experiments were conducted in positive ion mode with ions being generated in the external ionization source, transferred into cylindrical ion cyclotron resonance (ICR) cell by quadrupole ion guide, trapped, excited and then detected. The average base pressure during the experiments was ~$1*10^{-11}$ torr. Each spectrum was obtained as a sum of 5 scans, 10 laser shots each. External calibration of the spectra was performed using PEG 1500 as a calibrant. Three spectra were collected for each matrix:analyte ratio from three different spots on the target plate in order to check spot-to-spot reproducibility of the experiments. After the spectra were collected, Data Analysis® software was used to subtract the baseline and perform the calibration.

For the samples analyzed, number-average molecular weight (M_n), weight-average molecular weight (M_w) and polydispersity index (PDI) were calculated from obtained MALDI mass spectra using the following equations[64]:

$$M_n = \frac{\sum_{i=1}^{\infty} M_i N_i}{\sum_{i=1}^{\infty} N_i} \quad (1) \qquad M_w = \frac{\sum_{i=1}^{\infty} M_i^2 N_i}{\sum_{i=1}^{\infty} M_i N_i} \quad (2) \qquad PDI = \frac{M_n}{M_w} \quad (3)$$

where M_i is the molecular weight of the oligomer with i repeating units and N_i corresponds to the intensity of the peak i.

3. **Sample preparation**

- *Analysis of polyvinyl acetate*

The chosen sample preparation procedure for both TOF and FTMS was based on the protocol established by Hanton et al.[27] and was as follows. First, three different stock solutions of each matrix and polymer were prepared in methanol, acetone and ethyl acetate. These stock solutions prepared in the common solvent were then mixed in three different volume ratios. The concentrations of stock solutions were 0.25M for a matrix solution and 5 mg/ml for a polymer solution. Volume ratios of polymer-to-matrix used to investigate the influence of the amount of the matrix were 2:7, 1:7, 1:14. Sodium contamination from solvents, glassware and matrix material provided sufficient alkali cationization aid for ionization of the polymer sample. After mixing stock solutions in the ratios indicated, three 2 ml aliquots of each mixture were deposited on a stainless steel target plate, and allowed to air dry prior to spectral collection.

- *Analysis of chewing gum sample*

In view of the fact that there was no similar investigation found in the literature, the sample preparation protocol needed to be developed and optimized. The information about the overall composition of the sample given on a package did not provide any information about the chemical nature of gum base and attempts to find MSDS information were unsuccessful. Listed primary ingredients were sugar, gum base, dextrose, and corn syrup. Minor ingredients (less then 2%) were natural and artificial flavors, glycerol, soy lecitin, aspartame, acesulfame K, colors (yellow 5 lake, blue 1 lake) and BHT as a preservative. Since the main aim of this investigation was the determination of PVAc in the chewing gum base, the MALDI sample preparation protocol, which was optimized for the pure PVAc sample, was employed. DHB was used as a matrix since it was possible to obtain good quality spectra of the chewing gum base polyvinyl acetate sample. Matrix stock solution's concentration was 2.5M (a lower concentration of 0.25M was also tested but did not yield any PVAc signal), and concentration of the gum sample employed was 50 mg/ml (a lower concentration was tested also, but was found insufficient). Methanol and ethyl acetate were used as solvents to extract the PVAc from the gum sample and for matrix stock solution preparation. To extract the polyvinyl acetate from the chewing gum sample, appropriate amounts of sample and solvent were placed into a screw cap vial. The vial was then placed into the ultrasonic bath and held at 70°C for 30 min to ensure efficient extraction of the polymer. After 30

min, the supernatant solution containing the extracted PVAc was mixed with matrix stock solution to achieve a 2:7 sample-to-matrix volume ratio and then three 2 ml aliquots were spotted on the stainless steel target plate, allowed to air dry and analyzed.

C. *Results and Discussion*

1. **Analysis of low molecular weight polyvinyl acetate used as a chewing gum base**

- *Optimization of sample preparation protocol with MALDI-TOF*

Although the mechanism of MALDI is still the topic of the debate, it is widely known that the choice of proper sample preparation conditions plays a crucial role in the success of any MALDI analysis. However, due to the diverse chemical nature of synthetic polymers, no standard sample preparation protocol has been established for their analysis, although over the years multiple attempts have been made to optimize and rationalize the choice of such important parameters as the nature of the matrix[18, 19] and its concentration[20, 21], solvent[22] and cationizing agent[23].

Hanton and Owens investigated the influence of the chemical nature of matrix and determined that formation of a “solid solutions” when the polymer molecules are evenly dispersed in the matrix is observed when the polarity of the matrix matches the polarity of the polymer, in turn leading to superior quality mass spectra. Therefore, following these principles, DHB was chosen as a matrix for polyvinyl acetate analysis in this study, since these compounds match in polarity. The concentration of the matrix and of the polymer, along with matrix:analyte ratios were also chosen in accordance with guidelines suggested in the publications by these authors[27 26].

The choice of the suitable solvent is also essential for the success of any solvent-based polymer MALDI analysis. Generally, it is advisable to use the same solvent to prepare all solutions during the sample preparation process, this way preliminary segregation of the polymer from the matrix during crystallization of the MALDI sample could be minimized[9, 10, 22, 25]. This segregation of the matrix and analyte produces a non-homogeneous surface of the sample with clusters of analyte and matrix crystals of various sizes, and ultimately leads to very poor spot-to-spot and shot-to-shot reproducibility of analysis and can also lead to severe mass discrimination and errors in MWD calculations[29]. In order to improve homogeneity and reduce segregation of the sample, it was also suggested that the use of fast drying solvents (such as acetone) is beneficial, since when evaporation of the solvent happens quickly the

sample will have less time to segregate[25, 26, 34]. However, the use of fast drying solvent does not guarantee superior quality spectra every time, as was demonstrated in a recent comprehensive study of solvent effect on MALDI analysis of several different polymers.[35] It was concluded that as long as the all components of the sample are soluble in the solvent, reliable good quality data could be obtained regardless of the evaporation rate.

The solubility of polymers is an important characteristic since various industrial manufacturing procedures requires either the polymer's dissolution or swelling in order to be processed. Consequently, from the very beginning of macromolecular chemistry, solubility properties of polymers were investigated and quantified. Solubility, along with other physical properties of polymers, can be related to the strength of interactions between chains and of covalent bonds in individual molecules. Since the strength of intermolecular interaction is equal to cohesive energy density (CED), it can therefore be used to describe solubility behavior[60]. The square root of CED is defined as Hildebrand solubility parameter d and can be calculated based on the Hildebrand's theory of regular solutions[61]:

$$\delta = \sqrt{CED} = \sqrt{\frac{\Delta E_v}{V}} \qquad (4)$$

where DE_v is the molar energy of vaporization and V is the molar volume of the liquid. When the polymer and the solvent have the same d, maximum swelling (or solubility) will be observed. Therefore, the concept of solubility parameter allows evaluating whether or not the polymer and solvent are compatible. Solubility parameters can also appraise compatibility of polymers, predict swelling of elastomers in various solvents and predict chemical resistance. For these reasons, solubility parameters are widely accepted by industry and polymer chemists alike[61, 93]. However, the theory of regular solutions does not take into account strong interactions in the solvent, such as polar and hydrogen bonding interactions. In order to improve the accuracy of the Hildebrand's model, C. Hansen in 1966 suggested separating the total solubility parameter into different components, representing different interactions (Hansen parameters).[93] These are d_d – dispersion forces, d_p – polar interactions and d_h – hydrogen bonding. The total solubility parameter d_t can be calculated as a sum of these three components:

$$\delta_t^2 = \delta_d^2 + \delta_p^2 + \delta_h^2 \qquad (5)$$

These components can be visualized as a three-dimensional model where individual Hansen parameters are the coordinate axes and unique spherical volume of solubility with the center at coordinates (d_d, d_p, d_h) can be obtained for different polymers. A polymer is likely will be soluble in liquids, whose total solubility parameter lies within the radius of the solubility sphere (interaction radius, R) of the polymer. An equation can be used in order to calculate the distance of the solvent from the center of the solubility sphere (D_s)[35, 93]:

$$D_s^2 = 4(\delta_{d_S} - \delta_{d_P})^2 + (\delta_{p_S} - \delta_{p_P})^2 + (\delta_{h_S} - \delta_{h_P})^2 \qquad (6)$$

where δ_{i_S} represents Hansen parameters of the solvent and δ_{i_P} Hansen parameters of the polymer. If the distance D_s is smaller than the interaction radius, the solvent will most likely dissolve the polymer.

In order to investigate the influence of the solvent in MALDI analysis of polyvinyl acetate, three solvents were selected: ethyl acetate, methanol and acetone. Hansen parameters of these solvents were obtained from the literature[93] and along with calculated D_s values are presented in the Table 1. Vapor pressures of these solvents at 25°C[94] can also be found in the Table 3.1. The Hansen parameters of PVAc used in calculations were obtained from the literature as well[95]: d_d = 20.9 $MPa^{½}$, d_p = 11.3 $MPa^{½}$, d_h = 9.6 $MPa^{½}$ and interaction radius R = 13.7.

As it can be seen from Table 3.1, ethyl acetate and acetone are fast drying solvents, with close values of solubility parameters and D_s. Both should be considered good solvents for polyvinyl acetate since their Ds values are less than interaction radius for polyvinyl acetate. Methanol on the other hand, has a D_s value that is higher than R, and lies outside of solubility sphere of PVAc. Therefore, methanol should be considered as the worst solvent for PVAc out of all three, although it is more volatile than ethyl acetate and therefore might produce more homogeneous sample surface in MALDI sample preparation. Acetone is the most volatile solvent out of all selected, and therefore it can be expected that it will produce sample surfaces with the least segregation of analyte from the matrix. Although based on its D_s value, methanol should be a non-solvent for polyvinyl acetate, the polymer did dissolve in it at the concentration required for the sample preparation and it was possible to collect mass spectra for the samples prepared with this solvent. The explanation for this inconsistency might be explained by low concentration of the polymer solution that was needed for sample preparation (5 mg/ml) and also by low molecular weight of the polymer – the solubility of polymers is mass dependant. So, lower weight

fractions are usually more soluble than the higher molecular weight ones. MALDI analysis was successful for all chosen matrix:analyte ratios and all solvents investigated for the sample preparation optimization. The results of the optimization are presented in Fig. 3.1. Here, the average intensity of the base peak obtained from triplicate measurements for each solvent/matrix:analyte combination is plotted against the solvent in order to reveal which combination of these sample preparation parameters produces the highest ion yield. The error bars are the standard deviations obtained for the triplicate measurements and illustrate spot-to-spot reproducibility.

As it follows from Fig. 3.1, the best signal intensity was obtained when ethyl acetate was used as a solvent and volume ratio matrix-analyte was 7:2 (the lowest amount of matrix). Ethyl acetate as a solvent resulted in reproducible spectra with low signal-to-noise and fairly high signal for all matrix-analyte ratios investigated. It therefore was considered the best solvent for low molecular weight PVAc. Use of acetone as a solvent produced spectra with somewhat lower signal intensities as compared to ethyl acetate data. In addition, standard deviations obtained with acetone were significantly higher as compared with data obtained with the other solvents for all matrix-alnalyte ratios, which is consistent with observations made by other researchers[35]. Data obtained when methanol was used as a solvent is in good agreement with predictions based on comparison of solubility parameters of polymer and solvents – it consistently produced the lowest signal intensities for all matrix-analyte ratios. Results obtained with the other two solvents are not in the agreement with prediction based on their D_s values, since the highest average base peak intensities were obtained with ethyl acetate and not with acetone. However, it should be noted that the calculated D_s values of these two solvents are really close. It seems possible therefore, that when comparing two solvents that interact with the polymer in a very similar way, other factors may play major role in the outcome of MALDI experiment. For example, it is known that for successful MALDI analysis, a homogeneous microcrystalline surface of the sample is required, and therefore it is possible that ethyl acetate allows for a formation of more uniform, smaller crystals and less segregation of polymer from the matrix. Smaller standard deviations obtained with this solvent also support this hypothesis, since more uniform, homogeneous surfaces always give more reproducible spectra[26]. The MALDI-TOF spectrum of PVAc obtained with volume ratio matrix-analyte of 7:2 and ethyl acetate as a solvent is shown in Fig. 3.2. The overall look of the spectrum is typical for synthetic polymers, showing Gaussian-

type distribution of oligomers in the polymer sample. The inset in the Fig. 3.2 shows the expanded section of the spectrum, demonstrating the mass difference between individual peaks in the distribution is 86 Da, corresponding to the molecular weight of the ethyl acetate monomeric unit. Individual peaks are marked with the corresponding degree of polymerization (number of monomeric units in a molecule) values. The spectra were collected at low laser power (just above the threshold), and as it is evident from the spectrum, there was little evidence of the laser-induced fragmentation of the polymer. A secondary distribution was also detected in collected spectra, but had very low intensity. The peaks in this distribution are shifted towards higher molecular weights and the difference between corresponding peaks in main and secondary distributions is 16 Da, which matches the mass difference between sodium and potassium. Therefore, it can be concluded that peaks in secondary distribution corresponds to the same oligomers as in the main distribution, only with attached potassium cation instead of sodium. Number-average molecular weight (M_n), weight-average molecular weight (M_w) and polydispersity index (PDI) were calculated from obtained mass spectrum and were found to be M_n = 2293.23 Da, M_w = 3352.73 Da and PDI = 1.46. The relatively high value of PDI indicates that this sample is susceptible to a well-known problem of MALDI analysis of polydisperse polymers – mass discrimination against higher molecular weight species[10]. This phenomenon was thoroughly investigated over the years and multiple reasons for it were found[84, 96-98]. However, since the main goal of this analysis was to develop the method for the analysis of low molecular weight fractions of PVAc, the results obtained are deemed satisfactory.

The individual oligomeric peaks in the spectrum were assigned and the assignments for several selected peaks are presented in the Table 3.2 along with the values of ppm errors for these assignments. The values of calculated ppm errors were typical for MALDI-TOF analysis of polymers and were below 300 ppm for all peaks in the spectrum. However, even though the errors were not uncharacteristic, several compositional assignments for each mass value with different end-groups and attached cation were probable, as shown in the Table 3.2. Based just on the values of ppm error it is impossible to accurately identify end groups and cation attached for this polymer sample, since all ppm errors were close to each other and were within acceptable range for TOF measurements for polymers. In order to determine chemical composition of this PVAc sample correctly, additional measurements that are more

accurate were required and therefore FTMS analysis of the polymer using optimized sample preparation conditions was performed.

- *Structural analysis of polyvinyl acetate with MALDI-FTMS*

After the sample preparation procedure was optimized as described above, FTMS was used to identify the structure of the polyvinyl acetate sample. In addition, the influence of laser power on the quality of spectra was investigated. Fig. 3.3 demonstrates the spectrum obtained with the optimized conditions and on the lowest setting of laser power. The weight average molecular weight (M_w) calculated for the sample from this spectrum was 1823.35 Da, number average molecular weight (M_n) was 1761.98 Da, and PDI was found to be 1.04. These values differs significantly from those obtained with MALDI-TOF, since low intensity peaks in both low and high m/z ranges that are present in the TOF spectra were absent from FTMS spectra. This might be explained by several reasons: it is possible that sensitivity of FT-mass spectrometer is lower than that of TOF for this sample and therefore unable to detect low intensity ions; it is also possible that the instrumental settings were not optimized when FTMS analysis was performed, which resulted in mass discrimination. Overall, the spectrum obtained with FTMS has the same features as the one obtained with the time-of-flight mass spectrometer. It demonstrates the same general Gaussian shape of the MWD, with peaks distributed at equal distances of 86 Da from each other, corresponding to the mass of the polyvinyl acetate monomeric unit. The peaks in the spectrum are marked with degree of polymerization numbers.

However, there was a significant difference between FTMS and TOF data. As it can be seen from the Fig. 3.3, there is a secondary distribution present in the spectrum with fairly high intensity of the signals – in this regard the obtained spectrum was different from that obtained with the TOF mass analyzer. Upon closer inspection, it became evident that the mass difference between peaks in the main and secondary distributions is 60 Da, which corresponds to the molecular weight of acetic acid. It was therefore suggested that the secondary distribution of ions appears due to the fragmentation during MALDI-FTMS analysis, which leads to the loss of acetic acid. In order to test this hypothesis, laser power was systematically varied during the experiment and the spectra were recorded at four different values – 0.891 mJ, 1.264 mJ, 1.450 mJ and 1.637 mJ. It was discovered that as the value of laser power increased, the intensity and number of secondary peaks increased as well. The results of this

investigation are presented in Fig. 3.4 where spectra collected at four different values of laser power are shown. The expanded portion of the spectrum collected when the highest laser power was used clearly demonstrates (Fig. 3.5) the loss up to 4 acetic acid molecules from each individual oligomer of polyvinyl acetate. This unimolecular fragmentation of polyvinyl acetate results in the formation of macromolecular polyenes as demonstrated in Scheme 3.1. The fragmentation pattern with the loss of acetic acid and formation of several unsaturated compounds was observed previously during pyrolysis of PVAc[99, 100] and in the MS/MS experiments, such as the study performed by Collins et al[101] where tandem quadrupole time-of-flight electrospray mass spectrometry (qTOF-ESI-MS) was used for analysis of low molecular weight polyvinyl acetate. They discovered that under collision-induced dissociation (CID) MS/MS conditions, de-acetylation of the polymer occurs by either elimination of acetic acid or ketene molecules from the side groups. Similar results were obtained by Giguere and Mayer[102] who also employed CID ESI-mass spectrometry to study mechanism of dissociation of PVAc. It can be concluded therefore that this process is typical for polyvinyl acetate and happens not only under the harsh conditions of MS/MS or pyrolysis-MS but also in the conditions of soft MALDI mass spectrometry if the laser power is high enough and the transient length is long enough as it is during FTMS experiments.

The compositional analysis was performed in order to establish correct chemical composition of the sample. The results of this analysis are presented in the Table 3.3. As it is evident from the table, the use of FTMS allows unambiguous identification of the chemical structure of the polymer. There was only one assignment, which allowed for errors less than 10 ppm, whereas other possible chemical compositions produced errors of at least 20 ppm and therefore were unlikely. This assignment was found to be $[C_2H_5(C_4H_6O_2)_nOCH_3]Na^+$, where n stands for degree of polymerization (or for number of monomeric units in the oligomer). Interestingly, this assignment gave the highest error with the TOF data and usually would be rejected. This example illustrates the value of Fourier Transform mass spectrometry in the analysis of complex mixtures such as polymers – due to its unmatched resolving power, very high accuracy can be achieved and used to disambiguate chemical compositions when more than one option is possible.

2. Method development for the analysis of chewing gum

In order to test MALDI sample preparation methodology developed for pure PVAc chewing gum base on a more complex, 'real life' sample, it was suggested to apply it to the analysis of PVAc in chewing gum. In order to extract the polymeric component from the gum, an extraction protocol had to be developed. Methanol and ethyl acetate were chosen as solvents for extraction and for matrix solutions preparation. Two matrix concentrations of 0.25M (just as was used for the pure PVAc analysis) and 2.5M along with two concentrations of the chewing gum (5 mg/ml and 50 mg/ml) were used in the sample preparation process.

Two different extraction procedures were tested. In the first procedure, to reduce possible interference from dextrose and other sugars which are the major components of the gum sample, it was washed with hot water first (the reasoning was that sugars are very soluble in water and therefore could be removed from the sample, whereas PVAc is not soluble in water and would stay in the sample) as such:

- Enough of chewing gum and water to make 5 mg/ml solution were placed in a screw cap vial, which then was placed into ultrasonic bath kept at 70°C for 30 min.
- After that, the water from the tube was discarded, organic solvent was added and the vial was placed back into the ultrasonic bath for another 15 min.
- Appropriate amounts of resulting supernatant and 0.25 M matrix solutions were mixed and spotted on the target plate.

This approach did not produce any usable data, however very weak signals that belonged to PVAc (based on the difference between peaks) were detected. Also, despite the attempts to get rid of the sugar-related interference, there were signals present in the spectra equally distributed at 162 Da from one another, which is suitable for a poly/oligosaccharide, which consists of either glucose or fructose units (data not shown). The most likely reasons for a weak signal from the PVAc chewing gum base were the loss of the polymeric material due to its dissolution in water and low concentration of the gum sample, which might be problematic in this case, since the polymeric base is already greatly diluted in the gum by various fillers.

To address these issues, a different extraction procedure was tested:

- Enough of chewing gum and organic solvent to make 50 mg/ml solution were placed in a screw cap vial, which then was placed into ultrasonic bath kept at 70°C for 30 min.
- After that, appropriate amounts of resulting supernatant and of 2.5 M matrix solutions were mixed and spotted on the target plate.

This direct extraction approach was more successful and allowed spectra to be obtained with fairly high signal intensities. Ethyl acetate solutions produced significantly better spectra with respect to the ion yields compared with methanol, thus demonstrating once again its superiority in MALDI sample preparation of PVAc-based materials and pure PVAc. The spectrum of the chewing gum sample obtained by following direct extraction procedure with ethyl acetate as a solvent and 2.5 M DHB as a matrix is presented on the Fig. 3.6. The spectrum had the same features and looked very similar to the one acquired for pure PVAc with TOF mass analyzer, although the overall signal intensity obtained for the chewing gum was significantly lower than that in pure PVAc spectra. The inset in the Fig. 3.6 demonstrates the expanded section of the spectrum, from which the mass difference between individual peaks in the distribution can be seen. This difference was 86 Da, which corresponds to the molecular weight of ethyl acetate monomeric unit. Individual peaks are marked with the corresponding degree of polymerization values. The laser power was set just above the threshold, and as it is evident from the spectrum, there was no evidence of the laser-induced fragmentation. Number average and weight average molecular weights along with polydispersity index were calculated from the data obtained and were found to be M_n = 2181.19 Da, M_w = 2781.73 Da, PDI = M_w/M_n = 1.28. In addition, end group analysis of the sample was performed and chemical composition was established. Results of this analysis for several selected oligomers are presented in the Table 3.4. There was only one assignment found that was adequate from chemical point of view and allowed for errors less than 400 ppm. This assignment was found to be $[C_2H_5(C_4H_6O_2)_nCH_2]Na^+$, where n stands for number of monomeric units in the oligomer. Based on these results, it can be concluded that developed sample preparation procedure can be successfully used for identification and characterization of polymeric base in the chewing gum samples.

D. *Conclusions*

Matrix-assisted laser desorption/ionization mass spectrometry analysis of pristine low molecular weight polyvinyl acetate chewing gum base and chewing gum sample was performed. In order to ensure the best ionization efficiency for the polymer, sample preparation optimization was performed with time-of-flight mass spectrometry. This was accomplished by investigating the influence of the solvent and matrix:analyte ratio on the average base peak intensity of the pristine low molecular weight PVAc sample. It was demonstrated that comparison of polymer's and solvent's Hansen solubility parameters could be used as a guide when choosing the solvent for MADLI sample preparation. The highest intensity PVAc signals were obtained when ethyl acetate as a solvent and lowest matrix-analyte ratio were employed. It was impossible to accurately determine the identity of the end groups based just on the TOF data since more than one compositional assignment was possible and therefore FTMS analysis of this polymer was performed using optimized sample preparation conditions. The use of FTMS allowed disambiguation and accurate determination of chemical composition for this sample. The influence of laser power was investigated for MALDI-FTMS and it was discovered that PVAc undergoes unimolecular decomposition by losing acetic acid molecules from its backbone. It was demonstrated that the degree of this decomposition is laser power dependant – the higher the laser power, the more extensive fragmentation was observed. Number and weight average molecular weights as well as polydispersity index were determined with both methods. Developed sample preparation protocol was applied to the analysis of a chewing gum sample. It was shown that optimized MALDI-TOF mass spectrometry could be successfully used for the complete characterization of the polymeric chewing gum base.

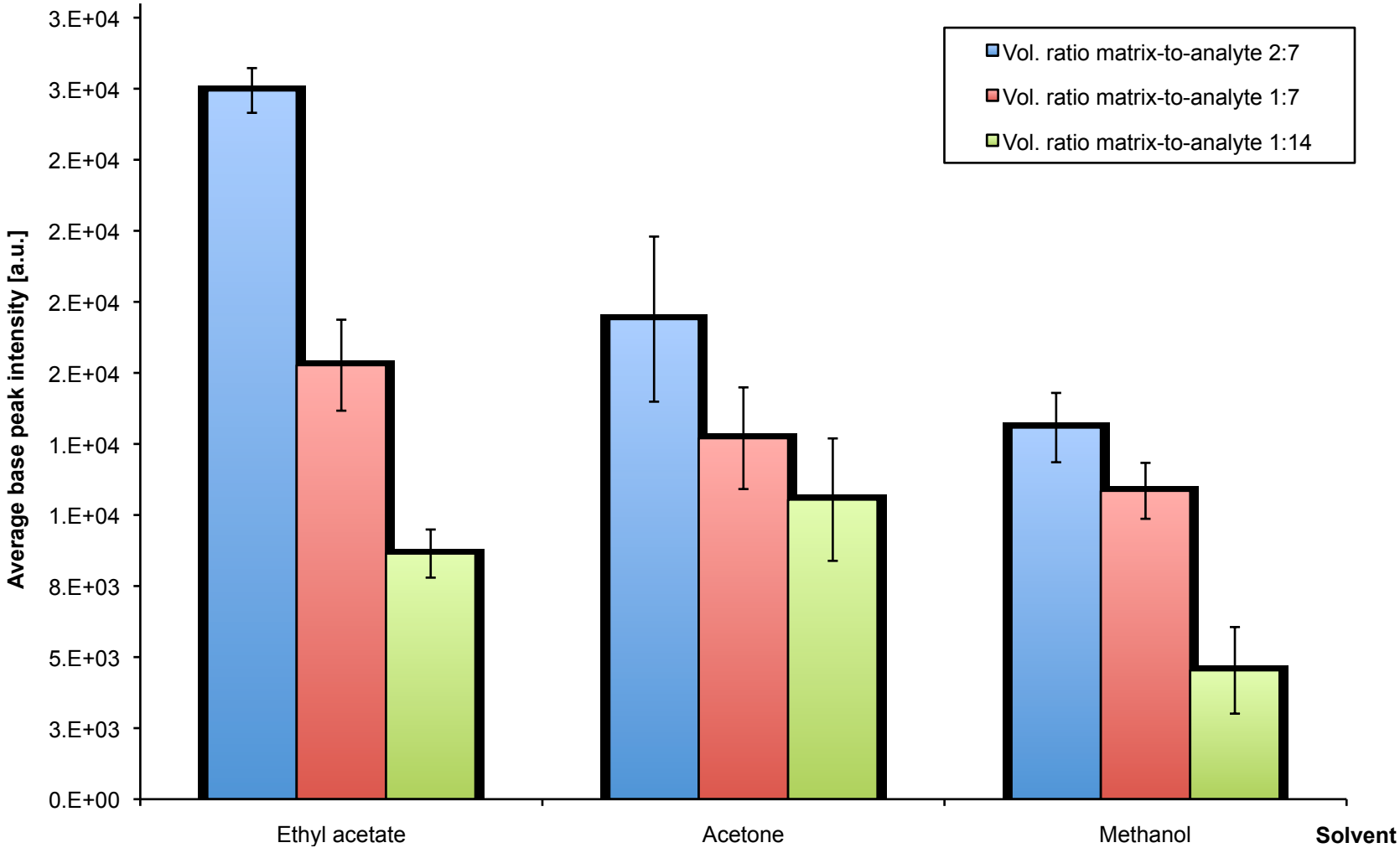

Figure 3.1 Average base peak signal intensities obtained with different solvents and matrix-analyte volume ratios for MALDI-TOF analysis of low molecular weight PVAc, employing 0.25M DHB as a matrix

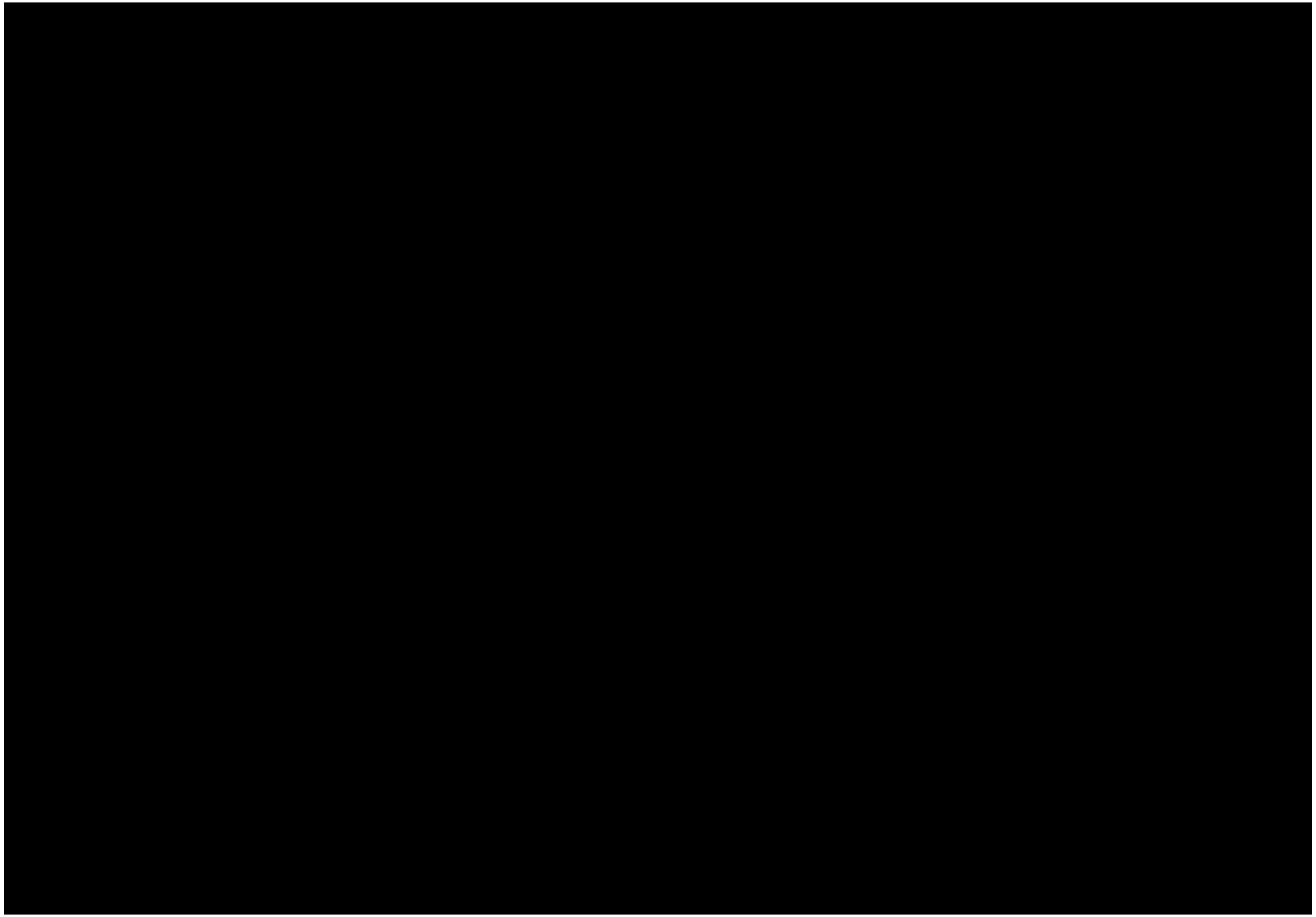

Figure 3.2 MALDI-TOF spectrum of polyvinyl acetate when ethyl acetate was used as a solvent, 0.25M DHB as a matrix and volume ratio matrix-analyte 7:2

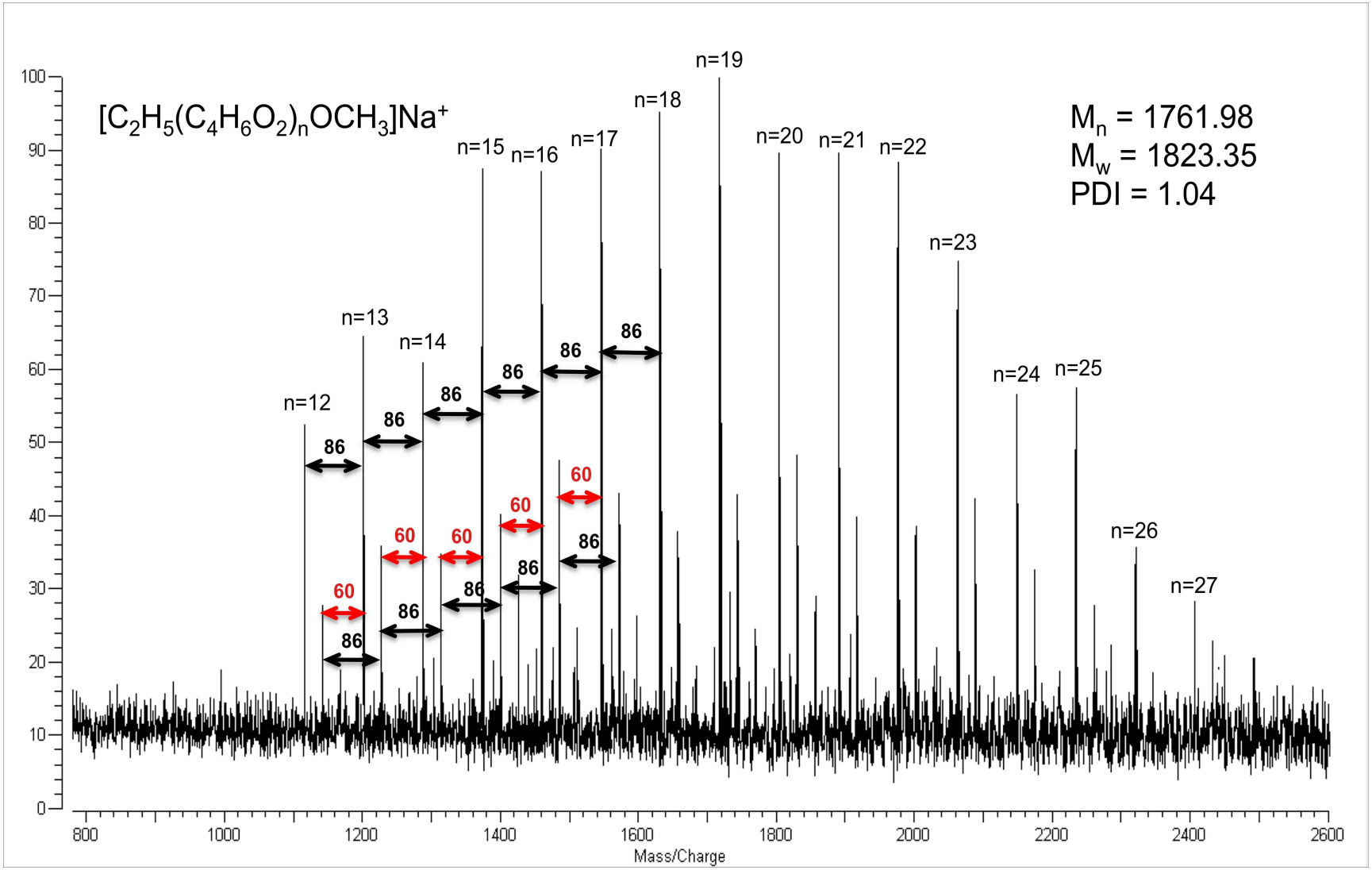

Figure 3.3 9.4T MALDI-FTMS spectrum of polyvinyl acetate when ethyl acetate was used as a solvent, 0.25M DHB as a matrix and volume ratio matrix-analyte 2:7

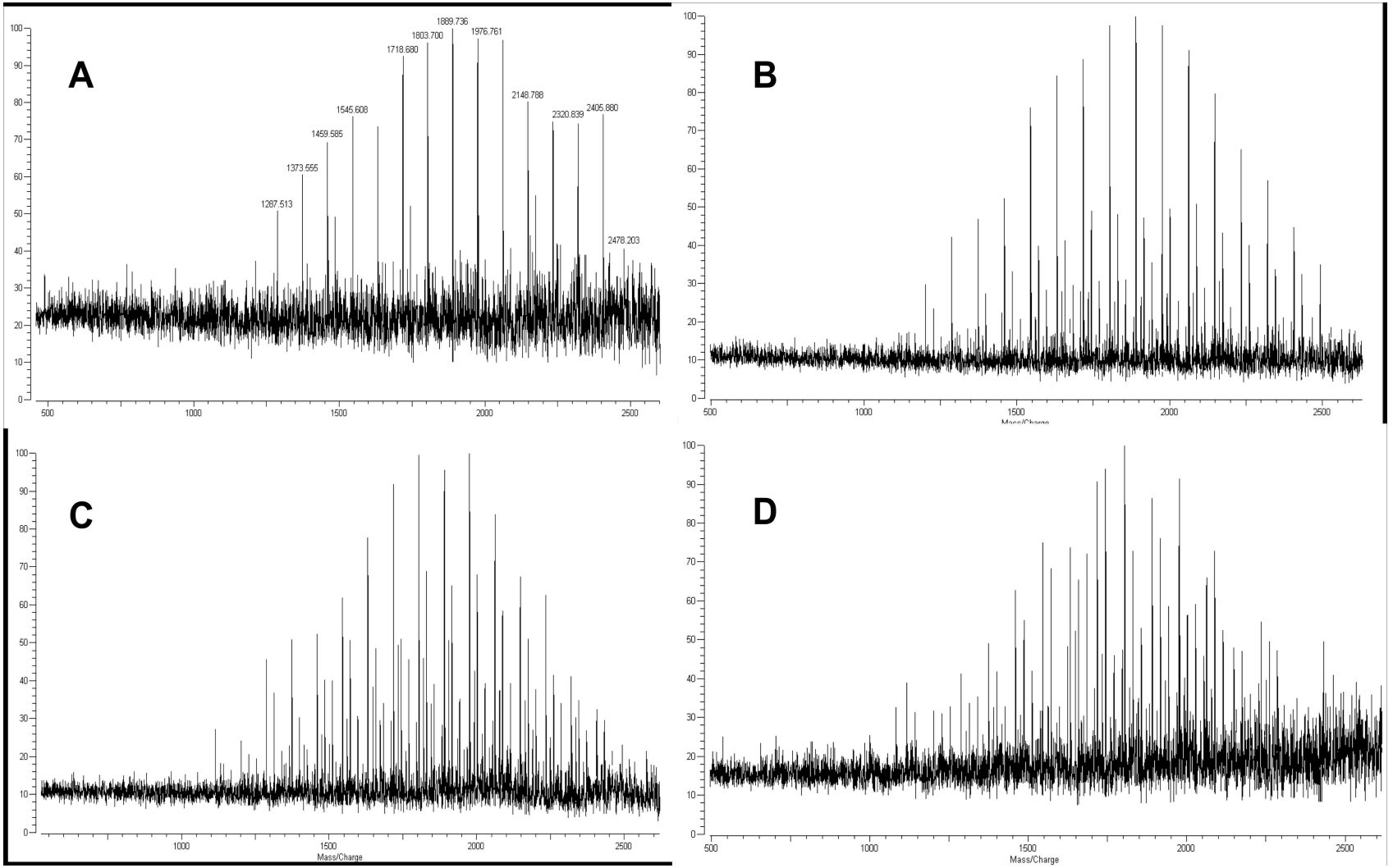

Figure 3.4 9.4T MALDI-FTMS spectra of polyvinyl acetate with ethyl acetate used as a solvent, 0.25M DHB as a matrix and volume ratio matrix-analyte 2:7 collected at different values laser power; A – 0.891 mJ, B – 1.264 mJ, C – 1.450 mJ, D – 1.637 mJ

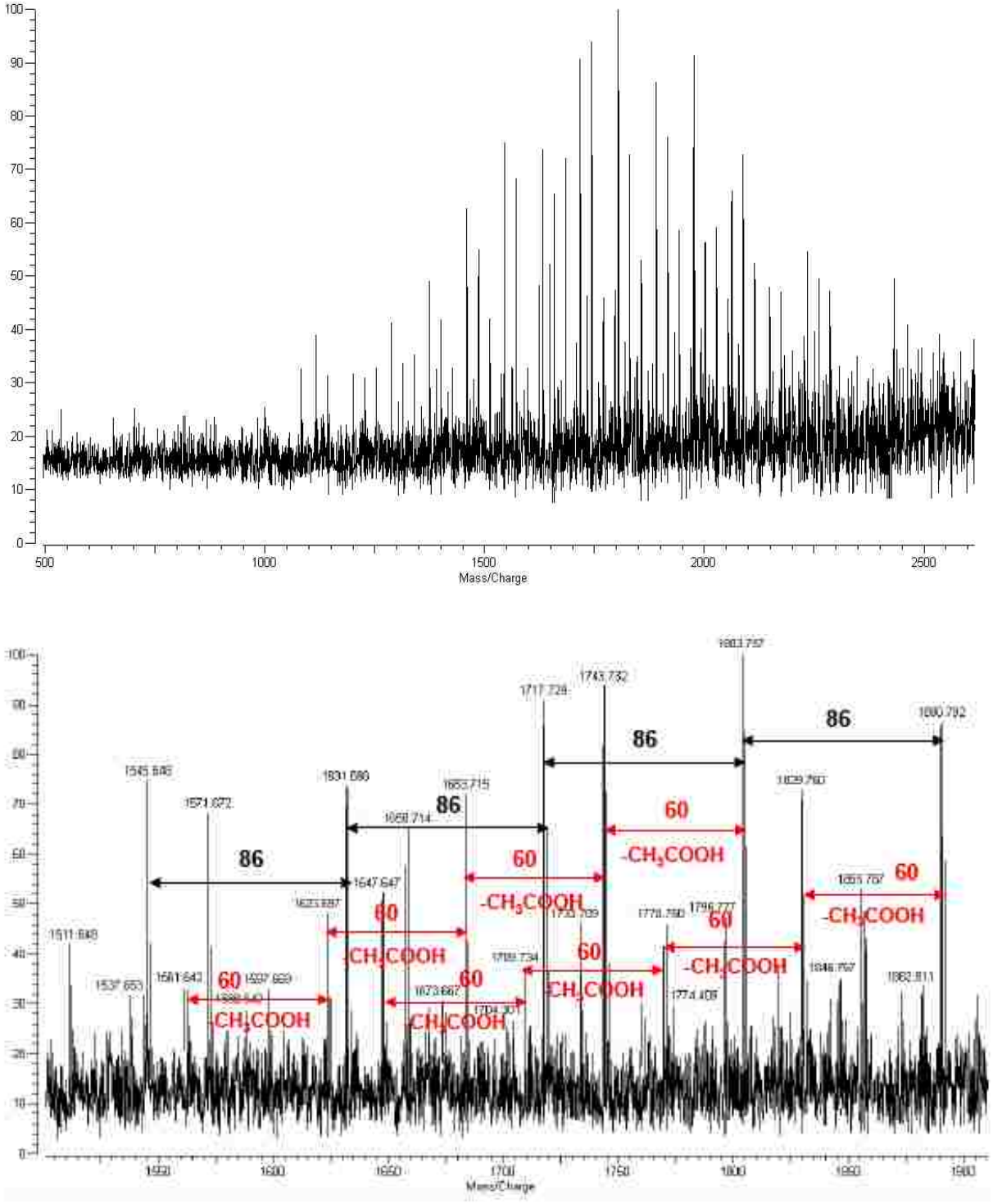

Figure 3.5. 9.4T MALDI-FTMS spectrum of polyvinyl acetate with ethyl acetate used as a solvent, 0.25M DHB as a matrix and volume ratio matrix-analyte 2:7 collected at highest value of laser power (1.637 mJ); expanded portion of the spectrum demonstrates excessive fragmentation

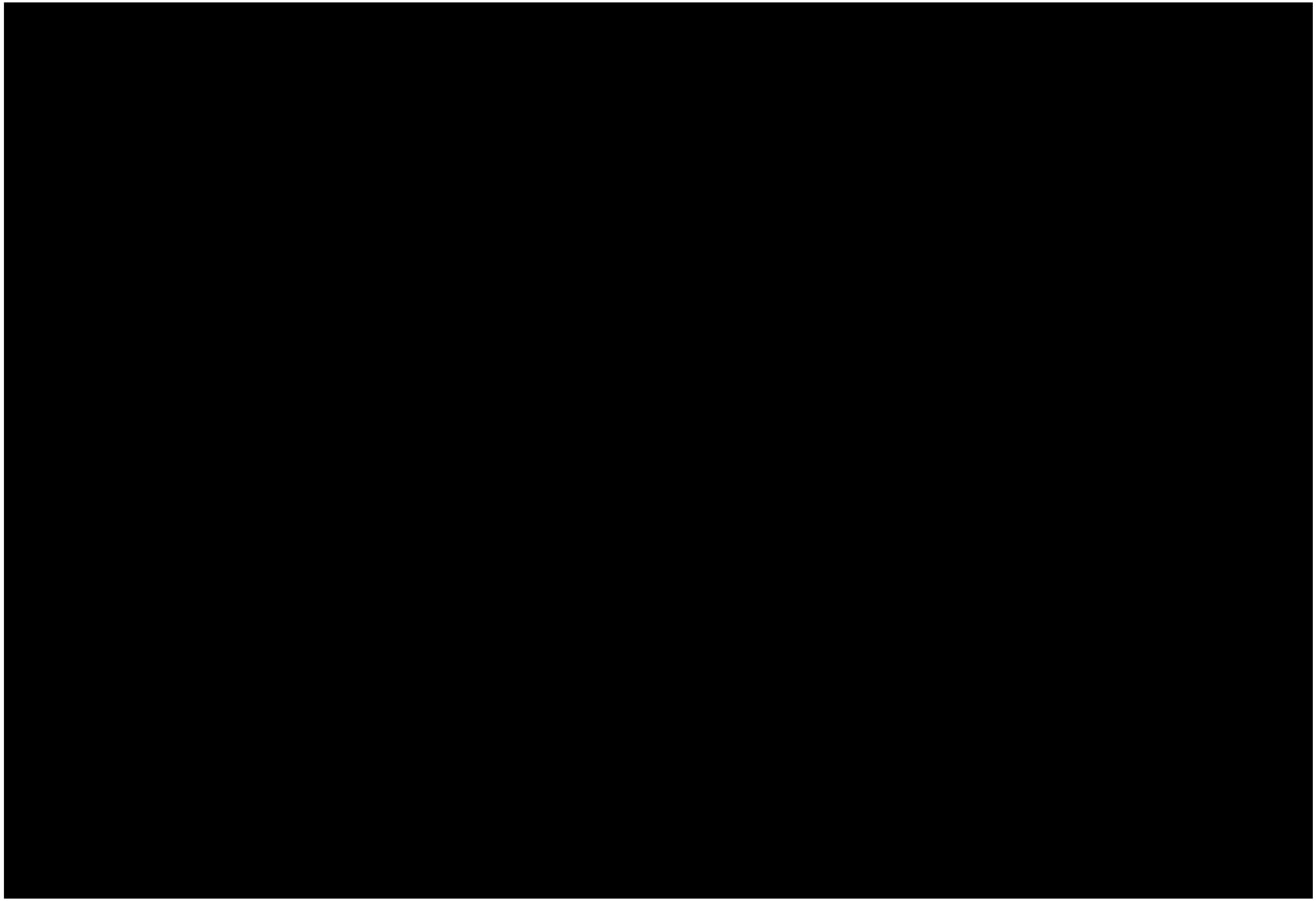

Figure 3.6 MALDI-TOF spectrum of Wrigley's chewing gum sample obtained by direct extraction with ethyl acetate; 2.5M DHB used as a matrix, volume ratio matrix-sample 2:7, ethyl acetate used as a solvent for the matrix

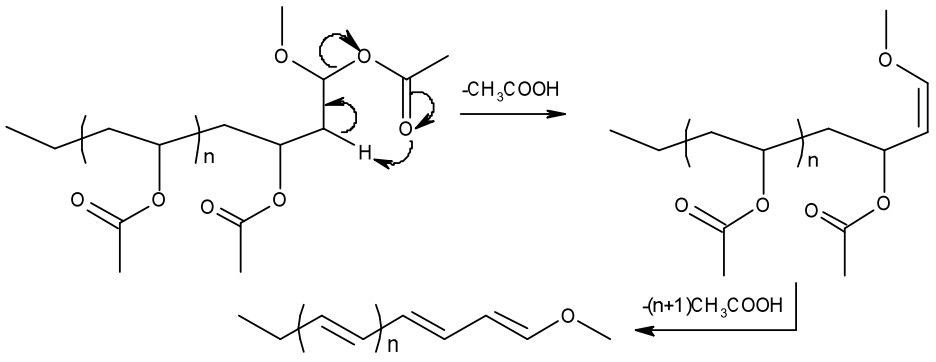

Scheme 3.1 Mechanism of unimolecular decomposition of polyvinyl acetate by elimination of acetic acid

Table 3.1 Hansen solubility parameters, D_s values and vapor pressure at 25°C of selected solvents

Solvent	d_d [MPa^{½}]	d_p [MPa^{½}]	d_h [MPa^{½}]	D_s (PVAc)	P_{vapor} [kPa]
Acetone	15.5	10.4	7.0	11.1	30.7
Ethyl acetate	15.8	5.3	7.2	12.1	12.7
Methanol	15.1	12.3	22.3	17.2	16.9

Table 3.2 Compositional analyses of selected PVAc oligomers obtained with MALDI-TOF using optimized sample preparation protocol (ethyl acetate as a solvent, volume ratio matrix-analyte 7:2)

Experimental mass	Compositional assignment	Theoretical mass	ppm error
1115.219	PVAc 6 CH3 C2H5 K	1115.468	223
	PVAc 6 CH2OH CHO Na	1115.452	209
	PVAc 6 CH3 CHO K	1115.431	190
	PVAc 6 C2H5 OCH3 Na	**1115.489**	**242**
1201.233	PVAc 7 CH3 C2H5 K	1201.504	226
	PVAc 7 CH2OH CHO Na	1201.489	213
	PVAc 7 CH3 CHO K	1201.468	196
	PVAc 7 C2H5 OCH3 Na	**1201.525**	**243**
1287.324	PVAc 8 CH3 C2H5 K	1287.541	169
	PVAc 8 CH2OH CHO Na	1287.526	157
	PVAc 8 CH3 CHO K	1287.505	140
	PVAc 8 C2H5 OCH3 Na	**1287.562**	**185**
1373.247	PVAc 9 CH3 C2H5 K	1373.578	241
	PVAc 9 CH2OH CHO Na	1373.563	230
	PVAc 9 CH3 CHO K	1373.542	214
	PVAc 9 C2H5 OCH3 Na	**1373.599**	**256**
1459.262	PVAc 10 CH3 C2H5 K	1459.615	242
	PVAc 10 CH2OH CHO Na	1459.599	231
	PVAc 10 CH3 CHO K	1459.578	217
	PVAc 10 C2H5 OCH3 Na	**1459.636**	**256**
1545.256	PVAc 11 CH3 C2H5 K	1545.652	256
	PVAc 11 CH2OH CHO Na	1545.636	246
	PVAc 11 CH3 CHO K	1545.615	232
	PVAc 11 C2H5 OCH3 Na	**1545.673**	**269**
1631.273	PVAc 12 CH3 C2H5 K	1631.688	255
	PVAc 12 CH2OH CHO Na	1631.673	245
	PVAc 12 CH3 CHO K	1631.652	232
	PVAc 12 C2H5 OCH3 Na	**1631.709**	**267**
1717.262	PVAc 19 CH3 C2H5 K	1717.725	270
	PVAc 19 CH2OH CHO Na	1717.710	261
	PVAc 19 CH3 CHO K	1717.689	248
	PVAc 19 C2H5 OCH3 Na	**1717.746**	**282**
1803.288	PVAc 20 CH3 C2H5 K	1803.762	263
	PVAc 20 CH2OH CHO Na	1803.746	254
	PVAc 20 CH3 CHO K	1803.726	243
	PVAc 20 C2H5 OCH3 Na	**1803.783**	**274**
1889.290	PVAc 21 CH3 C2H5 K	1889.799	269
	PVAc 21 CH2OH CHO Na	1889.783	261
	PVAc 21 CH3 CHO K	1889.762	250
	PVAc 21 C2H5 OCH3 Na	**1889.820**	**280**

Table 3.3 Compositional analyses of selected PVAc oligomers obtained with MALDI-FTMS using optimized sample preparation protocol (ethyl acetate as a solvent, volume ratio matrix-analyte 7:2)

Experimental mass	Compositional assignment	Theoretical mass	ppm error
1115.495	PVAc 6 CH3 C2H5 K	1115.468	-24
	PVAc 6 CH2OH CHO Na	1115.452	-38
	PVAc 6 CH3 CHO K	1115.431	-57
	PVAc 6 C2H5 OCH3 Na	**1115.489**	**-5**
1201.535	PVAc 7 CH3 C2H5 K	1201.504	-25
	PVAc 7 CH2OH CHO Na	1201.489	-38
	PVAc 7 CH3 CHO K	1201.468	-56
	PVAc 7 C2H5 OCH3 Na	**1201.525**	**-8**
1287.569	PVAc 8 CH3 C2H5 K	1287.541	-22
	PVAc 8 CH2OH CHO Na	1287.526	-34
	PVAc 8 CH3 CHO K	1287.505	-50
	PVAc 8 C2H5 OCH3 Na	**1287.562**	**-5**
1373.606	PVAc 9 CH3 C2H5 K	1373.578	-20
	PVAc 9 CH2OH CHO Na	1373.563	-32
	PVAc 9 CH3 CHO K	1373.542	-47
	PVAc 9 C2H5 OCH3 Na	**1373.599**	**-5**
1459.644	PVAc 10 CH3 C2H5 K	1459.615	-20
	PVAc 10 CH2OH CHO Na	1459.599	-31
	PVAc 10 CH3 CHO K	1459.578	-45
	PVAc 10 C2H5 OCH3 Na	**1459.636**	**-6**
1545.685	PVAc 11 CH3 C2H5 K	1545.652	-22
	PVAc 11 CH2OH CHO Na	1545.636	-32
	PVAc 11 CH3 CHO K	1545.615	-45
	PVAc 11 C2H5 OCH3 Na	**1545.673**	**-8**
1631.718	PVAc 12 CH3 C2H5 K	1631.688	-18
	PVAc 12 CH2OH CHO Na	1631.673	-28
	PVAc 12 CH3 CHO K	1631.652	-40
	PVAc 12 C2H5 OCH3 Na	**1631.709**	**-5**
1717.763	PVAc 19 CH3 C2H5 K	1717.725	-22
	PVAc 19 CH2OH CHO Na	1717.710	-31
	PVAc 19 CH3 CHO K	1717.689	-43
	PVAc 19 C2H5 OCH3 Na	**1717.746**	**-8**
1803.788	PVAc 20 CH3 C2H5 K	1803.762	-14
	PVAc 20 CH2OH CHO Na	1803.746	-23
	PVAc 20 CH3 CHO K	1803.726	-35
	PVAc 20 C2H5 OCH3 Na	**1803.783**	**-3**

Table 3.4 Compositional analyses of selected PVAc oligomers obtained with MALDI-TOF from the chewing gum sample using optimized sample preparation protocol (ethyl acetate as a solvent, volume ratio matrix-analyte 2:7, 2.5M DHB as a matrix)

Experimental mass	Compositional assignment	Theoretical mass	ppm error
1012.821	PVAc 11 C2H5 CH2 Na	1012.449	-367
1098.691	PVAc 12 C2H5 CH2 Na	1098.486	-187
1184.599	PVAc 13 C2H5 CH2 Na	1184.523	-64
1270.465	PVAc 14 C2H5 CH2 Na	1270.559	74
1356.268	PVAc 15 C2H5 CH2 Na	1356.596	242
1442.069	PVAc 16 C2H5 CH2 Na	1442.633	391

IV. MALDI MASS SPECTROMETRY ANALYSIS OF [6,6]-PHENYL-C61-BUTYRIC ACID METHYL ESTER (PCBM)

A. *Introduction*

Photovoltaic cells (PVCs) or solar cells are one of the most attractive ways to use solar energy, an inexhaustible renewable clean energy. Organic photovoltaic technology, as a potential competitor to silicon-based PVCs, has undergone gradual progress with power conversion efficiency (PCE) over 6%[103, 104]. The key innovation in the development of organic photovoltaic cells (OPC) was the introduction of an interface between two organic semiconductors, called the donor and the acceptor[105]. The organic semiconductor donor materials based on π-conjugated systems have a lower HOMO (highest occupied molecular orbital) and LUMO (lowest unoccupied molecular orbital) compared with the acceptor. Therefore, the donor is the hole transporting material and makes ohmic contact with the anode, while the acceptor material transports electrons and contacts the cathode. In a typical polymeric PVC, the photoactive blend layer is sandwiched between an indium tin oxide (ITO) positive electrode and a metal negative electrode, and is usually composed of a low band gap conjugated polymer donor and a soluble nanosized acceptor.[106-108] Fullerene and especially its soluble derivatives such as [6,6]-phenyl-C61-butyric acid methyl ester (PCBM) have been a key components for the development of bulk heterojunction (BHJ) solar cells and are widely used acceptors.[109, 110] Besides having a LUMO level which allows efficient photoinduced charge transfer from the donor, the spherical geometry of C_{60} leads to isotropic electron transport through a 3D percolation system, which seems “particularly appropriate for charge transport in disordered media”[111]. Physical properties and thus the efficiency of the OPCs depend on the variations of the chemical composition of their active layers. Accordingly, accurate information about their composition is of critical importance, motivating development of fast, simple, reliable, sensitive, and accurate analysis methods.

Matrix-assisted laser desorption/ionization (MALDI) is a soft ionization technique which allows for the sensitive detection of large, non-volatile, and labile molecules by mass spectrometry[9, 112]. The MALDI technique is based upon co-crystallizing the analyte with a compound called a matrix, which strongly absorbs laser radiation. Laser excitation of the matrix molecules results in the ejection of the irradiated material and the formation of a gas phase plume. The molecules of analyte are transported into the plume

as it expands into the vacuum and then, after undergoing primary and secondary ionization reactions involving the matrix and analyte, the desorbed species are detected in the form of ions [15].

Since its introduction in the late 80's[1, 2], MALDI has become a powerful analytical tool for the investigation of important properties of various classes of organic compounds including industrial polymer materials[3, 4]. The key aspects of the typical MALDI experiment are the generation of intact singly charged ions and an absence of fragmentation, which simplifies the analysis of complex multi-component samples. Other characteristics of MALDI that are important for analysis of chemically and physically heterogeneous samples are the exceptionally high sensitivity of this method (with modern instrumentation the attomole level is achievable)[9].

The choice of proper sample preparation conditions plays a crucial role in the success of any MALDI analysis. A significant drawback of this method is that the choice of the proper sample preparation protocol depends on the chemical nature of the analyte. The variations in methods being used for actual sample preparation include the choice of the solvents employed, choice of cationizing agents, matrix-to-analyte ratios, and deposition techniques. A general recommendation for the choice of the matrix for the successful analysis of heavy organic molecules (such as polymers) is to match the polarity of the molecule under the investigation and the polarity of the matrix[10, 27]. As for the choice of the solvent, when a fast drying solvent is employed, the segregation of matrix and analyte is lower, thus improving the homogeneity of the co-crystallized sample. Several sample deposition methods have been developed over the years, including the slow crystallization dried droplet method, and fast crystallization methods such as aerospray and electrospray which offer improved spot-to-spot and shot-to-shot reproducibility and better ion signals.[10, 45, 46] However, despite these developments the success of the analysis often depends on an empirical approach used to find an optimal matrix, solvent and matrix-to-analyte ratio.

It has been demonstrated by numerous researchers that the choice of matrix heavily influences the outcome of MALDI-analysis of fullerene derivatives in both positive and negative modes.[113-122] Several investigations concerning matrix performance comparisons, as applied to analysis of fullerene derivatives were conducted [113, 114, 116, 117] and show that some matrices consistently provided better quality spectra (low or no fragmentation, high intensity of the analyte signal, lower laser power threshold) compared with the others. These electron transfer matrices include dithranol, *trans*-4-tert-butyl-4'-nitrostilbene (TBNS), 9-

nitroanthracene and especially 2-[(2E)-3-(4-tert-butylphenyl)-2-methylprop-2-enylidene]malononitrile (DCTB). The reason for such distinctive differences in matrix performance is attributed to the fact that ionization of fullerene derivatives occurs predominantly due the electron transfer reactions between matrix and analyte, producing radical molecular ions $[M]^{\bullet+}$ (or $[M]^{\bullet-}$). This occurs rather than protonation or cation attachment, as is often observed for other compounds.

In this chapter, a sample preparation protocol for the successful MALDI analysis of PCBM was developed by investigating the influence of the matrix, solvent, deposition method and matrix-to-analyte ratio. Gas-phase reactions of PCBM in the high vacuum conditions of the FTMS and TOF mass spectrometry experiments were investigated and a possible mechanism for these reactions was proposed.

B. *Experimental*

1. **Materials**

The sample of [6,6]-phenyl-C61-butyric acid methyl ester (PBCM) was purchased from Nano-C and was analyzed as received. The matrix compounds 2,5-dihydroxybezoic acid, 9-nitroanthracene and dithranol (2,5-DHB, 9-NA, DH), as well as the solvents (toluene, o-dichlorobenzene, glacial acetic acid), trifluoroacetic acid (TFA) and the calibrants polyethylene glycol (PEG) with molecular weights of ~600 Da, and a standard mixture of peptides including angiotensin I, angiotensin II and substance P were purchased from Aldrich and used without further purification. Chemical structures of PCBM and the matrices used are given in Scheme 4.1.

2. **Instrumentation and analysis**

Time-of-flight experiments were carried out using a Bruker Ultraflex TOF/TOF mass spectrometer employing a Nd:YAG laser operating at l = 355 nm. Experiments were performed in reflectron mode using a delayed extraction pulse in the source region with a 20 kV acceleration voltage. The average base pressure during analysis was ~ $5*10^{-8}$ torr. The spectra obtained were calibrated externally with PEG 600 Da. All spectra resulted from averaging of 300 laser shots.

FTMS experiments were performed using the Bruker APEX Qe 9.4T FTMS (Bruker Daltonics, Billerica, MA) with a dual external ionization ESI and MALDI source. The mass spectrometer is equipped with Nd:YAG laser operating at l = 355 nm. Experiments were conducted in positive ion mode with ions

being generated in the external ionization source, transferred into cylindrical ion cyclotron resonance (ICR) cell by a hexapole ion guide, trapped, excited and then detected. Each spectrum was obtained as a sum of 5 scans 10 laser shots each. Laser power was set up for each experiment just above the threshold of the analyte signal for consistency of the analysis and to avoid fragmentation of PCBM. External calibration of the spectra was performed using a peptide mixture as a calibrant. Three spectra were collected for each matrix:analyte ratio from three different spots on the target plate in order to check spot-to-spot reproducibility of the experiments. After the spectra were collected, Data Analysis® software was used to subtract the baseline and perform the calibration.

3. **Sample preparation**

For the analysis of PCBM, optimization of ionization conditions was performed by using several different sample preparation protocols and by changing important variables, such as matrix-to-analyte ratios, matrices, solvents, and sample deposition techniques. To start, the procedure developed by Hummelen et al.[109] was reproduced as follows. PCBM solutions (0.02 mM) were prepared in two different solvent systems: toluene mixed with glacial acetic acid (3:4 by volume) and o-dichlorobenzene mixed with glacial acetic acid (1:1 by volume). A matrix solution consisting of 50 mM 2,5-DHB and 0.1% TFA in methanol was added to sample solutions to achieve a matrix/analyte ratio of 5000:1. Approximately 2 ml of this mixture was spotted onto a steel target plate and allowed to dry. Samples prepared using this protocol were analyzed using both Bruker APEX Qe 9.4T FTMS and Bruker Ultraflex TOF/TOF mass spectrometers.

In addition, another sample preparation protocol was used. The matrices 9-nitroanthracene and dithranol were used in combination with pure chlorobenzene or toluene to achieve several different molar matrix-to-analyte ratios. Molar matrix-to-analyte ratios of 5000:1, 2000:1, 1000:1, 750:1, 500:1, and 250:1 were prepared in toluene for both matrices. Further, molar matrix-to-analyte ratios of 5000:1, 2000:1, 1000:1, and 500:1 were prepared in chlorobenzene for both matrices. The prepared samples were then applied to a stainless steel target plate by a dry droplet technique. The 1000:1, 750:1, 500:1, and 250:1 molar matrix-to-analyte ratios composed in toluene for both matrices were applied using the aerospray technique. The dry droplet technique consisted of using approximately 2 ml of each sample and applying it to the stainless steel target plate followed by air-drying. The aerospray technique consisted of aerosol

particles being ejected from the end of a needle after being conveyed from the sample container by a controlled flow of nitrogen, each application consisting approximately of 50-75 µl of the sample. Samples prepared using this protocol with matrix-to-analyte ratios of 5000:1 and 1000:1 were analyzed using both Bruker APEX Qe 9.4T FTMS and Bruker Ultraflex TOF/TOF mass spectrometers. However, the remaining samples were analyzed only by FTMS.

For LDI analysis, ~2 µl of PCBM sample in corresponding solvent was applied to the stainless steel target plate and allowed to air dry.

C. *Results and Discussion*

1. **Sample preparation optimization – preliminary investigation**

Following the procedure developed by Hummelen et al.[109] described above, samples were prepared, and mass spectra of PCBM were collected. MALDI analysis of toluene-based solvent systems resulted in significant yields of PCBM molecular ion along with highly abundant fullerene C_{60} molecular ions. The spectrum of the PCBM sample obtained with TOF mass spectrometer is shown in Fig. 4.1. Along with fullerene signal and the products of gas phase reactions ($C_{46}H_2O$ and $C_{69}H_{36}O$), hydrogenated PCBM species with up to two hydrogens attached were observed in the spectrum (see inset on the Fig. 1). It should be noted that the molecular ions formed by fullerene and PCBM species are radical cations rather then protonated ions, which is consistent with literature reports.[117, 123]

FTMS analysis of the same sample resulted in a significantly different spectrum with large number of fragment ions as it can be seen in Fig. 4.2. Products of gas phase reactions of the parent molecule or fullerene were also observed. The intensity of the signal corresponding to PCBM was very low and so was the intensity of fullerene signal, which could be the result of excessive fragmentation. The noticeable variation between spectra collected with FTMS and TOF detection methods could be attributed to the much longer residence time in FTMS (milliseconds in FTMS versus microseconds in TOF), thus resulting in a higher probability of gas phase reactions occurring in the FT-ICR cell.

LDI analysis for both FTMS and TOF showed fullerene C_{60} as the most abundant molecular ion (spectra not shown). Very low intensity peaks corresponding to PCBM and few fragment ions were also observed. It can therefore be concluded that the LDI ionization method is not suitable for the analysis of

PCBM because it leads to the dissociation of the molecule resulting in the formation of fullerene C_{60} and various fragments.

Different results were obtained following the same sample preparation protocol but with the o-dichlorobenzene-based solvent system. Both MALDI-FTMS and MALDI-TOF produced spectra dominated by fragment ions and peaks corresponding to products of hydrogenation reactions of fullerene (e.g. 663.5, 685.4, 701.4 m/z) as it can be seen in Fig. 4.3 and 4.4. Fullerene and PCBM molecular ions were observed at very low abundances, which could be explained by excessive gas phase reactions, and abundant fragmentation products that were observed in the spectra.

LDI-FTMS spectra showed fullerene C_{60} as the most abundant peak with several products of its gas phase reactions (results are not shown). This observation is similar to MALDI-FTMS and MALDI-TOF spectra obtained with the toluene-based solvent system. On the other hand, LDI-TOF spectra demonstrated only a few low intensity peaks corresponding to fragment ions. The most abundant peak observed was also fullerene. In both cases of LDI analysis, no PCBM ions were detected. These results confirm the previous conclusion that the direct LDI ionization method is not suitable for the analysis of PCBM due to the complete fragmentation of this fragile molecule resulting in the formation of fullerene C_{60} and various products of gas phase reactions.

2. **New sample preparation protocol development: analysis with TOF mass spectrometry**

The outcome of the preliminary work described above was found unsatisfactory because the intensity of the ion of interest (PCBM) was comparatively low and fragments, namely fullerene C_{60} and products of gas phase reactions, dominated spectra. Therefore, in order to improve the quality of MALDI analysis of PCBM, the experiments with electron transfer matrices were repeated. It was hoped that this protocol would increase the yield of analyte molecular ion and reduce the unwanted fragmentation.

The results were compared with those obtained using DHB as a matrix. Other alterations of the sample preparation protocol included: 1) the use of the same solvent for both matrix and PCBM to avoid unwanted effects of phase separation during crystallization process; 2) elimination of glacial acetic acid from the solvents because of the high acidity of the medium. Therefore, the significant excess of protons might be responsible for formation of hydrogenated fullerene derivatives observed in the spectra; 3)

investigation of lower molar matrix-to-analyte ratios, since the general consensus is that low molecular weight molecules do not require a relatively large amount of matrix.

MALDI-TOF analysis was performed for the samples prepared with both 9-nitroanthracene and dithranol with matrix-to-analyte ratios 5000:1 and 1000:1. As a consequence, it was demonstrated that 9-nitroanthracene was much more efficient as a matrix for PCBM analysis when TOF was used as mass analyzer. When dithranol was used as a matrix, the spectrum is shown in Fig. 4.5 for the matrix-to-analyte ratio 5000:1. In can be observed that the features of the spectrum were similar to those obtained with DHB. The spectrum was dominated by the fullerene C_{60} molecular ion and hydrogenated fragments; the intact PCBM signal was not detected. However, when 9-nitroanthracene was used as a matrix, the appearance of the spectra was very different. Unlike spectra obtained with all other sample preparation protocols, the signal with highest intensity belong to PCBM. In addition, the presence of oxidized species with addition of up to 11 oxygen atoms was detected. The influence of matrix-to-analyte ratio investigation revealed that in the case of the dithranol a higher amount of sample (molar matrix-to-analyte ratio 1000:1) did not yield any PCBM or fullerene signals. However, when 9-nitroanthracene was used as a matrix, a higher amount of sample produced a spectrum (shown in Fig. 4.6) with PCBM signal intensity almost twice as high as the spectrum obtained with matrix-to-analyte ratio of 5000:1, although the intensity of fragment peaks stayed about the same. The feature of the spectra common with the ones obtained with sample preparation protocol involving DHB as a matrix was the presence of various products of gas phase reactions; however the abundance of these species was significantly lower than when DHB was used as a matrix, which can be attributed to the elimination of the source of protons (glacial acetic acid) from the solvent.

3. **Further sample preparation optimization and FTMS analysis**

The optimization of ionization conditions was continued with the help of the FTMS mass analyzer: several matrix-to-analyte ratios, two different solvents (chlorobenzene and toluene), two matrices (9-nitroanthracene and dithranol), and two deposition methods (dry droplet and aerospray) were investigated. The preliminary analysis using molar matrix-to-analyte ratios of 5000:1, 2000:1 and 1000:1 demonstrated that toluene was a better solvent for MALDI when compared to chlorobenzene as it resulted in an order of magnitude higher PCBM signal intensity. Therefore, further analysis was

conducted using only toluene as the solvent. As for the matrix comparisons, preliminary results showed that dithranol gave an order of magnitude higher PCBM signal intensity when compared with 9-nitroanthracne, which is inconsistent with previous findings performed with TOF mass analyzer. The influence of matrix: analyte ratio investigation however, revealed the same trend as it was observed with TOF analysis – the lowest ratio of 1000:1 produced the highest intensity of PCBM signal.

It was reasoned that lower matrix: analyte ratios might produce even better spectra and so ratios of 750:1, 500:1, and 250:1 were also examined. As expected, the use of the lowest matrix-to-analyte ratio of 250:1 produced spectra with the best PCBM signal yield for both matrices, regardless of sample deposition technique. The comparison between aerospray and dried droplet sample deposition techniques revealed the aerospray method to produce superior results with respect to signal-to-noise ratio and spot-to-spot reproducibility when compared to the dry droplet technique for all investigated matrix-to-analyte ratios with both matrices. The application of dithranol as a matrix at a molar matrix-to-analyte ratio of 250:1 with the use of aerospray deposition technique resulted in the best spectra (demonstrated in Fig. 4.7 and 4.8). The signal with highest intensity was assigned to PCBM, and only a few other fragment species with low intensities were observed in the spectra.

The unmatched resolution obtained with FTMS mass analyzer (the resolution of ~140,000 was achieved with FTMS opposed to ~5000 obtained with TOF mass spectrometer for PCBM samples) allowed resolving the fine structure of the spectra and detection of several types of oxidized and reduced species. In Fig. 4.8, the portion of the spectrum behind the PCBM peak is demonstrated with the assignments of the species. It can be seen that during or after desorption/ionization step of MALDI process, several kinds of PCBM derivatives are formed presumably due to the gas phase reactions. Hydrogenated species with up to four hydrogen atoms attached to the PCBM were detected (see the inset in the Fig. 4.8, the positions of peaks belonging to hydrogenated species are circled in red). These species has molecular weights isobaric to peaks, which are a part of the isotopic distribution of PCBM and would be impossible to detect unless the mass spectrometer has high enough resolving power.

Two different types of oxidized species were detected as well. There were scarce quantities of species with up to five oxygen atoms added and much more abundant species with one hydrogen atom and various numbers of oxygen atoms added. It is suggested that because of much higher abundance of

the latter, they could be products of either reactions of hydrogenated species $[PCBM+H]^{\bullet+}$ with various numbers of oxygen atoms or of addition of one hydrogen atom to oxidized species $[PCBM+nO]^{\bullet+}$. It was suggested in the previous report that the transfer of oxygen from the matrix to the analyte can easily occur under MALDI conditions. A possible mechanism of formation of all these species is presented in Scheme 4.2.

The quality of spectra when 9-nitroanthracene was used as a matrix was significantly improved when the sample was applied using the aerospray technique. However, the signal intensity and signal to noise ratio were an order of magnitude less than those obtained by with dithranol. Otherwise, the features of the spectra were essentially the same as the ones obtained with dithranol. The best spectrum obtained with this matrix is shown in Fig. 4.9.

A composite summary of absolute peak intensity of PCBM at various molar matrix-to-analyte ratios obtained with both matrices and with two deposition techniques is presented in Fig. 4.10. It can be clearly seen that the use of dithranol as a matrix with the aerospray sample deposition technique produces significantly improved results with respect to the PCBM signal intensity. It can also be concluded that the use of lower matrix-to-analyte ratios also produces superior quality spectra with the use of both matrices and sample deposition methods. The significant deviations in standard deviations (the data presented on the Fig. 4.10 are the average of three measurements) are intrinsic for laser ionization mass spectrometry methods and are attributed to several factors. These are inconsistent fluctuations in laser power and \the inequality of sample deposition on the target plate. The second factor is greatly reduced by the application of aerospray or electrospray deposition techniques. These methods result in much more even surface of the sample and more homogeneous analyte distribution.

D. *Conclusions*

The analysis of pristine PCBM was performed with the use of laser ionization techniques such as MALDI, LDI-TOF and FTMS. Extensive optimization of ionization conditions was performed for the analysis of PCBM and a new sample preparation protocol was developed. The influence of several important parameters was investigated – choice of the matrix, molar matrix:analyte ratio, solvent for both matrix and analyte and sample deposition technique. It was found that the application of lowest molar matrix:analyte ratio of 250:1, toluene as a solvent for both matrix and analyte and aerospray sample deposition technique for MALDI analysis produced spectra with the highest intensity of PCBM signal, the smallest amount of fragments, the fewest products of gas phase reactions and the best reproducibility. As for the choice of matrix, the results were inconsistent, since out of two electron-transfer matrices compared (9-nitroanthracene and dithranol), dithranol was found superior when the FTMS mass analyzer was employed, whereas 9-nitroanthracene gave higher PCBM signal with TOF mass spectrometer. Direct laser desorption/ionization (LDI) analysis was found unsuitable for the analysis of PCBM due to the complete fragmentation of this molecule under conditions of LDI and resulting in the formation of fullerene C_{60} and various products of gas-phase reactions. The extremely high resolving power achieved with FTMS mass spectrometer allowed detecting and identifying the species formed under MALDI experiment conditions. It was suggested that during or after desorption/ionization step of MALDI process, several kinds of oxidized and reduced PCBM derivatives are formed, presumably due to the gas phase reactions. Hydrogenated (reduced) species included derivatives with the loss of one hydrogen atom or with up to four hydrogen atoms added. Two different types of oxidized species were detected as well: species with up to five oxygen atoms added and much more abundant species with one hydrogen atom and various numbers of oxygen atoms added.

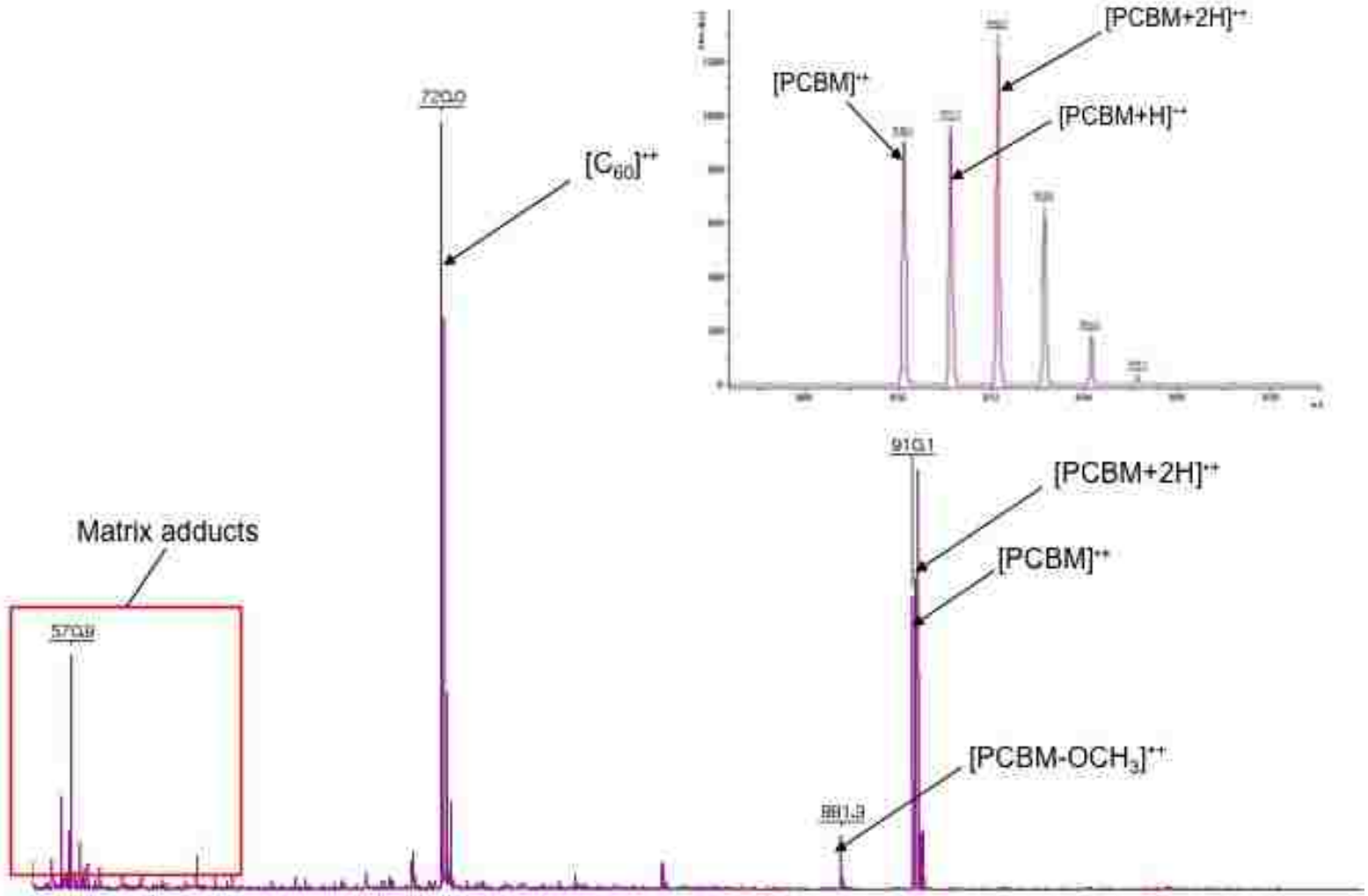

Figure 4.1 MALDI-TOF spectrum of PCBM (positive ion mode); toluene/glacial acetic acid (3:4 vol) as a solvent for the sample, 50 mM DHB/0.1% TFA in methanol as a matrix, molar ratio matrix:analyte is 5000:1

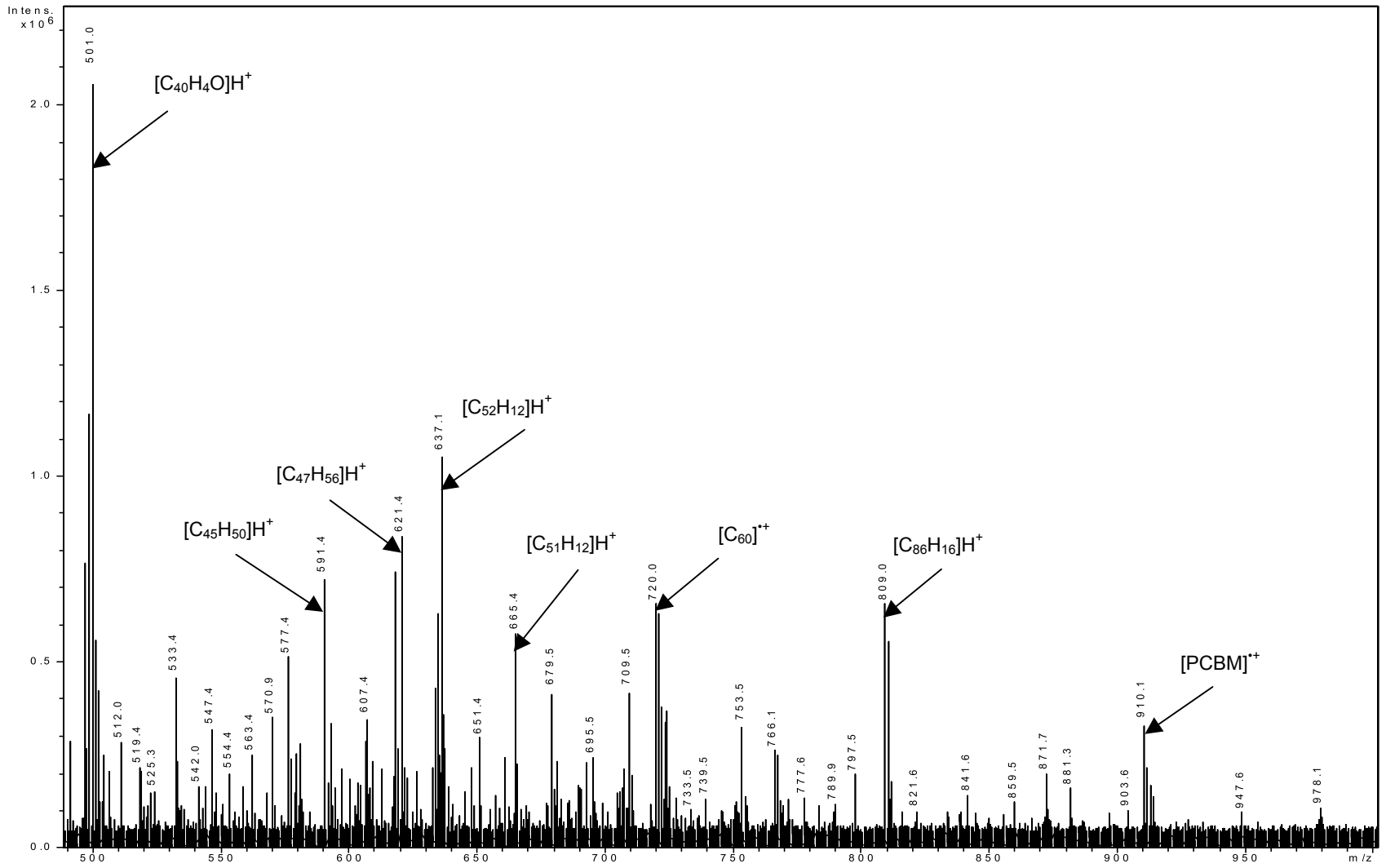

Figure 4.2 9.4T MALDI-FTMS spectrum of PCBM (positive ion mode); toluene/glacial acetic acid (3:4 vol) as a solvent for the sample, 50 mM DHB/0.1% TFA in methanol as a matrix, molar ratio matrix:analyte is 5000:1

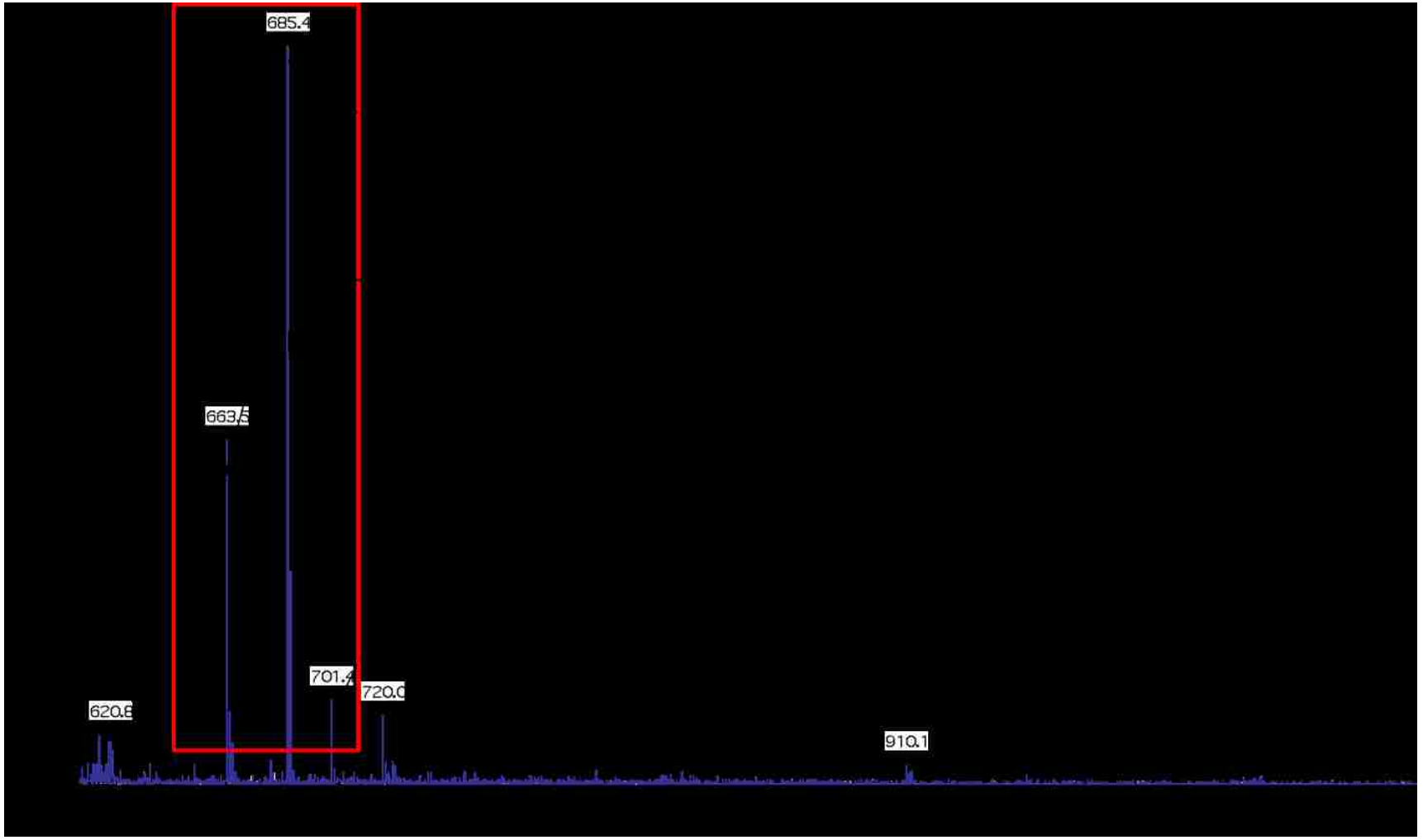

Figure 4.3 MALDI-TOF spectrum of PCBM (positive ion mode); o-dichlorobenzene/glacial acetic acid (1:1 vol) as a solvent for the sample, 50 mM DHB/0.1% TFA in methanol as a matrix, molar ratio matrix:analyte is 5000:1

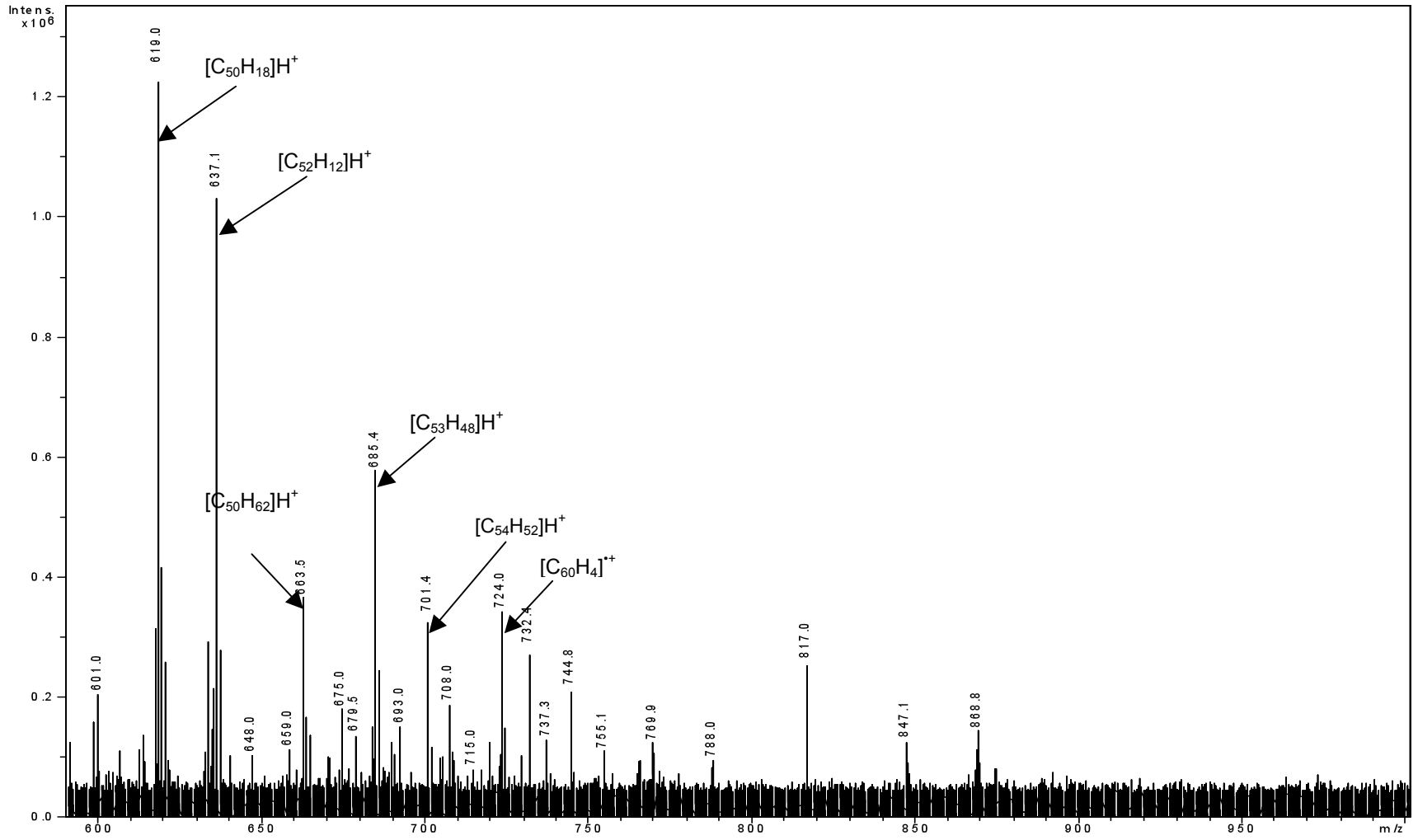

Figure 4.4 9.4T MALDI-FTMS spectrum of PCBM (positive ion mode); o-dichlorobenzene /glacial acetic acid (1:1 vol) as a solvent for the sample, 50 mM DHB/0.1 % TFA in methanol as a matrix, molar ratio matrix:analyte is 5000:1

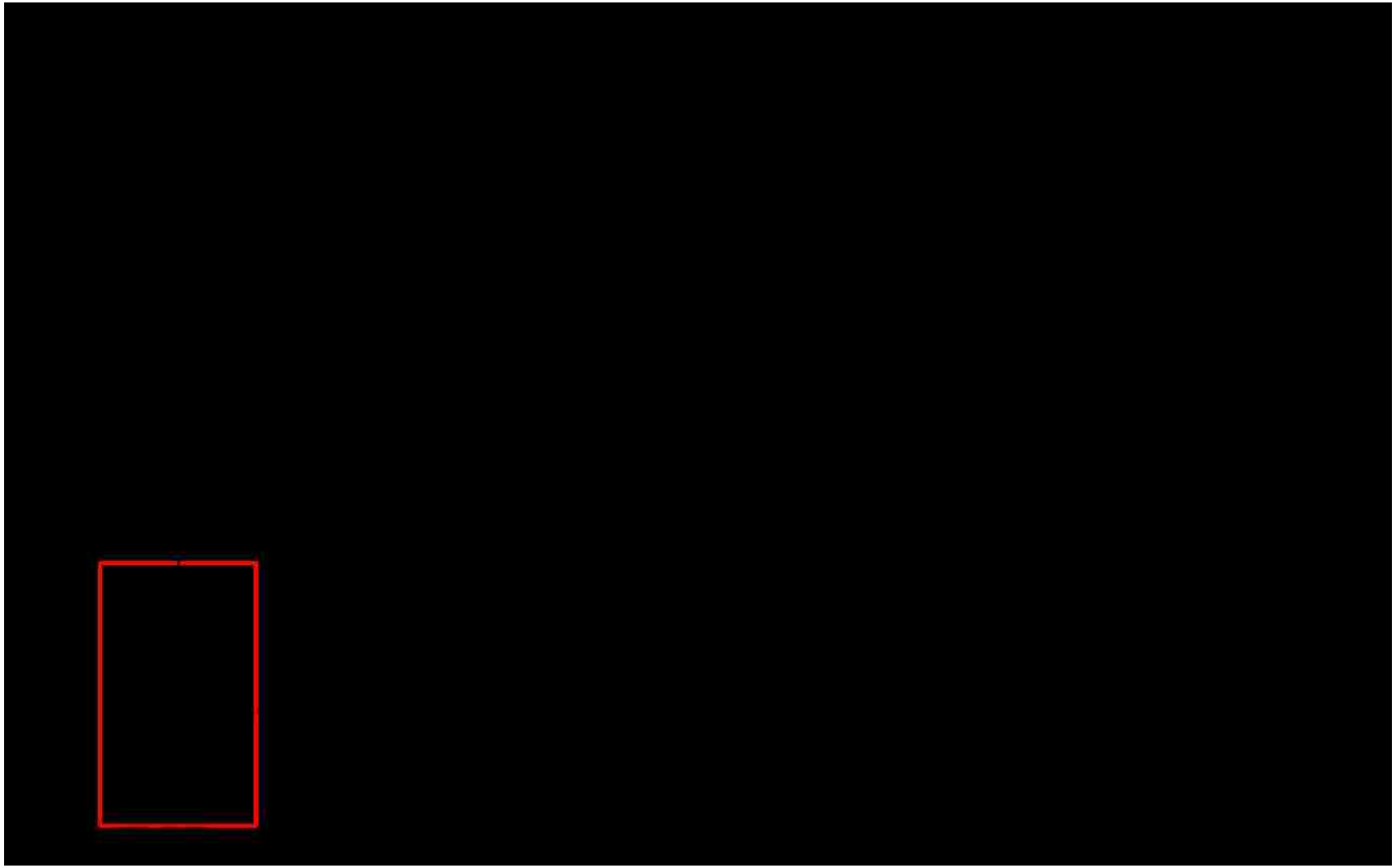

Figure 4.5 MALDI-TOF spectrum of PCBM (positive ion mode); toluene as a solvent, 50 mM dithranol as a matrix, molar ratio matrix-to-analyte is 5000:1

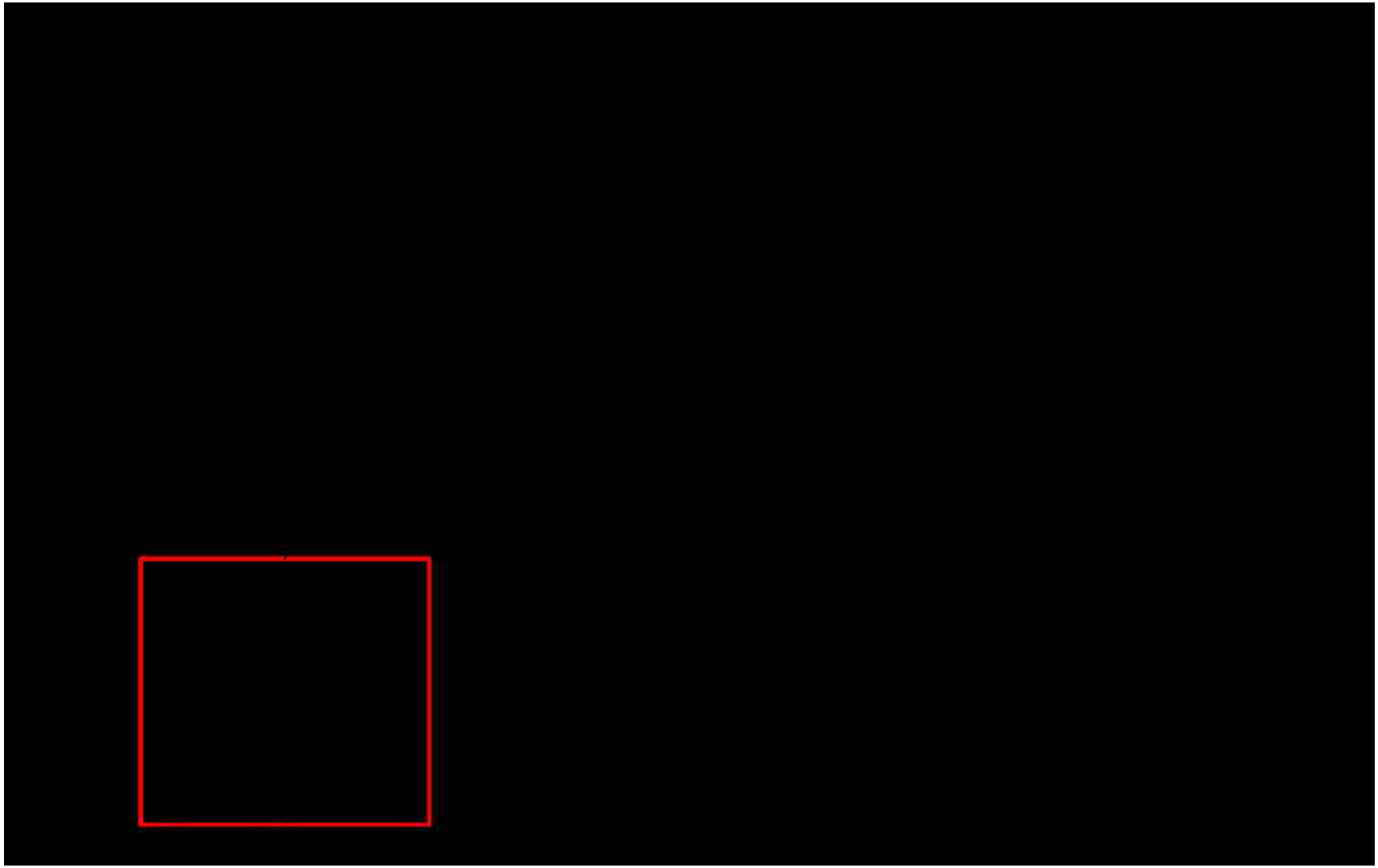

Figure 4.6 MALDI-TOF spectrum of PCBM (positive ion mode); toluene as a solvent, 50 mM 9-nitroanthracene as a matrix, molar ratio matrix:analyte was 1000:1

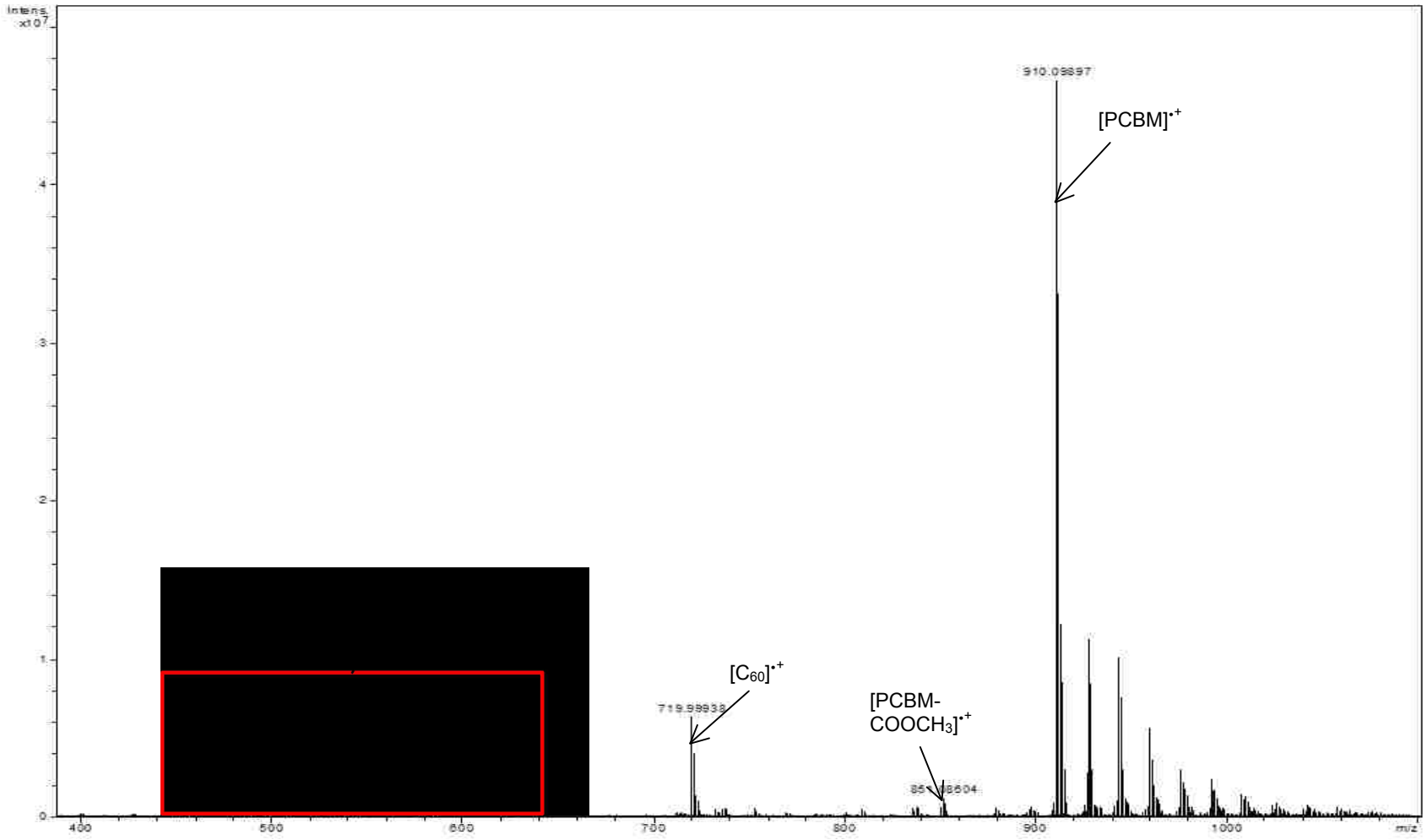

Figure 4.7 9.4T MALDI-FTMS spectrum of PCBM (positive ion mode); toluene as a solvent, 50 mM Dithranol as a matrix, molar ratio matrix-to-analyte was 250:1, aerospray deposition technique

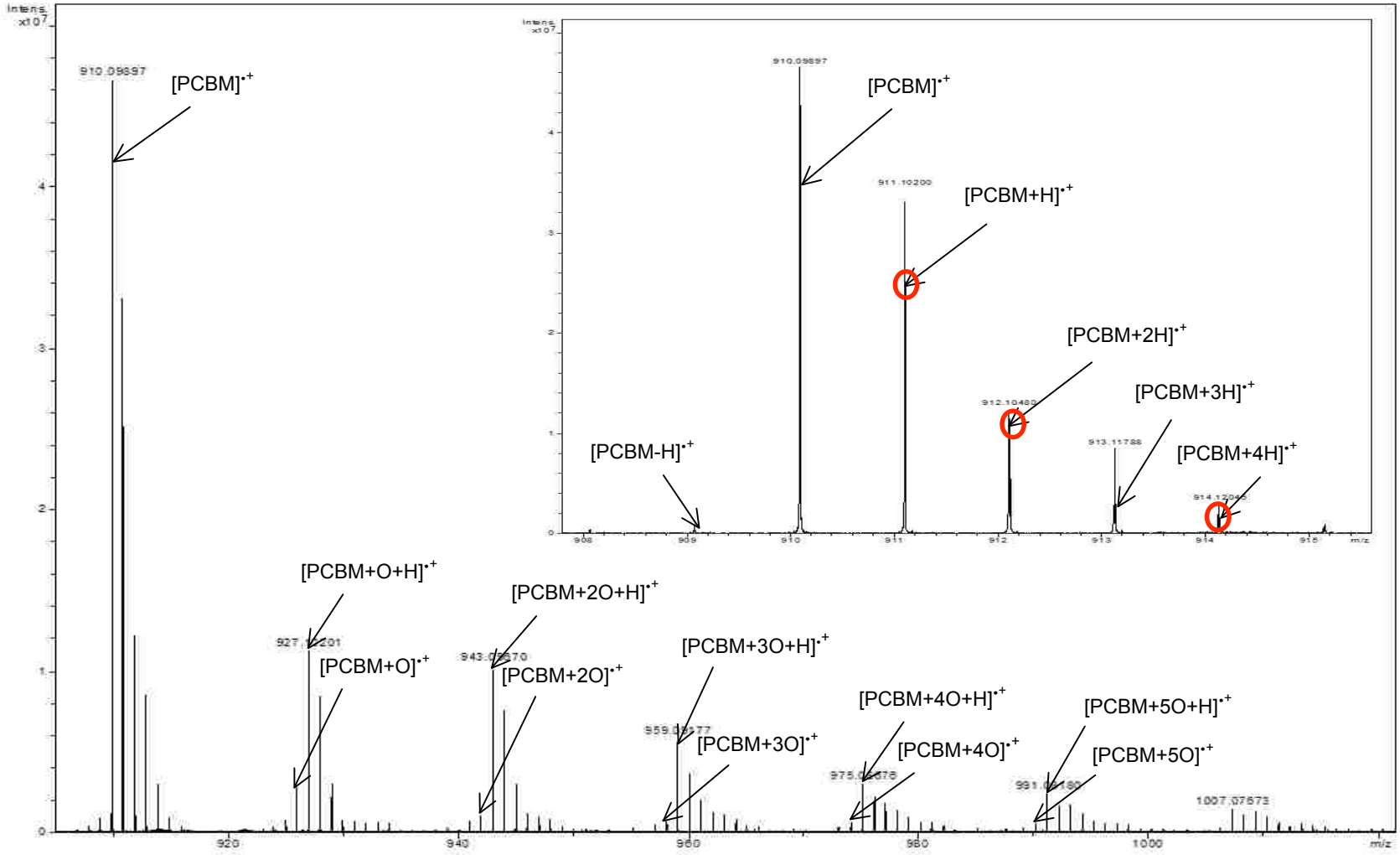

Figure 4.8 9.4T MALDI-FTMS spectrum of PCBM (positive ion mode) – enlarged portion of the spectrum behind PCBM peak; toluene as a solvent, 50 mM dithranol as a matrix, molar ratio matrix-to-analyte was 250:1, aerospray deposition technique

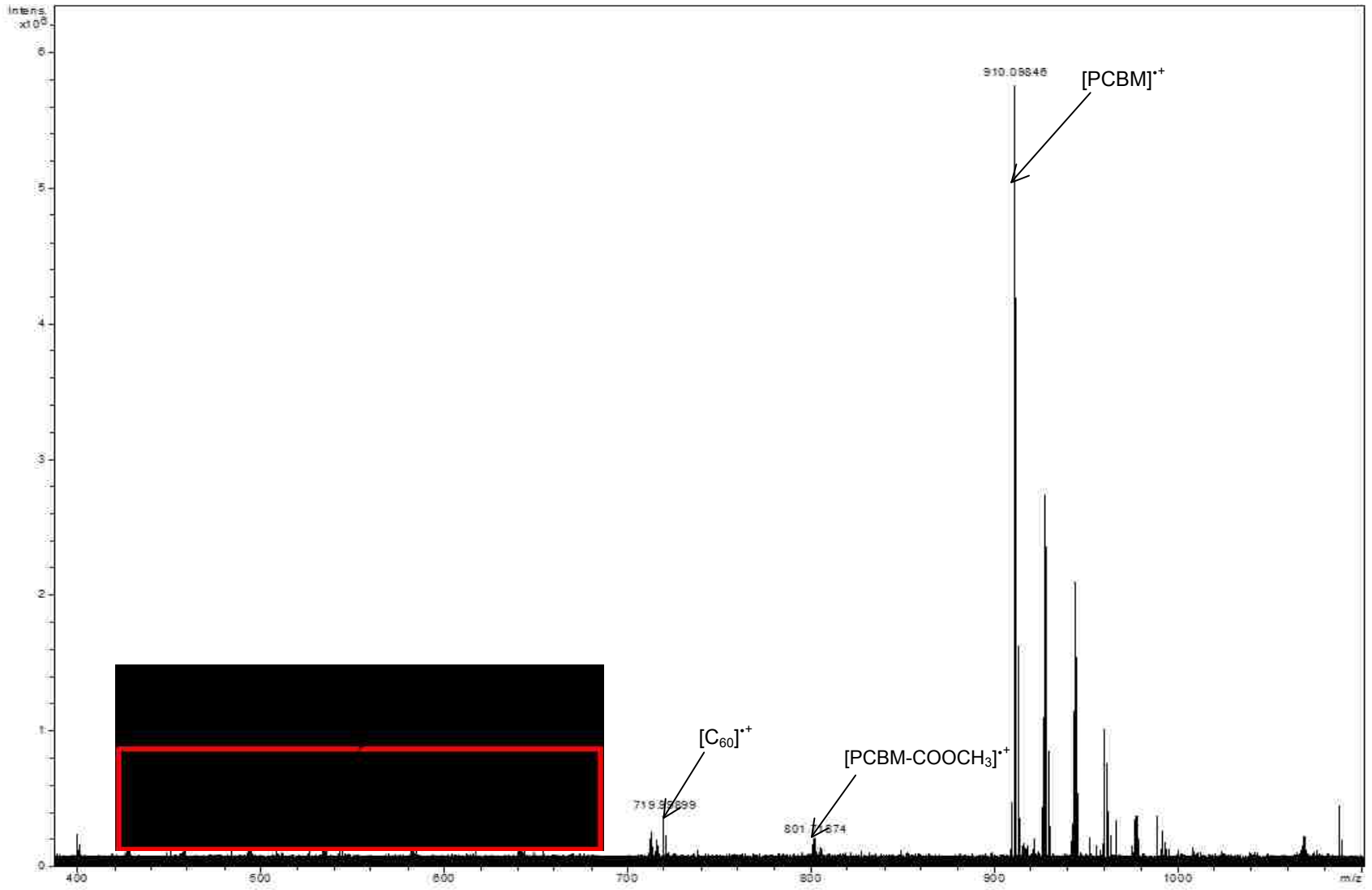

Figure 4.9 9.4T MALDI-FTMS spectrum of PCBM (positive ion mode); toluene as a solvent, 50 mM 9-nitroanthracene as a matrix, molar ratio matrix-to-analyte was 750:1, aerospray deposition technique

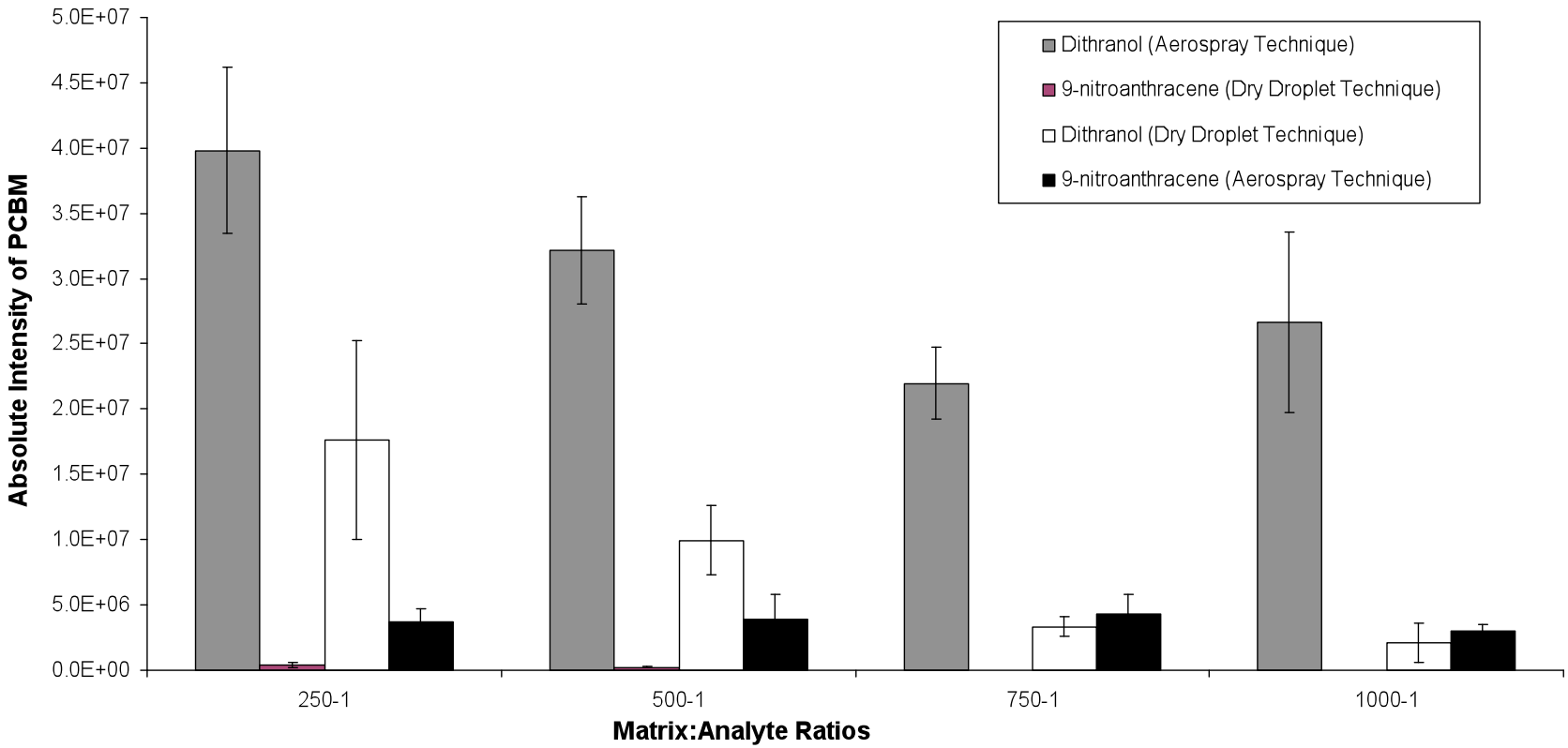

Figure 4.10 Composite summary of average absolute peak intensity of PCBM at various molar matrix-to-analyte ratios obtained with 9.4T MALDI-FTMS with dithranol and 9-nitroanthracene as matrices and toluene as a solvent. Dried droplet and aerospray methods were employed for sample deposition

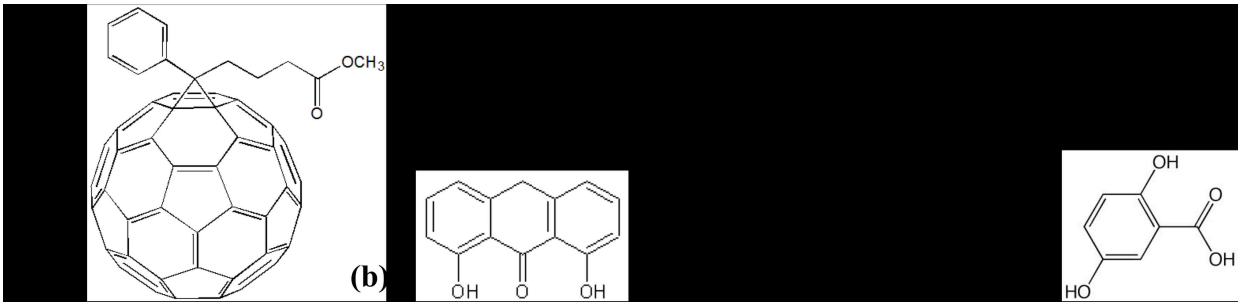

Scheme 4.1 Chemical structures of [6,6]-phenyl-C61-butyric acid methyl ester (PBCM) (a); Dithranol (DH) (b); 9-Nitroanthracene (9-NA) (c) and 2,5-Dihydroxybenzoic acid (2,5-DHB) (d)

Scheme 4.2 Proposed mechanism of formation of hydrogenated and oxydenated PCBM derivatives

V. STRUCTURAL CHARACTERIZATION OF FLUORINATED POLYSTYRENES BY MALDI MASS SPECTROMETRY

A. *Introduction*

Fluorinated polymers are a class of specialty polymers which aside from being morphologically very versatile (can be thermoplastic, elastomeric of totally crystalline) they possess many unique properties. They are properties are related to the high electronegativity of the fluorine atom and strong C-F bonds present in their molecular structures[124]. Such properties include[125-129] low surface energy and therefore great water and oil repelling qualities, exceptional chemical, thermal, aging and weather resistance, inertness to the corrosive mediums (acids, strong bases) and organic solvents, resistance to the photo-oxidation, low flammability, low dielectric constants and optical transparency. Because of these extraordinary characteristics, fluorinated polymers found their way into various branches of industry and are used for numerous functions[124, 125, 130]. Some examples include use as transmission fluids and lubricants for moving parts in automotive industry; as pipes liners resistant to the corrosive environments in petroleum industry; as antioxidants in paints and coating formulations; as elastomeric seals and O-rings capable to withstand extreme temperature conditions in aerospace applications; as non-linear optical materials in optics and microelectronics[127, 130-132].

Because many advantages of fluorinated polymers have been realized, the there have been attempts to develop rapid and reliable methods for their analysis. Among those are the application of techniques such as MALDI[133-141] and ESI[133, 142, 143] mass spectrometry. Matrix-assisted laser desorption/ionization (MALDI) is one of the soft ionization mass spectrometry techniques which was developed for the sensitive detection of large, non-volatile, and labile molecules [9, 112]. The MALDI technique is based on the co-crystallizing of analyte with a matrix compound, which strongly absorbs laser irradiation. Laser excitation of the matrix molecules results in the ejection of the irradiated material and the formation of a gas phase plume. The molecules of analyte are transported in the plume as it expands into the vacuum and then after primary and secondary ionization reaction involving the matrix and analyte, desorbed species are detected in the form of ions[15]. Because the key features of a typical MALDI experiment are the generation of intact, singly charged ions and an absence of fragmentation, since its introduction by Karas and co-workers[1] and by Tanaka et al.[2], MALDI has became a powerful

analytical tool for the investigation of important properties of industrial polymer materials. These properties include the identity of polymer chain repeat units, end groups[3, 4], absolute molecular weights, molecular weight distributions[5-8]. In addition, MALDI can reveal the presence and nature of any additives. Other characteristics of MALDI important for the analysis of chemically heterogeneous samples such as synthetic polymers, are the exceptionally high sensitivity of this method, With modern instrumentation the attomole level is achievable.,[9] This technique allows high speed of analysis, small sample size,and a large, potentially unlimited, mass range. However, as applied to the analysis of polymers, MALDI method has one significant drawback. Due to the diverse chemical nature of polymers, no standard sample preparation protocol or universal matrix has been developed. Therefore, the success of the analysis often depends on the empirical approach used to find the optimal matrix, solvent and matrix-to-analyte ratio. The choice of proper sample preparation conditions plays a crucial role in the success of any MALDI analysis. Over time, several attempts to rationalize the sample preparation protocols for the analysis of polymers have been made. The general recommendation for the choice of the matrix in polymers analysis is to match the polarity of the polymer under the investigation and the polarity of the matrix[10, 27]. It was demonstrated that when the polarity of the polymer matches that of the matrix, much better quality spectra were obtained with higher signal intensities due to the lower degree of segregation between the matrix and a polymer in the deposited samples. As for the choice of the solvent, when a fast drying solvent is employed, it was also demonstrated that segregation of matrix and analyte is lower thus improving the homogeneity of the sample. The choice of the cationizing agent is determined only by the nature of the polymer. The polymer should have high affinity with the chosen cation, because only then will cationization be efficient and the ion yield high. Several sample deposition methods have been developed over the years, including slow crystallization (the dried droplet method) and fast crystallization methods which offer improved spot-to-spot and shot-to-shot reproducibility and better ion signal, such as aerospray and electrospray deposition of the sample[10, 45, 46] All these important variables were studied by various research groups over the years except for one - matrix:analyte molar ratio. When it comes to this parameter, no rationalization on why to choose one ratio over another is usually offered despite the recognition of its importance. So far it have been only a few publications dedicated to the investigation of the influence of this parameter[144-146].

Fluorinated polymers are a challenging subject for mass spectrometry analysis and there have been very few successful MALDI studies reported, despite significant interest to these compounds. The reason for this lies in the chemical nature of this class of polymers. Their hydrophobicity leads to their poor solubility in most solvents, consequently complicating the sample preparation. It is also difficult for these compounds to form solid mixtures with commonly used MALDI matrices without significant segregation, thus making the ionization process inefficient and therefore producing low ion yields. A possible solution to this problem suggested by Marie et al.[140] was to use fluorinated derivatives of the common matrices. In their study, a sample of perfluoropolyether was analyzed using pentafluorocinnamic acid (PFCA) and pentafluorobenzoic acid (PFBA) since when the conventional matrices of a-Cyano-4-hydroxycinnamic acid (HCCA) and 2,5-dihydroxybenzoic acid (DHB) were used, no signal was obtained for the polymer. The choice of cationizing agent was also found to have profound influence on the outcome of the MADLI experiment. In these studies cations investigated were Na^+, Li^+, Fe^{2+}, Cu^{2+} and Ag^+. However, only when Ag^+ was present, were intense oligomer signals observed. In later years, other researchers applied the combination of PFCA with Ag^+ to the analysis of other types of fluorinated polymers: Ameduri et al[135] used this technique to characterize the vinylidene fluoride telomers and Kostjuk et al[134] successfully characterized perfluoropolyethers they synthesized by ring-opening polymerization of hexafluoropropylene oxide.

However, it must be noted that conventional MALDI matrices were also successfully applied to the analysis of fluorinated polymers. A dithranol and Na^+ combination was used by Wesdemiotis et al.[138] to characterize poly(fluorooxetane) and poly(fluorooxetane-co-THF) and Marie et al.[139] applied DHB to the analysis of one of the industrial fluorinated polymers. Latourte, et al.[133] performed MALDI sample preparation optimization for a model fluorinated compound by comparing various common and fluorinated matrices, such as DHB, dithranol, PFBA, 2,4-bis(trifluoromethyl)benzoic acid (TFMBA), HCCA and others and by varying composition and polarity of the solvent systems used. It was also discovered that the use of DHB produced spectra with the highest signal intensities for protonated oligomers of the model fluorinated phosphazine. The optimized sample preparation protocol which included DHB as a matrix was then successfully applied to the analysis of two industrial fluorinated polymers – poly(perfluorooctadecyl)acrylate and a poly(acrylic acid) polymer with a perfluorinated end group.

Therefore, in can be concluded that there is no consensus on the best sample preparation approach within the same class of fluorinated polymers. Thus, it would be prudent to perform a study of the sample preparation conditions, in order to properly characterize new polymer samples.

In this work, we explore the possibilities of method optimization for MALDI TOF-MS analysis of several poly(styrene-co-pentafluorostyrene) copolymers produced by the atom transfer radical polymerization (ATRP) technique. To the best of our knowledge this is the first attempt to optimize the analysis of STY-co-PFS copolymers synthesized via ATRP with MALDI mass spectrometry. In the first part of this investigation, sample preparation conditions were optimized for one out of three samples by investigating the influence of the matrix, polymer-to-salt and matrix-to-polymer ratios on the quality of the spectra. Optimized conditions were then applied to the other two samples, evaluating several important characteristics such as molecular weight distributions, end group identities and sequence distributions for all samples in order to determine how the change in the synthesis conditions affected these properties of the polymers.

B. *Experimental*

1. **Materials**

Matrix materials 2,3,4,5,6-Pentafluorocinnamic acid (PFCA), *all*-trans-Retinoic acid (RA) and Dithranol (DH) were obtained from Alfa Aesar, 2,5-dihydroxybenzoic acid (2,5-DHB), *trans*-2-[3-(4-tert-Butylphenyl)-2-methyl-2-propenylidene]malononitrile (DCTB) were purchased from Sigma Alrdich and 2,3,4,5,6-Pentafluorobenzoic acid (PFBA) was acquired from Tokyo Chemical Industry co. LTD. Silver trifluoroacetate (AgTFA) was used as a cationizing agent, HPLC grade THF was used as a solvent to prepare all solutions and both were obtained from Sigma Aldrich. Poly(ethylene glycol) (PEG) with molecular weight of ~ 4000 g/mol was used as a calibrant and purchased from Fluka (now Sigma Aldrich, St. Louis, MO). Three samples of poly(styrene-co-pentafluorostyrene) (STY-co-PFS) synthesized by atom transfer radical polymerization (ATRP) were received as a generous gift from Dr. Coleen Pugh of University of Akron, Ohio. All chemicals were used without further purification. Chemical structures of STY-co-PFS and matrices used are given in Scheme 5.1.

2. **Instrumentation and analysis**

MALDI mass spectra were acquired using a Bruker REFLEX III Time-of-Flight (TOF) mass spectrometer (Bruker Daltonics, Billerica, MA). The mass spectrometer was equipped with pulsed nitrogen laser (National Electronics, Inc. Miami, FL, USA) operating at 337 nm. Collected spectra represent the average of 1200 laser shots. All spectra were recorded in positive ion mode under delayed extraction conditions (250 ns) and in reflector mode. The accelerating voltage was 20 kV. The pressure in the TOF mass spectrometer was ~1x10^{-7} torr. External calibration of the spectra was performed using PEG 4000 as a calibrant. Three spectra were collected for each matrix:analyte:salt ratio from three different spots on the target plate in order to check spot-to-spot reproducibility of the experiments. After the spectra were collected, Bruker's Data Analysis® software was used to subtract the baseline, perform the calibration and smooth the spectrum. Contour maps of chemical composition of the copolymers were prepared with Origin® 8.5 software (OriginLab Corporation).

For the copolymer samples analyzed, number-average molecular weight (M_n), weight-average molecular weight (M_w) and polydispersity index (PDI) were calculated from obtained MALDI mass spectra using the following equations[64]:

$$M_n = \frac{\sum_{i=1}^{\infty} M_i N_i}{\sum_{i=1}^{\infty} N_i} \quad (1) \qquad M_w = \frac{\sum_{i=1}^{\infty} M_i^2 N_i}{\sum_{i=1}^{\infty} M_i N_i} \quad (2) \qquad PDI = \frac{M_n}{M_w} \quad (3)$$

where M_i is the molecular weight of the oligomer with i repeating units and N_i corresponds to the integrated area under the peak i.

3. **Sample preparation**

The solutions of all matrices were prepared at concentrations of 0.2M in THF and stored in the dark. Fresh solutions of AgTFA in THF were prepared at the concentration of 5 mg/ml before every analysis and kept wrapped while preparing samples to protect from decomposition induced by light. Copolymer solutions were also prepared fresh before the analysis in THF at the concentrations of 5 mg/ml. To perform the optimization study, one out of three copolymer samples was chosen. After the solutions of copolymer, matrices and salt were prepared, they were mixed to achieve chosen matrix:analyte:salt volume ratios. Several matrix:analyte ratios were investigated for each matrix while

keeping the amount of added AgTFA solution constant: 20:5:1; 40:5:1; 80:5:1; 100:5:1; 160:5:1; 320:5:1. Also, to reveal the influence of the amount of added salt to the signal intensity, three additional samples were prepared by adding various amounts of salt solution, while keeping matrix:analyte ratio the same: 40:5:0.2; 40:5:2; 40:5:5. Once mixed, approx. 2 ml of the combined solution was deposited onto a stainless steel target plate at three different spots and allowed to air-dry. The sample target plate was then submitted to MALDI experiments. After the best matrix:analyte:salt ratio was established, the procedure above was repeated with the rest of the samples.

C. *Results and Discussion*

1. **Sample preparation optimization for MALDI-TOF mass spectrometry analysis**

- *Choice of the matrix*

MALDI-mass spectrometry is a powerful soft ionization technique, which allows for ionization and subsequent detection of the intact molecules of high molecular weight and various chemical structures. However, the mechanism and processes that take place during MALDI are poorly understood and are still a topic of a debate. However, what is evident is that the choice of the proper matrix is extremely important to the success of the MALDI analysis since it is responsible for transfer of the absorbed laser energy to the analyte. It is also established that reactions which take place immediately after the ablation of the matrix-analyte mixture in the primary plume, and the kinetic energy of the desorbed molecules strongly depends on the chemical nature of the matrix[147] among other factors.

As is discussed above, there seems to be no consensus on which matrix should be used for the analysis of fluorinated polymers. It is possible that this is because this is a chemically diverse class of compounds. For example, a matrix suitable for fluorinated ethers will not work for fluorinated aromatic polymers. In addition, to the best of our knowledge up to date there is no tested sample preparation protocol available for the MALDI mass spectrometry analysis of STY-co-PFS copolymers. The only example containing MALDI-MS measurements obtained for STY-co-PFS we were able to find was the work by Becer at al.[137] where copolymers were synthesized via nitroxide-mediated polymerization, but unfortunately it did not contain information about sample preparation procedures. Thus, to begin the optimization of sample preparation conditions several matrices needed to be tested. The sample preparation protocol was optimized for the sample STY-co-PFS(B) and then applied to the analysis of the

other two samples.

The matrices were chosen because they were either successfully used for analysis of other classes of fluorinated polymers (such as PFCA, PFBA, 2,5-DHB, DCTB) or to the analysis of the polystyrene or the substituted polystyrene (RA, DH). Silver trifluoroacetate (AgTFA) was used as a cationizing agent also because it is well known that silver salts are very efficient in promoting ionization of polystyrene and its derivatives[41, 148]. When RA, DH and DCTB were used as matrices, no signals corresponding to the copolymer oligomers were observed at any of the matrix:analyte:salt molar ratios investigated. Instead, intense peaks corresponding to the silver clusters up to 6000 Da and in some cases to the carbon clusters were present in the spectra. Therefore, it can be concluded that these matrices are unsuitable for the analysis of the fluorinated polystyrene copolymers. This conclusion is somewhat surprising, considering that RA and DH are well known matrices that work particularly well for the analysis of polystyrene and its derivatives[149-151]. It was suggested that the reason for the success of these matrices lies in their chemical structures – both are highly conjugated, non-polar molecules and in that, they are similar to the chemical structure of polystyrene and match its polarity. When PFCA was used as a matrix, very weak copolymer signals were observed, barely above the noise level, and only for lowest matrix:analyte ratios out of all tested (20:5:1, 40:5:1). Silver clusters dominated the spectra collected with this matrix, and combined with low analyte signal intensities deemed spectra unusable. The situation was different when the other fluorinated matrix was used. Although silver clusters were also present in most of the spectra collected with PFBA as a matrix, the copolymer signal intensity was significantly higher when compared with spectra acquired with PFCA. The best signal intensity for this matrix was obtained when matrix:analyte ratio was 40:5:1. It must be noted however, that with PFBA usable spectra were obtained for only a few matrix:analyte ratios tested and the reproducibility of the data was problematic. Out of the all matrix compounds tested, 2,5-DHB allowed acquisition of spectra with highest intensities for peaks corresponding to the copolymer and with minimal amount of silver cluster interference. Also, meaningful data was collected for every matrix:analyte ratio tested, thus making this matrix much more reliable as compared to the PFBA.

- *Choice of the matrix:analyte:salt ratio*

Several matrix:analyte ratios were tested for each matrix in order to establish which combination would allow to obtain the highest signal from the polymer sample. The best signal intensity out of all combinations tested was observed when 2,5-DHB was used as a matrix and when matrix:analyte:salt ratio used was 40:5:1, in this case the intensity of the base peak was twice as high as that obtained with PFBA. The matrix-to-analyte vs maximum average signal intensity plot obtained with this matrix for sample STY-co-PFS(B) is presented on the Fig. 5.1. This plot demonstrates that the maximum of signal intensity is observed when matrix-to-analyte ratio is around 40:5 (vol) and decreases drastically when more matrix is added (higher M/A ratios) or when more analyte is present (lower M/A ratios) – in other words, the signal "saturates" at 40:5 (vol). The M/A response curves with maximum at the saturation point are typical and were observed previously for various analytes, including peptides and proteins[152, 153] as well as synthetic polymers[154, 155]. The exact location of the maximum on the curve as well as its slope depends on the analyte and on the matrix chosen. For example, Chavez-Eng[152] used a mixture of low molecular weight peptide and high molecular weight protein to prepare response saturation curves with different matrices by changing the amount of analyte used in sample preparation. It was demonstrated that the compounds in the mixture had drastically different saturation points that changed based on the matrix used, thus revealing significant variation in desorption/ionization efficiency for low and high molecular weight components at any given M/A ratio. To explain the phenomenon of a "saturation point", it is suggested that at low M/A values, there was not enough matrix to efficiently desorb and ionize the analyte[25]. When there is an excess of matrix present, too much energy is transferred to the ions thus promoting fragmentation of the analyte and decreasing of the overall signal.

Similar arguments can be used in order to explain observed signal intensities as a function of amount of salt added to the sample. When there is not enough cationizing agent, the cationization will not be efficient, but when too much salt is present, clusters of cations dominate the spectra and the analyte signal is suppressed. Therefore, evaluation of the influence of cationizing agent amount is critical in any optimization study. In this work, after the optimum M/A volume ratio was established as 40:5, the same optimization procedure was performed to find the amount of salt needed to obtain the highest polymer signal. The polymer-to-salt ratio vs maximum average signal intensity plot obtained with DHB for sample

STY-co-PFS(B) is presented on the Fig. 5.2. The plot demonstrates that the “saturation point” is observed when polymer-to-salt ratio is around 5:1 (vol) and that signal drops significantly when more analyte is present (vol. ratio 5:0.2). When more salt was added, high intensity signals produced by silver clusters were observed and the intensity of polymer peaks greatly diminished.

Based on the results of the optimization, it can be concluded that DHB as a matrix at matrix:analyte:salt volume ratio of 40:5:1 should be used in order to obtain maximum ionization efficiency and therefore the highest signal for the analytes under investigation.

2. **Structural characterization of fluorinated copolymers synthesized by ATRP**

In order to better understand the structure-function relationship of copolymers with respect to their physical, chemical and mechanical properties, complete characterization of their molecular composition is needed. This includes the information about nature and compositional distribution of monomeric units in oligomer chains, the degree of polymerization, the identity and structure of the end groups, calculations of molecular weight distributions and molar fractions of monomers. The usual analytical methods employed to obtain these characteristics include Gel-Permeation Chromatography (GPC) along with infrared (IR) and nuclear magnetic resonance (NMR) spectroscopy, viscosimetry and calorimetry[61]. Although all these methods are well established and have been applied successfully to the analysis of (co)polymers, mass spectrometry has a significant advantage over them: the classical methods provide an average distributions and are not suitable for the characterization of the individual oligomers that compose a sample, but mass spectrometry analysis *can* provide such information. More importantly, from this precise chemical composition of a polymer, details about polymerization mechanism can be obtained[25].

The mass spectrometry analysis of copolymers is significantly more difficult than analyses of homopolymers due to the presence of more than one repeating unit in their structure. This complicates the mass spectra tremendously. One must also take into account the possibility of structural mass discrimination due to the different ionization efficiency of the species with slightly different compositions, such as different end-groups or a variation in number and identity of repeating units[31, 156]. Furthermore, it is possible that for some types of copolymers, multiple composition assignments can exist for the same mass/charge ratio, and therefore ultra-high resolution mass analyzers must be employed in order to disambiguate them[52]. Despite these difficulties, when successful, MALDI mass spectrometry can provide

a wealth of structural information and therefore is an extremely useful complimentary technique in copolymers analysis.

- *Atom-Transfer Radical Polymerization of styrene with pentafluorostyrene*

The fluorinated copolymer samples in this work were synthesized by atom transfer radical polymerization (ATRP), which is one of the examples of controlled/living radical polymerization (CRP). Since its introduction, CRP techniques have became very popular with polymer chemists because they combine advantages of radical polymerization (simplicity, tolerance of functional groups and impurities, versatility) with controlled nature, which allowed synthesis of (co)polymers with well defined molecular weight distributions (MWDs), functionality distributions and architectures.[68, 157, 158] Main CRP methods, including ATRP, utilize the same basic principle: establishing equilibrium between a small amount of active, growing propagating radicals and a large amount of dormant chains, which can't propagate or self-terminate. In ATRP the radicals are produced by a reversible redox reaction, which involves a transition metal complex, typically a Cu^{I}–X/Ligand (activator, catalyst). The catalyst undergoes an inner sphere one-electron oxidation with acquisition of a halogen atom X from dormant species R–X – this key atom transfer step is responsible for the uniform growth of the chains. Polymer chains grow by the addition of propagating radicals to monomers, and after propagation step react reversibly with the oxidized metal complex Cu^{II}–X_2/Ligand to restore dormant species and the catalyst. The mechanism of ATRP is presented in scheme 5.2

The components of ATRP system include the monomer, a suitable initiator containing a halogen atom (usually an alkyl halide) and a catalyst. For the synthesis of copolymer samples examined in this work, the ATRP system consisted of styrene and pentafluorostyrene as monomers, ethyl-2-bromoisobutyrate as initiator and CuBr/PMDETA complex as a catalyst. In one case (sample C), a small fraction of CuBr was substituted with $CuBr_2$, which acts as deactivator during poymerization. It was demonstrated that the addition of a minor amounts of copper (II) halides leads to better-controlled polymerization and a decrease in polydispersity, can reduce the proportion of terminated (dead) chains and help establish atom transfer equilibrium[68, 159]. The ATRP reaction conditions used for the synthesis of three copolymer samples are listed in the Table 5.1. From this table, it can be seen the only difference between samples A and B was that the reaction was quenched much sooner when STY-co-PFS (A) was

synthesized: after just 8 min versus 90 min for STY-co-PFS (B). As it was noted above, the composition of catalyst was different for STY-co-PFS (C) as compared with sample B, but the reaction time and other parameters were the same. These differences influence the resulting MWD and compositional distributions and the mass spectra of the samples should be able to demonstrate this influence.

Any ATRP reaction includes several fundamental kinetic steps, which include initiation, activation, deactivation, propagation, termination and side reactions, such as elimination of HBr (loss of end group) induced by the deactivator. Based on the accepted mechanism of ATRP[68, 159] and on the kinetic models suggested for compositionally similar systems[128, 158] elementary reactions corresponding to the main kinetic steps as applicable to the systems under investigation were suggested and are outlined on Scheme 5.3.

- *Identification of peaks in MALDI-TOF mass spectra – end groups analysis*

The MALDI-TOF mass spectra obtained for samples A, B and C using the optimized protocol described in the previous section are presented in Fig. 5.3-5.6. The overall organization and main features of the spectra obtained for all three samples were practically identical. As is can be seen from the Fig. 5.3, 5.4, and 5.6, all spectra are complex displays showing multiple clusters of peaks. Closer investigation shows that these clusters consist of at least 4 peaks, each corresponding to a molecular ion, produced by different oligomeric species present in the sample (Fig. 5.5). Every such molecular ion consists of several units of pentafluorostyrene (molecular weight M_{PFS} = 194 Da), a few segments of styrene (molecular weight M_{STY} = 104 Da); two end groups (molecular weights M_{END1} and M_{END2}) and the cationizing species (molecular weight M_{cat}). Therefore, the theoretical calculated molecular weight of the cationized molecular ions can be defined as a sum:

$$(m/z)_{calculated} = nM_{PFS} + mM_{STY} + M_{END1} + M_{END2} + M_{cat} \qquad (4)$$

where n and m are the number of PFS and STY units respectively. Thus, in order to determine the individual composition of oligomers present in the sample, the identity of cationizing species as well as end groups must be established first and then measured value of *m/z* obtained from the spectrum should be compared with the calculated mass value. Since AgTFA was added during sample preparation to promote ionization of the copolymers, it was suggested that Ag^+ is the cationizing specie in this case. The identity of the end groups was proposed to be Br and $C_6H_{11}O_2$ based on the mechanism of ATRP outlined

in Scheme 5.3. Using equation (4), theoretical *m/z* values of various oligomers were calculated and compared with those observed in the spectra. It must be noted that other possibilities for end-group compositions were considered as well, since it is known that polymers synthesized by ATRP are prone to loose their Br functionality[157]. It is possible that the dead chains – products of bimolecular coupling and b-elimination terminations, in fact produced the molecular ions visible in the spectra and therefore would have very different end-groups as it can be seen in Scheme 5.3. However, it was discovered, that only with Br and $C_6H_{11}O_2$ as end groups and Ag^+ as a cation, was it possible to produce compositional assignments for every peak in the spectra for all three samples while keeping the accuracy of the assignments within acceptable range for the analysis of such samples with TOF mass analyzer (the average ppm error was ~300 ppm). Therefore It can be concluded that overall chemical composition of the copolymer samples can be expressed with the following formula: $[C_6H_{11}O_2\,(C_8H_3F_5)_n(C_8H_8)_m\,Br]Ag^+$

- *Compositional distributions in styrene-pentafluorostyrene copolymers*

Since copolymers have a distribution over the chain length as well as the chemical composition, their mass spectra can be extremely complex and difficult to interpret. This complexity is demonstrated in Fig. 5.5, where the expanded portion of the spectrum obtained for sample B is presented. It reveals that each individual molecular ion is a part of two different series of ions at the same time: one with peaks evenly distributed 104 Da apart from each other and the second one with peaks 194 Da apart. Becer et al[137] also observed this pattern in the MALDI-TOF spectra of STY-co-PFS obtained via nitroxide-mediated polymerization. The first type of series are observed due to the subsequent addition of styrene monomer to the oligomer containing an unchanging number of PFS units. For example, the ions in a series marked with red markers on the Fig. 5.5 contain the same number of PFS monomeric units (six), whereas the number of STY units systematically changes from nine to twenty. The second type of series is observed due to the chain's growth through successive addition of PFS monomer: series marked with blue markers on the Fig. 5.5 begins with an oligomer which is 194 Da apart from the oligomer with composition of n=6, m=9 (marked with red), and therefore it has one more PFS unit, but the same number of STY units, which gives it a composition of n=7, m=9. Because all peaks in the spectra are interconnected this way, it was only necessary to obtain accurate compositional assignment for a few most abundant peaks for each sample and after that the elucidation of the (n, m) combinations for the rest of the peaks was simple.

After structural identification was carried out for every peak in each spectrum, resulting n and m values obtained were plotted against each other to reveal overall chemical composition of the copolymers under investigation. The resulting plots are presented as insets on the corresponding spectra on the Fig. 5.3, 5.4 and 5.6. Another, more informative way to present compositional data obtained from MALDI mass spectra of copolymers was first introduced by Wilzec-Vera et al.[160, 161] and later was successfully applied to the characterization of various types of copolymers[52, 162-164]. This method includes representation of a mass spectrum as a matrix consisting of n_i rows and m_j columns, where each position corresponds to a composition of the oligomer possibly present in the sample. In this way, the peak in the mass spectrum with intensity $I_{i,j}$ can be assigned to a location in the matrix based on the compositional assignment (n_i, m_j) obtained for the corresponding oligomer as follows (the example of the matrix and notations are taken from the paper by Willemse et al[163]):

	m_0	m_1	….	m_j
n_0	$I_{0,0}$	$I_{0,1}$	….	$I_{0,j}$
n_1	$I_{1,0}$	$I_{1,1}$	….	$I_{1,j}$
….	….	….	….	….
n_i	$I_{i,0}$	$I_{i,1}$	….	$I_{i,j}$

This matrix can be then presented as a two-dimensional contour plot, also known as copolymer ‘fingerprint’. These plots give an overview of the chain length distribution and the chemical distribution of copolymers under investigation and can provide a valuable insight into the mechanism of a polymerization reaction.

The fingerprint plots were constructed as described above for all three samples and presented on the Fig. 5.7. On the y-axis the number of styrene monomeric units (STY) is shown and on the x-axis the number of pentafluorostyrene units (PFS) is displayed. The corresponding intensities of the peaks in the mass spectra are indicated by color. From these fingerprint plots it is evident that the polystyrene chain length varies from 2 to 16 units for sample A, from 6 to 22 units for sample B and from 8 to 20 units for sample C. Pentafluorostyrene chain length ranges from 2 to 11 units for sample A, from 2 to 16 units for sample B and from 1 to 17 units for sample C. The compositions (n, m) of most abundant oligomers

corresponding to the peaks with highest intensities also can be easily obtained from the plots: (5, 10) for STY-co-PFS(A), (9, 14) for STY-co-PFS(B) and (7, 12) for STY-co-PFS(C). Examination of fingerprint plots makes the similarities and differences between copolymers compositions very evident. First, when comparing the plots of samples A and B, it is clear that as polymerization reaction progresses, the number of both PFS and STY units in polymeric chains changes, but in a different way. From the PFS chain lengths listed above it can be noted that the distribution obtained for sample B includes all values obtained for sample A plus 5 more units, therefore it gets broader, but starts at the same point. However, when considering distributions of STY chain lengths, it is evident that the size of the range for both copolymers is comparable, but for sample B the distribution is shifted towards higher values and chains with smaller number of STY units that were present in sample A disappear. This indicates that the number of STY units during polymerization grows by adding monomers to the already existing chains with lower number of styrene units, which allows keeping the chain length distribution fairly constant. In case of PFS the situation is different – the chain length distribution becomes broader because as polymerization progresses, more and more molecules with a various number of PFS units (high as well as low) are made, but not inevitably by adding them to already existing chains. When comparing the fingerprints of samples B and C, it can be concluded that the PFS chain length distributions for both copolymers if practically identical, but in case of sample C there is less variation in number of STY units.

Another way to follow the polymerization reaction and make these differences in chemical composition more evident is to consider the individual distribution curves of STY and PFS units, also called marginal probability distributions G_{exp}. The distribution for STY can be obtained by summing all measured intensities for the peaks along the PFS axis (values in columns in the matrix of intensities above) and by summing the intensities along STY axis (the values in rows) in order to find distribution for PFS as shown in eq. 5[160]:

$$\Gamma_{exp}(n_i) = \sum_j I(n_i, m_j)$$
$$\Gamma_{exp}(m_j) = \sum_i I(n_i, m_j) \qquad (5),$$

where I (n_i, m_j) is the intensity of the peak with the given n and m. The marginal probability distributions constructed for all three samples are presented in the Fig. 5.8.

The PFS chain length curves on Fig. 5.8(1) confirms the observations discussed above and clearly demonstrates that samples B and C have nearly identical distributions (including their intensities), the only difference being that the maximum on the curve for sample C is slightly shifted towards a lower number of PFS units as compared with curve for sample B. It also shows the notable shift of the maximum on the curves for samples A and B from 5 to 9 units respectively, which is to be expected considering that polymerization was carried out much longer for STY-co-PFS(B). The curves on the Fig. 5.8(2) reveal several features. First, when comparing samples A and B, the maximum shifts towards a higher number of STY units in the same way as is observed in the PFS distribution curves and is expected. Most interesting are the discrepancies clearly observed between the samples B and C: 1) the distribution of STY units for sample C is visibly narrower than that in sample B; 2) there is a shift in maxima between two curves from 15 STY units for sample B to 12 STY units in sample C; 3) there is a significant difference in intensity of the most abundant oligomer. The fact that none of these differences are detected for the PFS distributions, leads to the conclusion that the alteration of the composition of catalyst, namely introduction of a small amount of deactivator $CuBr_2$ is responsible for these changes and that the styrene compositional distribution is more sensitive to the presence of deactivator than pentafluorostyrene unit distribution. Therefore, it can be suggested that if the objective is to produce the material with a narrow compositional distribution of styrene units, the addition of deactivator to the ATRP system will accomplish that goal.

- *Molecular weight and PDI calculations*

Number-average, weight average molecular weight and polydispersity index values were calculated for all three samples using equations 1-3 and compared with the values obtained by Gel-Permeation Chromatography (GPC). These results are presented in the Table 5.2. As it is evident from the Table 5.2, the molecular weight and PDI values obtained for the sample A from MALDI-TOF spectra, are in very good agreement with the ones obtained with GPC. However, for the other two samples with higher molecular weights, there is a notable discrepancy between the values obtained with two methods. The reasons for such discrepancy can be two-fold. On one hand, GPC method of determination of molecular weight relies on the use of calibration curves obtained by measuring hydrodynamic volumes of polymer standards with narrow PDI values and known molecular weights. However, because the

hydrodynamic volumes of polymers heavily depend on their chemical structure and macromolecular architecture, the use of standards that are very unlike the polymers under investigation will introduce an error into the measurements (sometimes very significant error). Another well known, very common and more likely reason for the observed discrepancy is the discrimination effects in MALDI-TOF analysis. The multiple reasons for discrimination effects can be roughly divided in two categories: mass differences and differences in ionization efficiency due to the variation in chemical composition within the copolymer sample. It has been established that discrimination due to the mass differences can be minimized by pre-separation of polydisperse polymer samples (with PDI>1.2), careful attention to the MALDI sample preparation and to the instrumental parameters[10]. However, in case of compositionally heterogeneous samples such as copolymers, the differences in ionization efficiency of the species present in the sample can cause significant deviation between compositions and molecular weight measured by conventional methods such as ^{1}H NMR or GPC and mass spectrometry data[161]. For the samples analyzed in this investigation, mass discrimination due to the polydispersity is unlikely since all three samples have PDI values less than 1.2. Therefore, it can be concluded that the observed inconsistency in molecular weight values obtained with GPC and MALDI-TOF is due to the unequal ionization efficiency of lower and higher molecular weight oligomers present in these samples.

D. *Conclusions*

The optimization of sample preparation conditions for MALDI-TOF mass spectrometry analysis of three poly(styrene-co-pentafluorostyrene) copolymers prepared by ATRP was performed by investigating the influence of the nature of the matrix, choice of matrix-to-analyte and analyte-to-salt ratio. It was determined that out of all matrix compounds tested, only DHB produced high ion yield consistently for all ratios examined. It was also established that when matrix:analyte:salt volume ratio was 40:5:1, the highest analyte ion intensity was observed.

Using the optimized sample preparation conditions, MALDI-TOF spectra were obtained for all copolymer samples and then used to carry out compositional analysis of copolymers. Chemical composition for all samples was elucidated and using copolymer 'fingerprint' method it was possible to determine the individual length distributions of both styrene and pentafluorostyrene monomers. These distributions provided detailed information about polymerization of the systems under investigation not attainable by any other method. It was possible to observe the changes in the composition of copolymers as the polymerization reaction progressed and also to investigate how the alteration in the catalyst composition (the addition of small amount of deactivator $CuBr_2$) would affect the chemical composition of the resulting copolymers. It was discovered that individual styrene chain length distribution is more sensitive to the change in the catalyst composition than pentafluorostyrene. As a consequence, this observation can be possibly used to manipulate the overall chemical composition of the material.

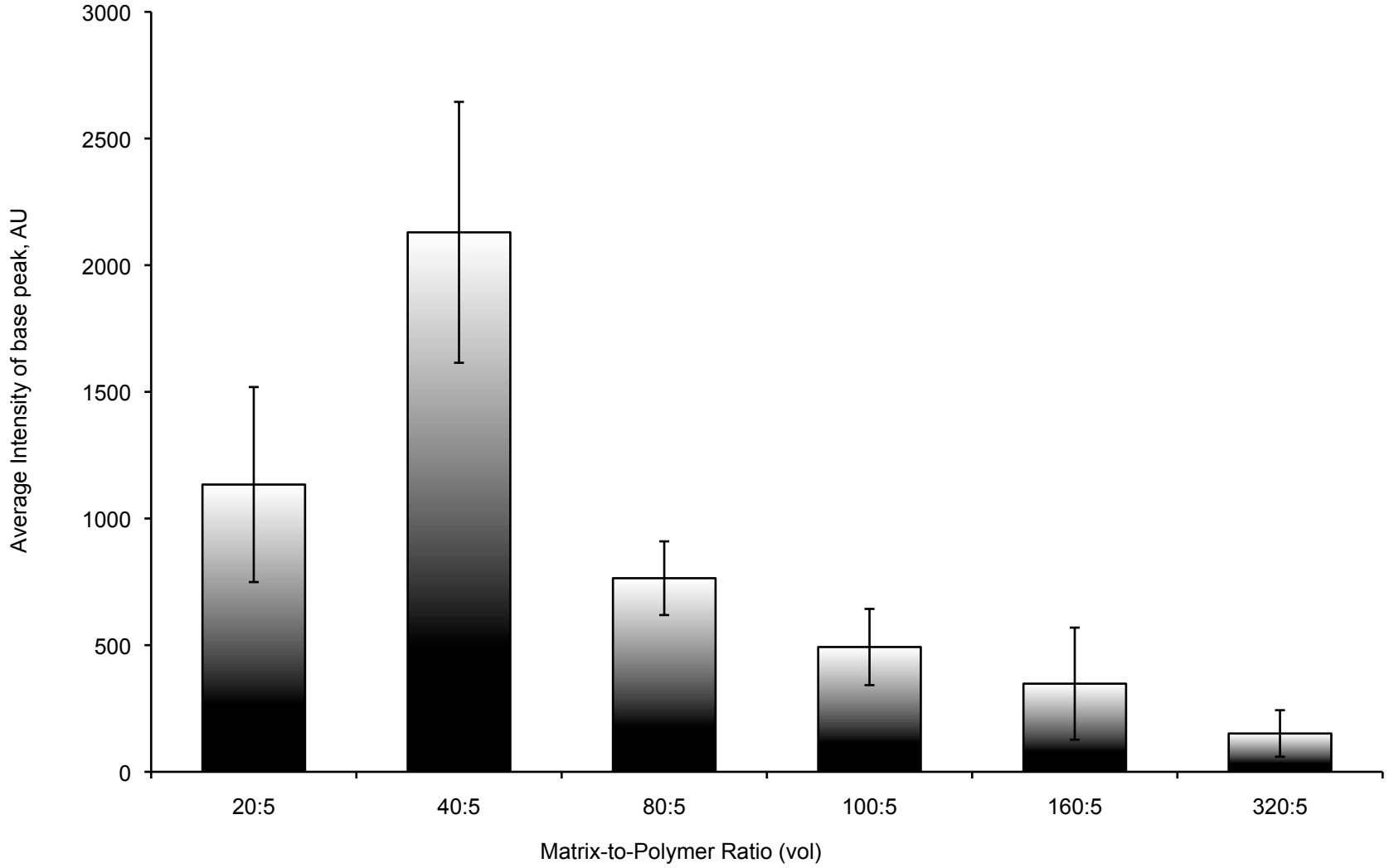

Figure 5.1 Matrix-to-analyte ratios versus maximum average signal intensity plot obtained for STY-co-PFS(B) with 0.2M DHB as a matrix, AgTFA as a cationizing agent and THF as a solvent. Polymer-to-salt ratio was kept constant at 5:1 (vol) for all samples. Error bars represent standard deviations obtained from triplicate measurements carried out for each data point.

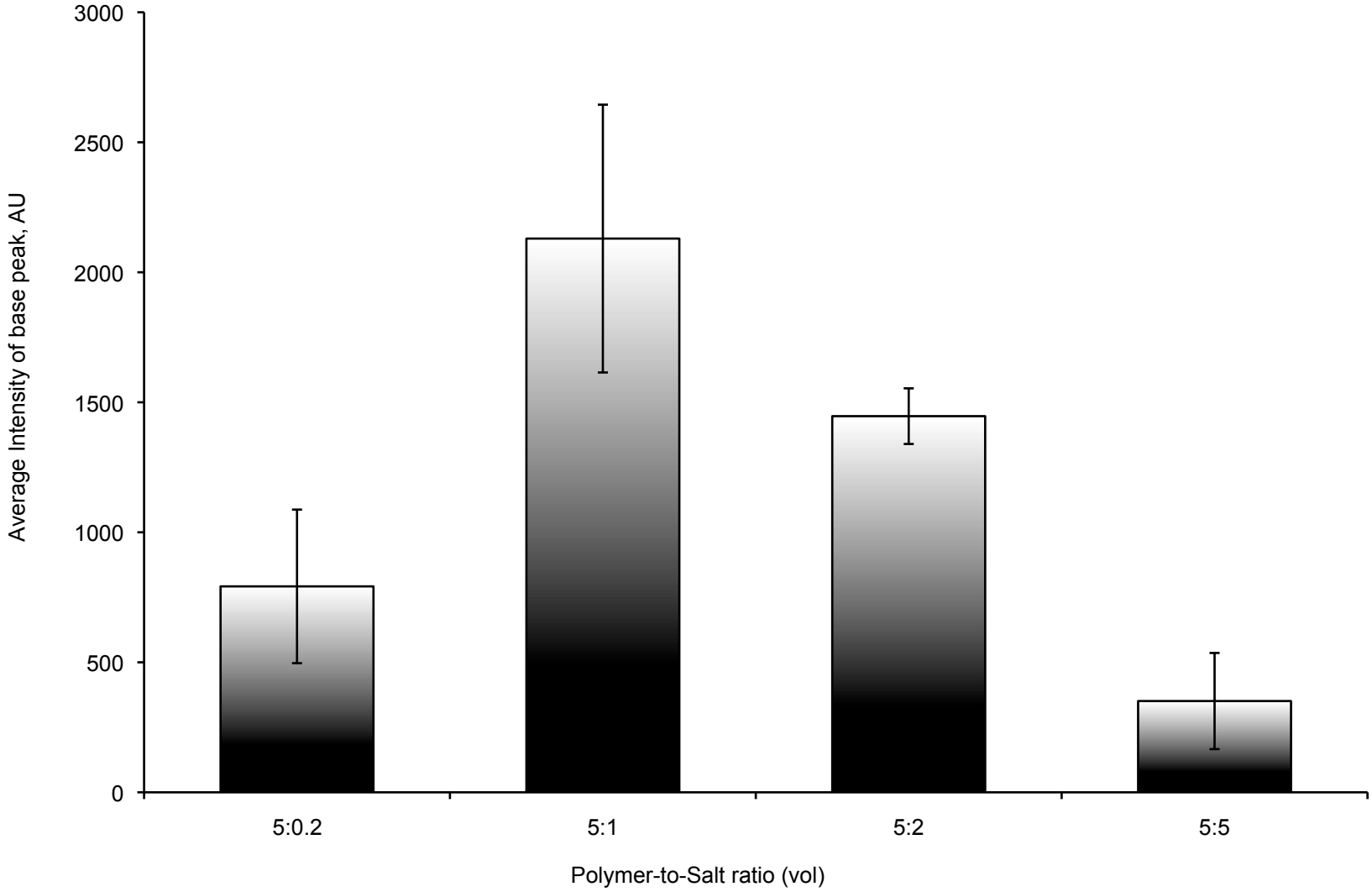

Figure 5.2 Polymer-to-salt ratios versus maximum average signal intensity plot obtained for STY-co-PFS(B) with 0.2M DHB as a matrix, AgTFA as a cationizing agent and THF as a solvent. Matrix-to-analyte ratio was kept constant at 40:5 (vol) for all samples. Error bars represent standard deviations obtained from triplicate measurements carried out for each data point.

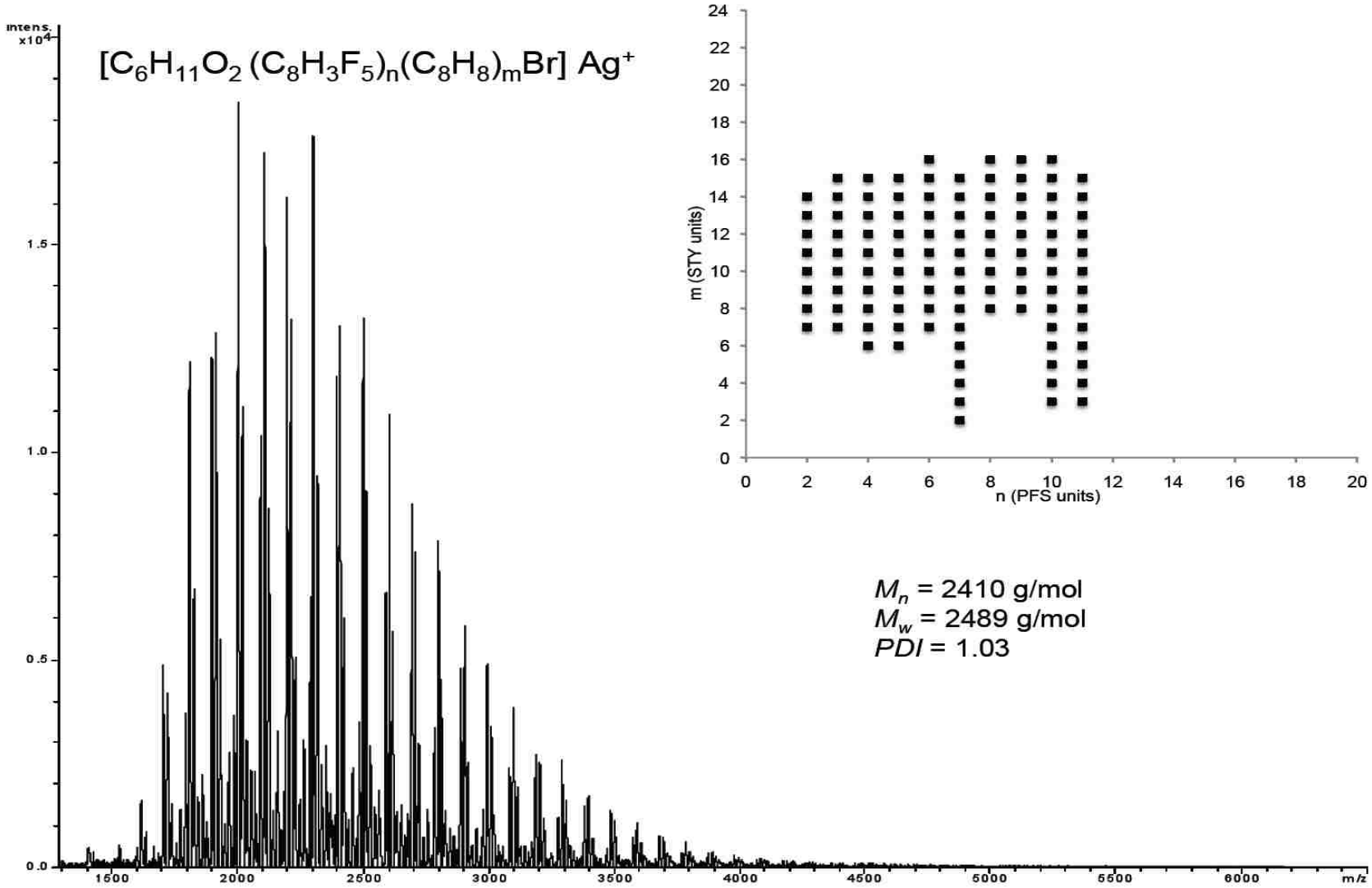

Figure 5.3 MALDI-TOF-MS spectrum of poly(styrene-co-pentafluorostyrene) sample STY-co-PFS(A) obtained with DHB as a matrix, AgTFA as a cationizing agent and optimized matrix:analyte:salt ratio of 40:5:1; the inset represents a compositional plot of the Sty versus PFS segments

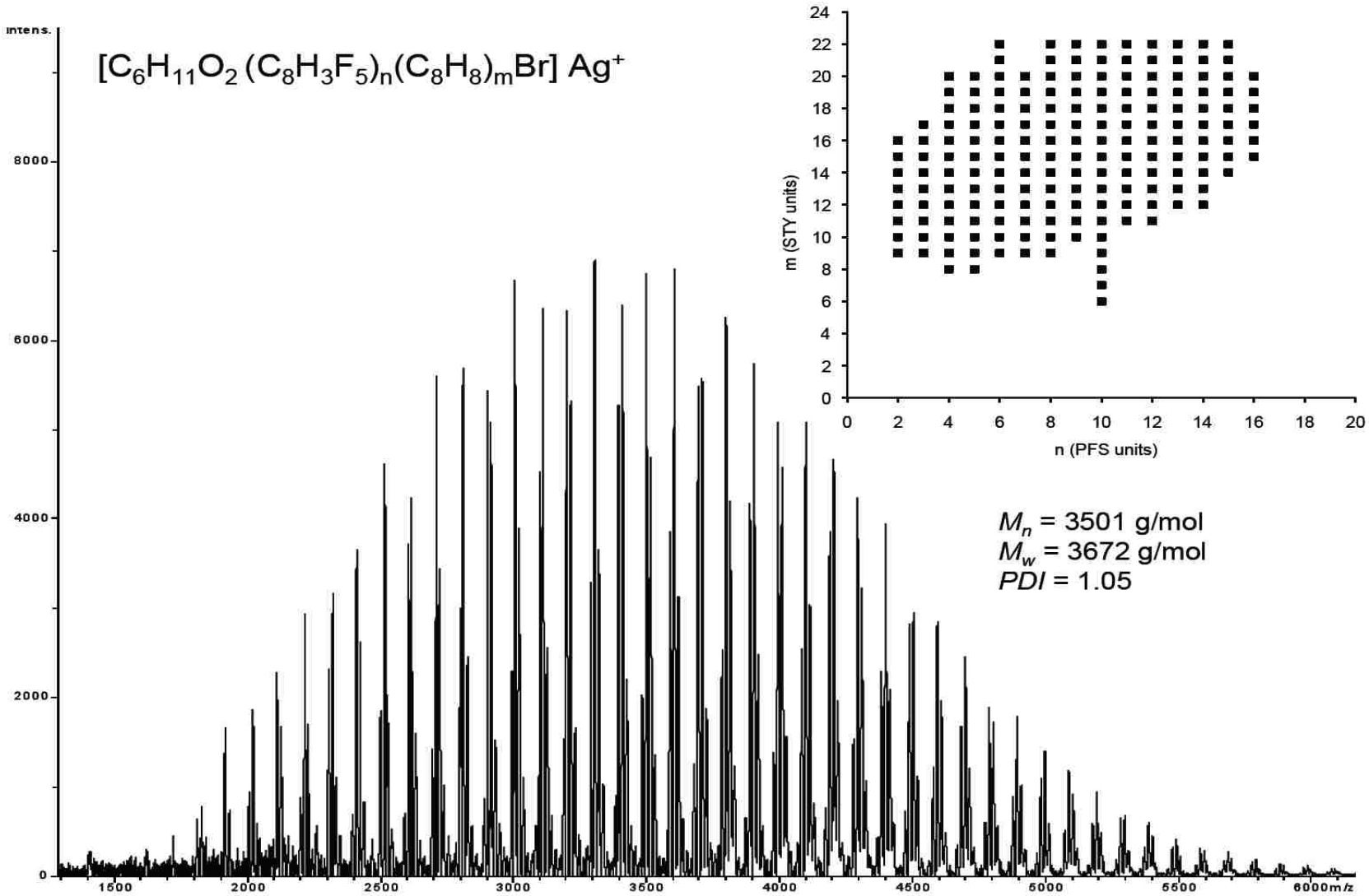

Figure 5.4 MALDI-TOF-MS spectrum of poly(styrene-co-pentafluorostyrene) sample STY-co-PFS(B) obtained with DHB as a matrix, AgTFA as a cationizing agent and optimized matrix:analyte:salt ratio of 40:5:1; the inset represents a compositional plot of the Sty versus PFS segments

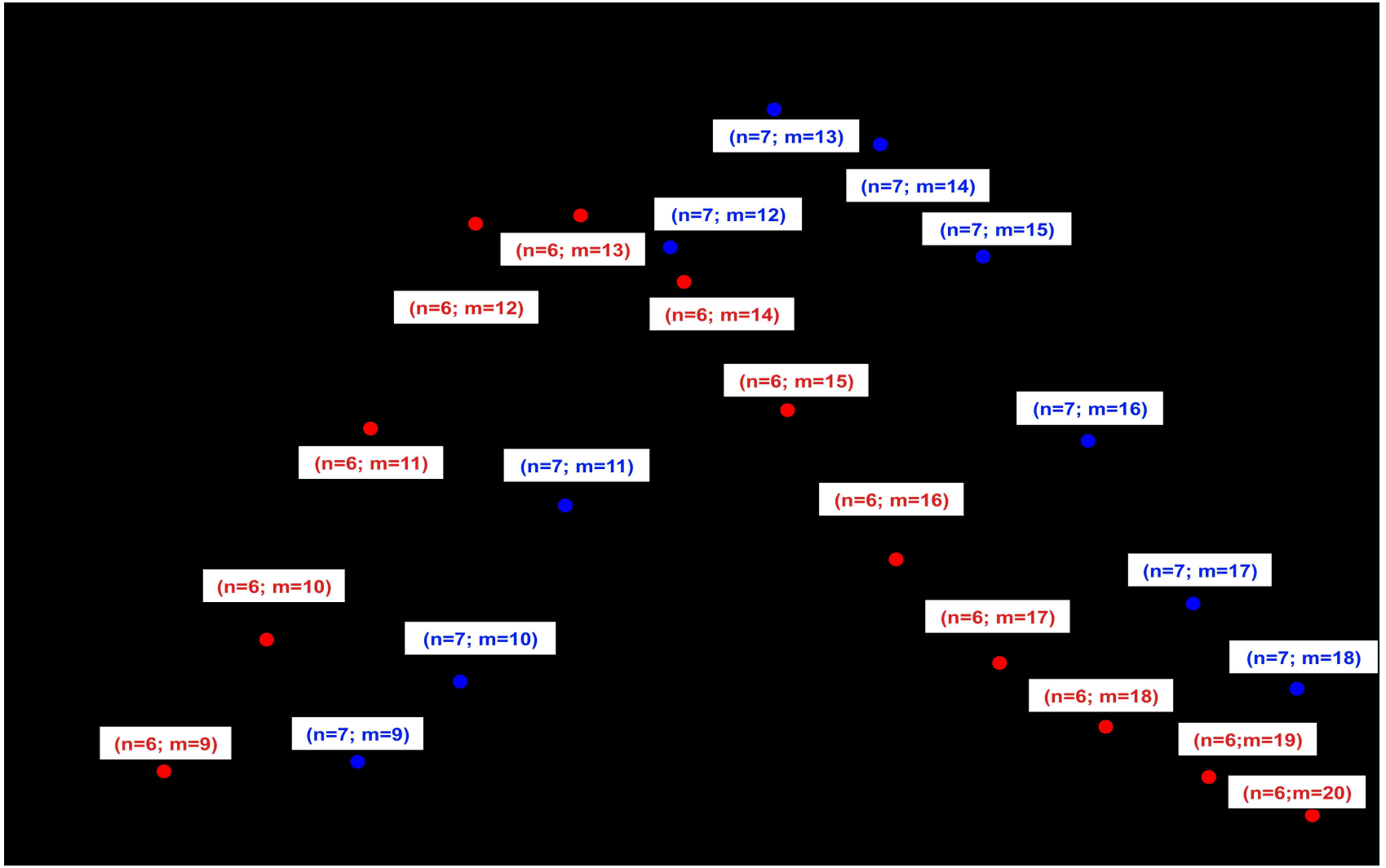

Figure 5.5 Expanded portion of MALDI-TOF-MS spectrum of STY-co-PFS(B) obtained with DHB as a matrix, AgTFA as a cationizing agent and at optimized matrix:analyte:salt ratio of 40:5:1, demonstrating overlapping mini-series of peaks that compose overall molecular weight distribution. Two series of oligomers are marked with red and blue: n represents number of PFS units; m stands for number of Sty units in each oligomer

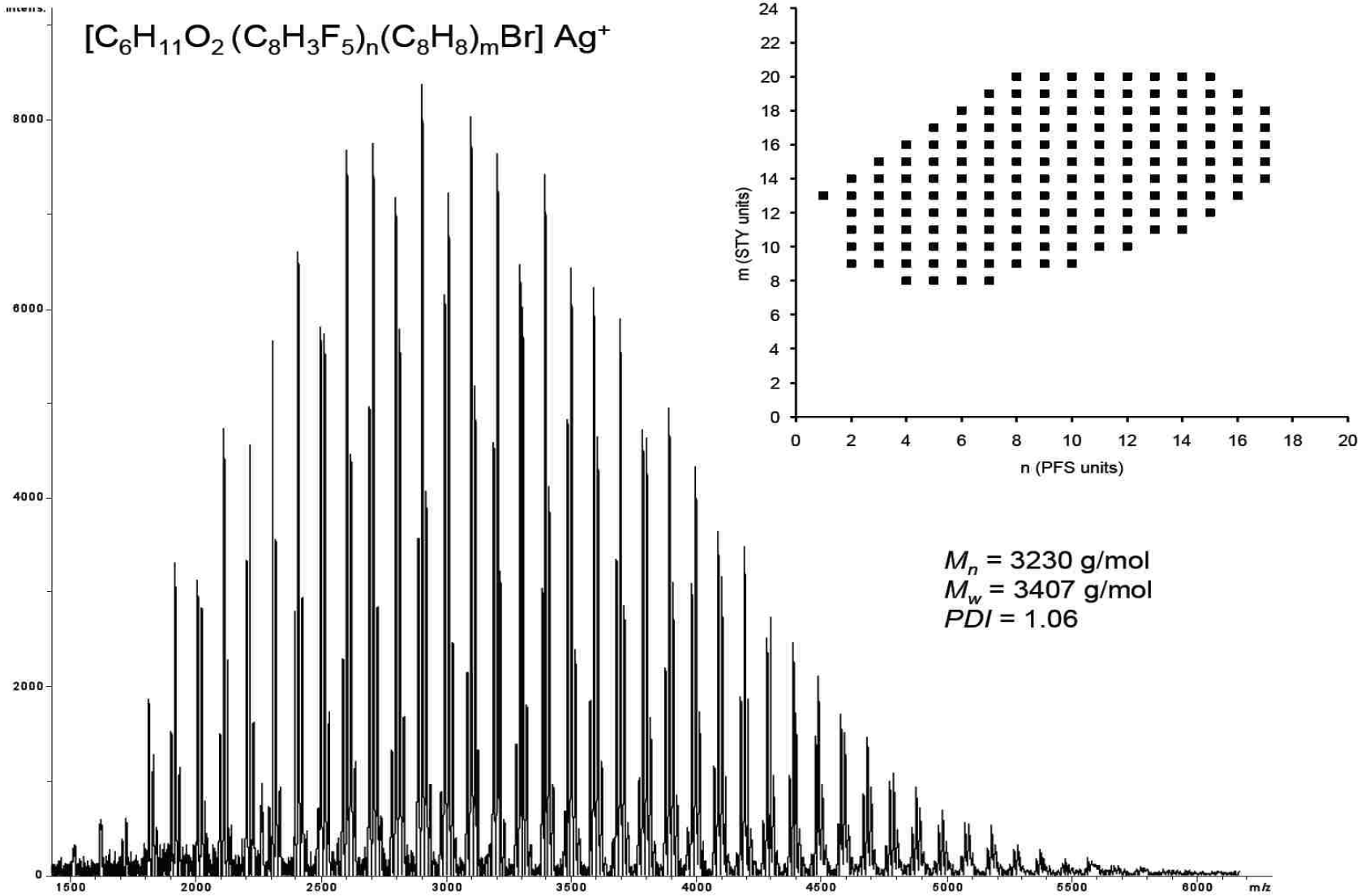

Figure 5.6 MALDI-TOF-MS spectrum of poly(styrene-co-pentafluorostyrene) sample STY-co-PFS(C) obtained with DHB as a matrix, AgTFA as a cationizing agent and optimized matrix:analyte:salt ratio of 40:5:1; the inset represents a compositional plot of the Sty versus PFS segments

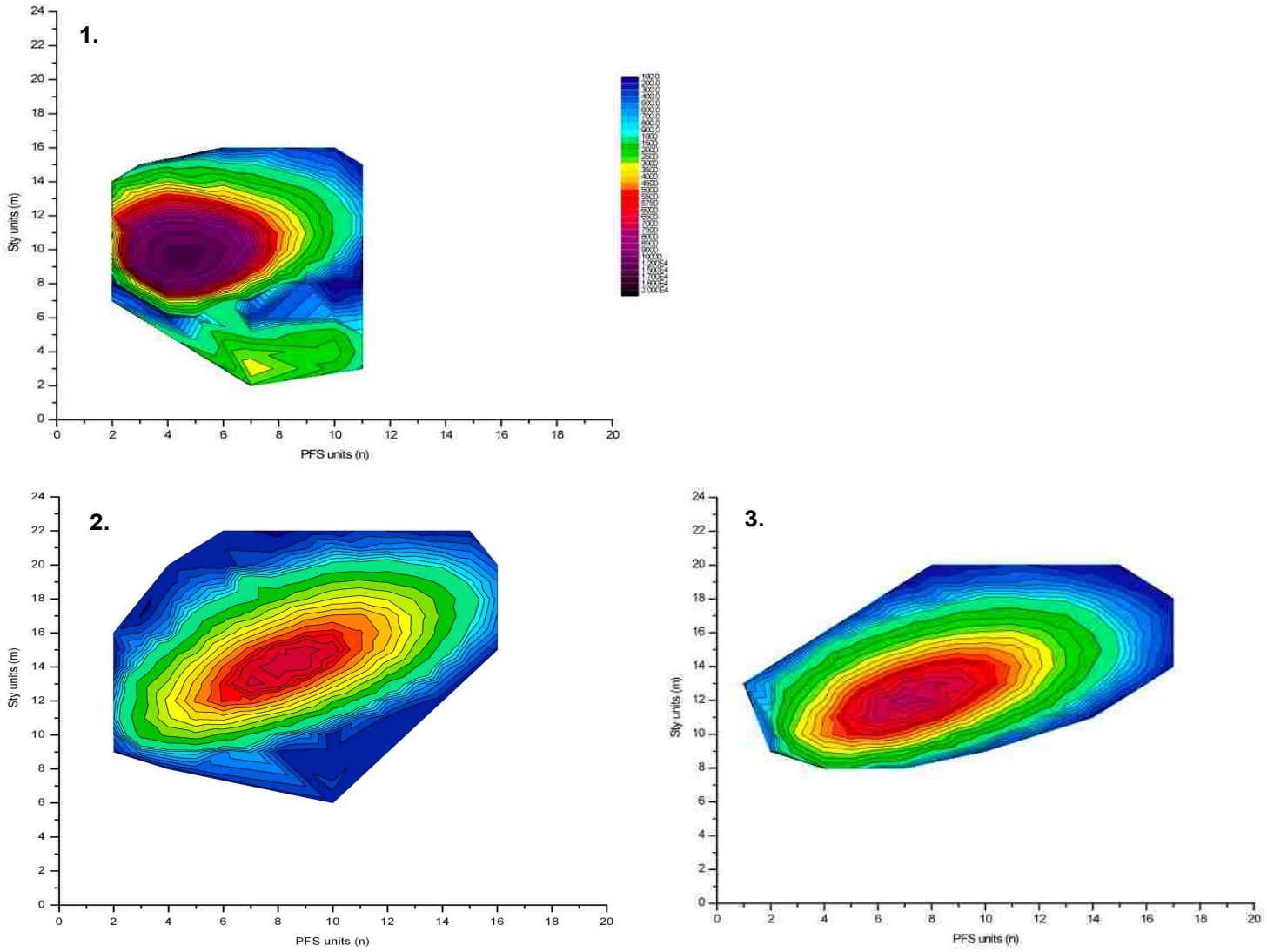

Figure 5.7 Contour “fingerprint” maps of the overall chemical composition distribution as a function of the individual monomer units in the copolymers: (1) for sample STY-co-PFS(A); (2) for sample STY-co-PFS(B); (3) for sample STY-co-PFS(C). The color scale indicates the intensities of the peaks in the corresponding spectra

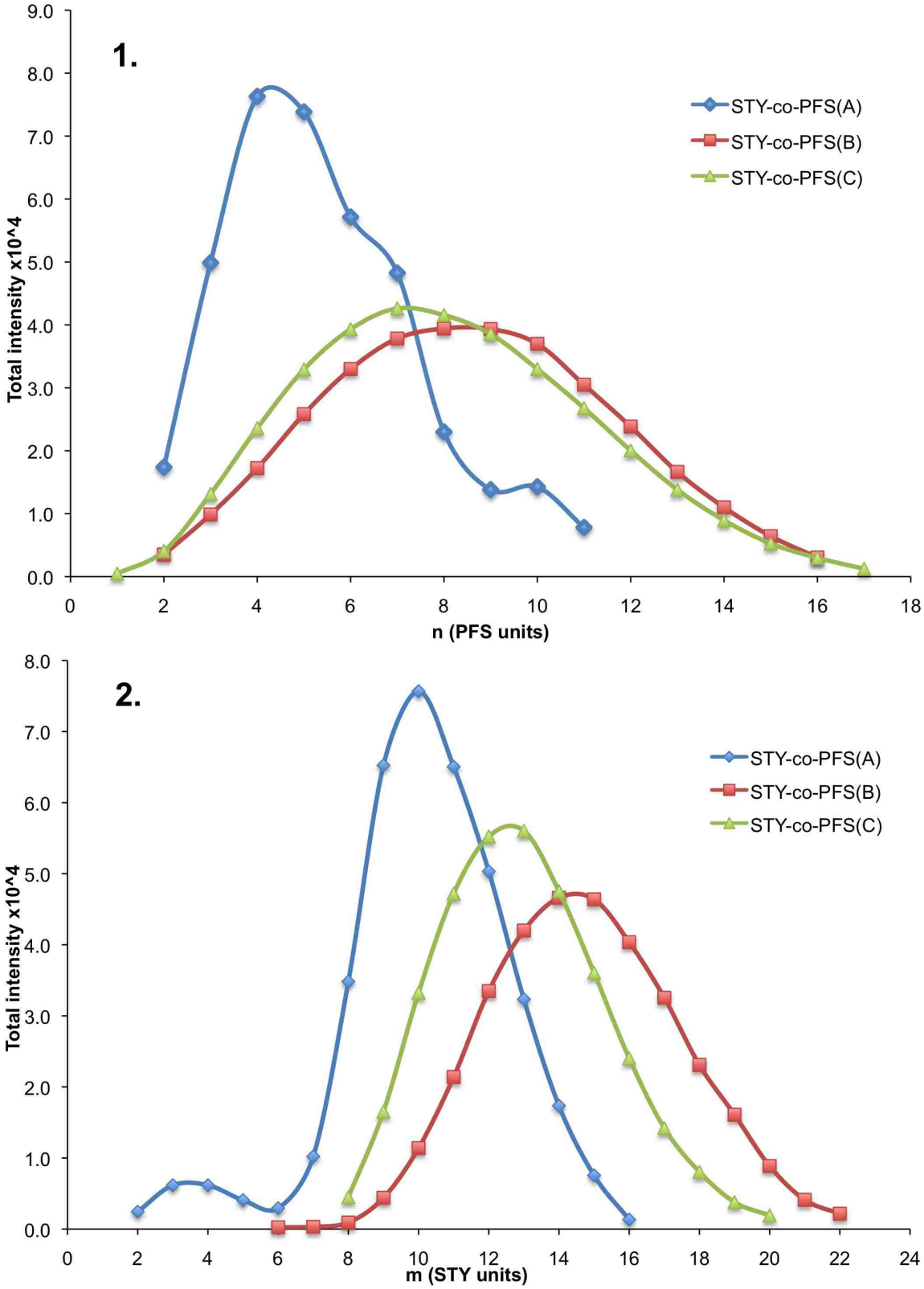

Figure 5.8 Chain length distributions obtained from MALDI-TOF spectra for STY-co-PFS samples: 1) PFS distributions; 2) STY distributions

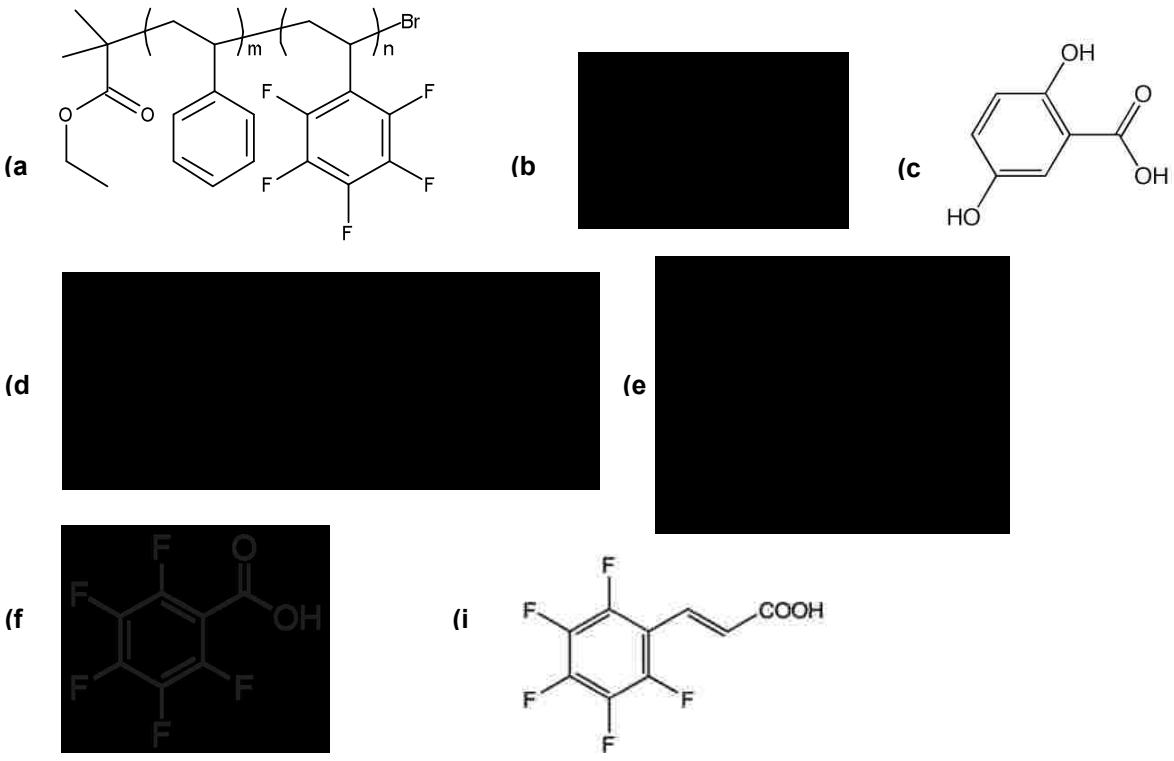

Scheme 5.1 Chemical structures of (a) poly(styrene-co-pentafluorostyrene) (STY-co-PFS); (b) Dithranol (DH); (c) 2,5-Dihydroxybezoic acid (DHB); (d) all-trans-Retinoic acid (RA); (e) *trans*-2-[3-(4-tert-Butylphenyl)-2-methyl-2-propenylidene]malononitrile (DCTB); (f) 2,3,4,5,6-Pentafluorobenzoic acid (PFBA); (i) 2,3,4,5,6-Pentafluorocinnamic acid (PFCA)

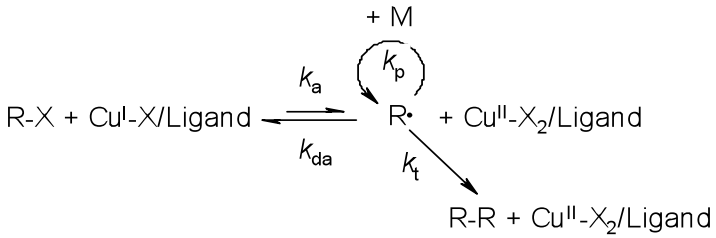

Scheme 5.2 Mechanism of ATRP. Here k_p stands for constant of polymerization, k_t – constant of termination, k_a – constant of activation, k_{da} – constant of deactivation. M represents a monomer molecule

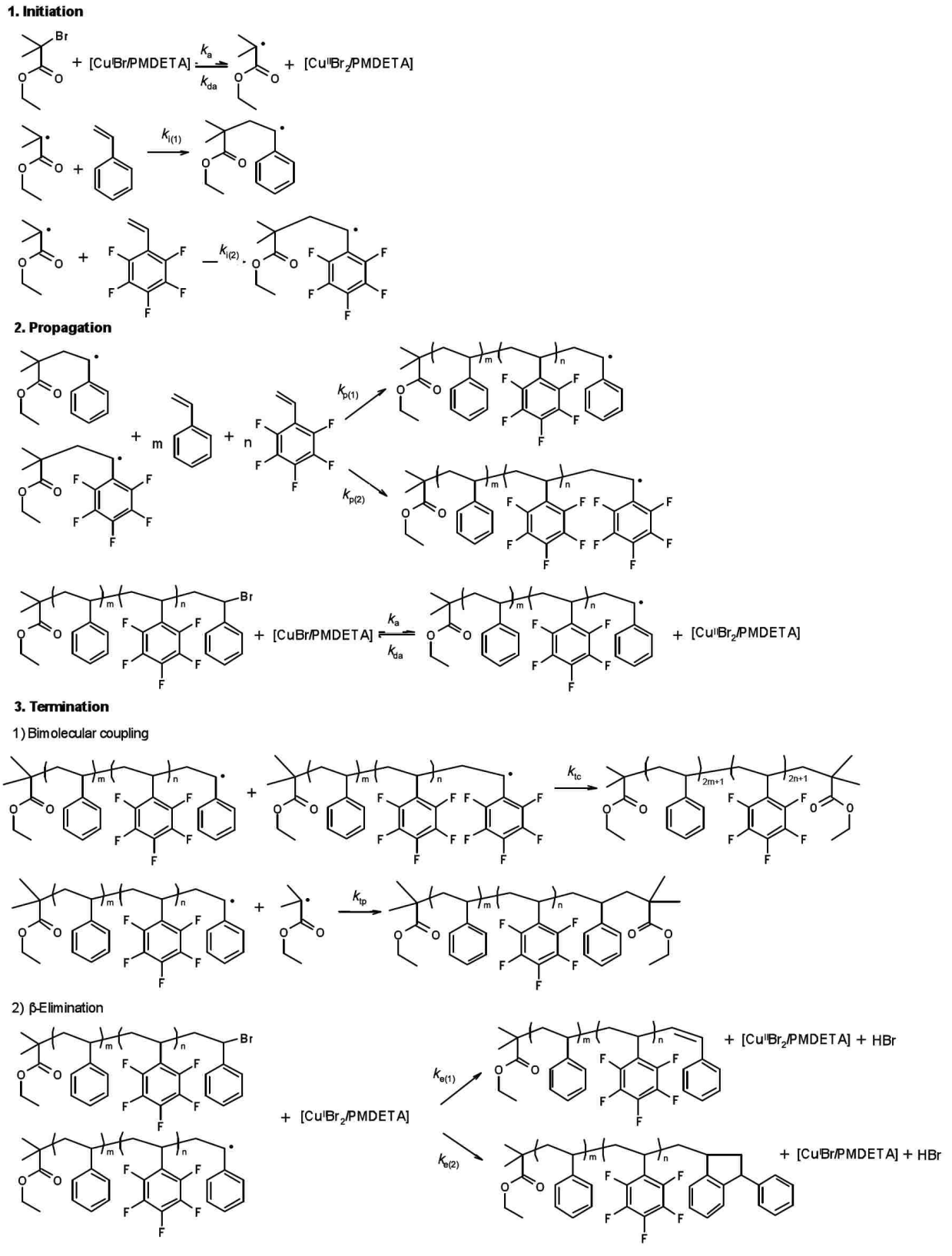

Scheme 5.3 Proposed elementary reactions in atom-transfer radical copolymerization of polystyrene with pentafluorostyrene using ethyl-2-bromoisobutyrate as the initiator

Table 5.1 Reaction conditions for Atom Transfer Radical Polymerization Synthesis of poly(styrene-co-pentafluorostyrene) samples

Copolymer	Sty/PFS/EBriB/CuBr/$CuBr_2$/PMDETA (mol ratio)*	Reaction time, min
STY-co-PFS(A)	10/10/2/1/0/2	8
STY-co-PFS(B)	10/10/2/1/0/2	90
STY-co-PFS(C)	10/10/2/0.95/0.05/2	90

* Sty represents styrene, PFS represents pentafluorostyrene, EBriB represents ethyl-2-bromoisobutyrate, PMDETA represents *N,N,N',N'',N''*-pentamethyldiethylenetriamine

Table 5.2 Molecular mass values (g/mol) and PDI of poly(styrene-co-pentafluorostyrene) samples determined by GPC and MALDI-TOF mass spectrometry

Copolymer	M_n (by GPC)	M_n (by MALDI)	M_w (by GPC)	M_w (by MALDI)	PDI (by GPC)	PDI (by MALDI)
STY-co-PFS(A)	2313	2410	2549	2489	1.10	1.03
STY-co-PFS(B)	4160	3501	4709	3672	1.13	1.05
STY-co-PFS(C)	3656	3230	4201	3407	1.15	1.06

VI. REFERENCES

(1) Karas, M.; Bachman, D.; Bahr, U.; Hillenkamp, F. *Int. J. Mass Spectrom. Ion Process.* **1987**, *78*, 53-68.

(2) Tanaka, K.; Waki, H.; Ido, Y.; Akita, S.; Yoshida, Y.; Yoshida, T.; Matsuo, T. *Rapid Comm. Mass Spectrom.* **1988**, *2*, 151-153.

(3) Jackson, A. T.; Yates, H. T.; Lindsay, C. I.; Didier, Y.; Segal, J. A.; Scrivens, J. H.; Critchley, G.; Brown, J. *Rapid Commun. Mass Spectrom.* **1997**, *11*, 520-526.

(4) van Rooij, G. J.; Duursma, M. C.; Heeren, R. M. A.; Boon, J. J.; de Koster, C. J. *J. Am. Soc. Mass Spectrom.* **1996**, *7*, 449-457.

(5) Räder, H. J.; Schrepp, W. *Acta Polymerica* **1998**, *49*, 272-293.

(6) Montaudo, G.; Garozzo, D.; Montaudo, M. S.; Puglisi, C.; Samperi, F. *Macromolecules* **1995**, *28*, 7983-7989.

(7) Montaudo, G.; Montaudo, M. S.; Puglisi, C.; Samperi, F. *Rapid Commun. Mass Spectrom.* **1995**, *9*, 453-460.

(8) Tatro, S. R.; Baker, G. R.; Flemming, R.; Harmon, J. P. *Polymer* **2002**, *43*, 2329-2335.

(9) *MALDI MS. A Practical Guide to Instrumentation, Methods and Appplications*; Willey-VCH Verlag GmbH&Co. KGaA, Weinheim, 2007.

(10) Nielen, M. W. F. *Mass Spectrom. Rev.* **1999**, *18*, 309-344.

(11) Karas, M.; Hillenkamp, F. *Anal. Chem.* **1988**, *60*, 2299-2301.

(12) Castoro, J. A.; Köster, C.; Wilkins, C. L. *Rapid Comm. Mass Spectrom.* **1992**, *6*, 239-241.

(13) Danis, P. O.; Karr, D. E.; Mayer, F.; Holle, A.; Watson, C. H. *Org. Mass Spectrom.* **1992**, *27*, 843-846.

(14) Zhigilei, L. V.; Kodali, P. B. S.; Garrison, B. J. *J. Phys. Chem. B* **1998**, *102*, 2845-2853.

(15) Zenobi, R.; Knochenmuss, R. *Mass Spectrom. Rev.* **1998**, *17*, 337-366.

(16) Karas, M.; Gluckmann, M.; Shafer, J. *J. Mass Spectrom.* **2000**, *35*, 1-12.

(17) Knochenmuss, R. *Analyst* **2006**, *131*, 966-986.

(18) Meier, M. A. R.; Adams, N.; Schubert, U. S. *Anal. Chem.* **2007**, *79*, 863-869.

(19) Batoy, S. M. A.; Akhmetova, E.; Miladinovic, S.; Smeal, J.; Wilkins, C. L. *Applied Spectroscopy Reviews* **2008**, *43*, 485-550.

(20) Chan, D. T. W.; Colburn, A. W.; Derrick, P. J. *Org. Mass Spectrom.* **1991**, *26*, 342-344.

(21) Knochenmuss, R.; Karbach, V.; Wiesli, U.; Breuker, K.; Zenobi, R. *Rapid Comm. Mass Spectrom.* **1998**, *12*, 529-534.

(22) Chen, H.; Guo, B. *Anal. Chem.* **1997**, *69*, 4399-4404.

(23) Hoberg, A.-M.; Haddleton, D. M.; Derrick, P. J.; Jackson, A. T.; Scrivens, J. H. *Eur. J. Mass Spectrom.* **1998**, *4*, 435-440.

(24) Van Rooij, G. J.; Boon, J. J.; Duursma, M. C.; Heeren, R. M. A. *Int. J. Mass Spectrom. Ion Process.* **2002**, *221*, 191-207.

(25) *Mass Spectrometry in Polymer Chemistry*; Wiley-VCH Verlag GmbH & Co. KGaA: Weinheim, Germany, 2011.

(26) Hanton, S. D.; Cornelio Clarl, P. A.; Owens, K. G. *J. Am. Soc. Mass Spectrom.* **1999**, *10*, 104-111.

(27) Hanton, S. D.; Owens, K. G. *J. Am. Soc. Mass Spectrom.* **2005**, *16*, 1172-1180.

(28) Liu, J. S.; Loewe, R. S.; McCullough, R. D. *Macromolecules* **1999**, *32*, 5777-5785.

(29) Yalcin, T.; Dai, Y.; Li, L. *J. Am. Soc. Mass Spectrom.* **1998**, *9*, 1303-1310.

(30) Arakawa, R.; Watanabe, S.; Fukuo, T. *Rapid Comm. Mass Spectrom.* **1999**, *13*, 1059-1062.

(31) Chen, R.; Zhang, N.; Tseng, A. M.; Li, L. *Rapid Comm. Mass Spectrom.* **2000**, *14*, 2175-2181.

(32) Hoteling, A. J.; Mourey, T. H.; Owens, K. G. *Anal. Chem.* **2005**, *77*, 750-756.

(33) Weidner, S. M.; Falkenhagen, J. *Rapid Comm. Mass Spectrom.* **2009**, *23*, 653-660.

(34) Vorm, O.; Roepstorff, P.; Mann, M. *Anal. Chem.* **1994**, *66*, 3281-3287.

(35) Brandt, H.; Ehmann, T.; Otto, M. *Rapid Comm. Mass Spectrom.* **2010**, *24*, 2439-2444.

(36) Yokoyama, Y.; Hirajima, R.; Morigaki, K.; Yamaguchi, Y.; Ueda, K. *J. Am. Soc. Mass Spectrom.* **2007**, *18*, 1914-1920.

(37) Rashidezadeh, H.; Wang, Y.; Guo, B. *Rapid Comm. Mass Spectrom.* **2000**, *14*, 439-443.

(38) Scrivens, J. H.; Jackson, A. T.; Yates, H. T.; Green, M. R.; Critchley, G.; Brown, J.; Bateman, R. H.; Bowers, M. T.; Gidden, J. *Int. J. Mass Spectrom. Ion Process.* **1997**, *165/166*, 363-375.

(39) Fujii, T. *Mass Spectrom. Rev.* **2000**, *19*, 111-.

(40) Kahr, M. S.; Wilkins, C. L. *J. Am. Soc. Mass Spectrom.* **1993**, *4*, 453-460.

(41) Deery, M. J.; Jennings, K. R.; Jasieczek, C. B.; Haddleton, D. M.; Jackson, A. T.; Yates, H. T.; Scrivens, J. H. *Rapid Comm. Mass Spectrom.* **1997**, *11*, 57-62.

(42) Macha, S. F.; Limbach, P. A.; Savickas, P. J. *J. Am. Soc. Mass Spectrom.* **2000**, *11*, 731-737.

(43) Keki, S.; Deak, G.; Zsuga, M. *Rapid Comm. Mass Spectrom.* **2001**, *15*, 675-678.

(44) Llenes, C. F.; O'Malley, R. M. *Rapid Comm. Mass Spectrom.* **1992**, *6*, 564-570.

(45) Rader, H. J.; Schrepp, W. *Acta Polymer.* **1998**, *49*, 272-293.

(46) Hanton, S. D. *Chem. Rev.* **2001**, *101*, 527-569.

(47) Hanton, S. D.; Owens, K. G.; Blair, W.; Hyder, I. Z.; Stets, J. R.; Guttman, C. M.; Giuseppetti, A. *J. Am. Soc. Mass Spectrom.* **2004**, *15*, 168-.

(48) Hensel, R. R.; King, R. C.; Owens, K. G. *Rapid Comm. Mass Spectrom.* **1997**, *11*, 1785-1793.

(49) Yao, J.; Scott, J. R.; Young, M. K.; Wilkins, C. L. *J. Am. Soc. Mass Spectrom.* **1998**, *9*, 805-813.

(50) In *The encyclopedia of Mass Spectrometry*; Armentrout, P. B., Ed.; Elsevier, 2003; Vol. 1, pp 121-144.

(51) Pasch, H.; Schrepp, W. *MALDI-TOF Mass Spectrometry of Synthetic Polymers*; Springer-Verlag Berlin Heidelberg New York, LLC, 2003.

(52) Van Rooij, G. J.; Duursma, M. C.; de Koster, C. J.; Heeren, R. M. A.; Boon, J. J.; Schuyl, P. J. W.; Van der Hage, E. R. E. *Anal. Chem.* **1998**, *70*, 843-850.

(53) Dienes, T.; Pastor, S. J.; Schurch, S.; Scott, J. R.; Yao, J.; Cui, S.; Wilkins, C. L. *Mass Spectrom. Rev.* **1996**, *15*, 163-211.

(54) Barrow, M. P.; Burkitt, W. I.; Derrick, P. J. *Analyst* **2005**, *130*, 18-28.

(55) Marshall, A. G.; Hendrickson, C. L.; Jackson, G. S. *Mass Spectrom. Rev.* **1998**, *17*, 1-35.

(56) Amster, J. *J. Mass Spectrom.* **1996**, *31*, 1325-1337.

(57) Wilkins, C. L.; Gross, M. L. *Anal. Chem.* **1981**, *53*, 1661A-1676A.

(58) Nibbering, N. M. M. *Analyst* **1992**, *117*, 289-293.

(59) Montaudo, G.; Lattimer, R. P., Eds. *Mass Spectrometry of Polymers*; CRC Press, 2001.

(60) Carraher, C. E. *Introduction to polymer chemistry*; CRC Press, Taylor & Francis Group: Boca Raton, Florida, 2007.

(61) Rodriguez, F.; Cohen, C.; Ober, C. K.; Archer, L. A. *Principles of Polymer Systems*, 5th ed.; Taylor & Francis Group: New York, NY, 2003.

(62) Peters, E. N. In *Comprehensive Desk Reference of Polymer Characterization and Analysis*; Brady, R. F., Ed.; Oxford University Press, Inc.: New York, NY, 2003, pp 3-29.

(63) Allcock, H. R.; Lampe, F. W.; Mark, J. E. *Contemporary polymer chemistry*, 3rd ed.; Pearson Education, Inc.: Upper Saddle River, New Jersey, 2003.

(64) Peacock, A. J.; Calhoun, A. *Polymer Chemistry: properties and applications*; Hanser Gardner Publications, Inc.: Cincinnati, Ohio, 2006.

(65) Painter, P. C.; Coleman, M. M. *Fundamentals of Polymer Science: an Introductory Text*; CRC Press, 1997.

(66) Hiemenz, P. C. *Polymer Chemistry: The Basic Concepts*; Marcell Dekker, Inc., 1984.

(67) Petrie, E. M. *Handbook of Adhesives and Sealants*; McGraw-Hill, 2000.

(68) Matyjaszewski, K.; Xia, J. *Chem. Rev.* **2001**, *101*, 2921-2990.

(69) Barth, H. G. In *Comprehensive Desk Reference of Polymer Characterization and Analysis*; Brady, R. F., Ed.; Oxford University Press, Inc.: New York, NY, 2003, pp 30-45.

(70) Brydson, J. *Plastics Materials (7th Edition)*; Elsevier, 1999.

(71) Fink, J. K. *Reactive Polymers Fundamentals and Applications - A Concise Guide to Industrial Polymers*; William Andrew Publishing/Plastics Design Library, 2005.

(72) *Food Chemicals Codex*, 5th ed.; National Academies Press, 2003.

(73) Bunczek, M. T.; Greenberg, M. J.; Urnezis, P. W., A23G4/00; A23G4/08; A23G4/06; A23G3/30 ed.; WRIGLEY W M JUN CO: USA, 2000.

(74) Koch, E. R.; Abbazia, L. P.; Puglia, W. J., A23G4/00; A23G4/08; A23G4/06; A23G3/30 ed.; WARNER LAMBERT CO: USA, 1980.

(75) Hill, V. A.; Schulz, G. O., A23G4/00; A23G4/08; A23G4/06; A23G3/30 ed.; GOODYEAR TIRE & RUBBER: USA, 2004.

(76) Fritz, D. *Formulation and Production of Chewing and Bubble Gum*; Kennedys Publications Ltd: London, UK, 2006.

(77) James, M. G., A23G4/00; A23G4/06; A23G4/08; A23G4/00; A23G4/06 ed.; SHAWINIGAN CHEM LTD, 1942.

(78) Pickett, O. A., A23G4/00; A23G4/06; A23G4/08; A23G4/00; A23G4/06 ed.; HERCULES POWDER CO LTD: USA, 1944.

(79) Cherukuri, S. R.; Mansukhani, G., A23G4/00; A23G4/02; A23G4/06; A23G4/08; A23G4/00; A23G4/02; A23G4/06; (IPC1-7): A23G3/3 ed.; Warner-Lambert Company (Morris Plains, NJ) : USA, 1988.

(80) Witzel, F., A23G4/00; A23G4/06; A23G4/08; A23G4/00; A23G4/06; (IPC1-7): A23G3/30 ed.; Life Savers, Inc. (New York, NY): USA, 1976.

(81) Comollo, A. J., C08L23/00; A23G4/00; A23G4/06; A23G4/08; A23G4/20; C08L7/00; C08L21/00; C08L101/00; C08L23/00; A23G4/00; A23G4/06; A23G4/18; C08L7/00; C08L21/00; C08L101/00; (IPC1-7): A23G3/30; A23G3/00 ed.; Wm. Wrigley Jr. Company (Chicago, IL) : USA, 1976.

(82) Haefliger, O. P.; Jeckelmann, N. *Rapid Comm. Mass Spectrom.* **2007**, *21*, 1361-1366.

(83) Niederer, B.; Le, A.; Cantergiani, E. *Journal of Chromatography A* **2003**, *996*, 189-194.

(84) Schriemer, D. C.; Li, L. *Anal. Chem.* **1997**, *69*, 4169-4175.

(85) Alicata, R.; Montaudo, G.; Puglisi, C.; Samperi, F. *Rapid Comm. Mass Spectrom.* **2002**, *16*, 248-260.

(86) Murgasova, R.; Hercules, D. M. *Anal. Chem.* **2003**, *75*, 3744-3750.

(87) Barman, B. N.; Cebolla, V. L.; Mehrotra, A. K.; Mansfield, C. T. *Anal. Chem.* **2001**, *73*, 2791-2804.

(88) Robins, C.; Limbach, P. A. *Rapid Comm. Mass Spectrom.* **2003**, *17*, 2839-2845.

(89) Millan, M.; Morgan, T. J.; Behrouzi, M.; Karaca, F.; Galmes, C.; Herod, A. A.; Kandiyoti, R. *Rapid Comm. Mass Spectrom.* **2005**, *19*, 1867-1873.

(90) Apicella, B.; Ciajolo, A.; Millan, M.; Galmes, C.; Herod, A. A.; Kandiyoti, R. *Rapid Comm. Mass Spectrom.* **2004**, *18*, 331-338.

(91) Danis, P. O.; Karr, D. E. *Org. Mass Spectrom.* **1993**, *28*, 923-925.

(92) Danis, P. O.; Saucy, D. A.; Huby, F. J. In *American Chemical Society. Division of Polymer Chemistry*, 1996; Vol. 37, pp 311-312.

(93) Hansen, C. M. *Hansen Solubility Parameters: A User's Handbook*, 2nd ed.; CRC Press, Taylor & Francis Group: Boca Raton, FL, 2007.

(94) *Lange's Handbook of Chemistry*, 15th ed.; McGraw-Hill Professional, 1998.

(95) Barton, A. F. M. *CRC Handbook of Polymer-Liquid Interaction Parameters and Solubility Parameters*; CRC Press LLC: Boca Raton, FL, 1990.

(96) Dey, M.; Castoro, J. A.; Wilkins, C. L. *Anal. Chem.* **1995**, *67*, 1575-1579.

(97) Martin, K.; Spickermann, J.; Rader, H. J.; Mullen, K. *Rapid Comm. Mass Spectrom.* **1996**, *10*, 1471-1474.

(98) Schriemer, D. C.; Li, L. *Anal. Chem.* **1997**, *69*, 4176-4183.

(99) Ballistreri, A.; Foti, S.; Montaudo, G.; Scamporrino, E. *J. Polym. Sci. Polym. Chem. Ed.* **1980**, *18*, 1147-1153.

(100) Fabbri, D. *J. Anal. Appl. Pyrolysis* **2001**, *58-59*, 361-370.

(101) Collins, S.; Rimmer, S. *Rapid Comm. Mass Spectrom.* **2004**, *18*, 3075-3078.

(102) Giguere, M. S.; Mayer, P. M. *Int. J. Mass Spectrom. Ion Process.* **2004**, *231*, 59-68.

(103) Kim, J. Y.; Lee, K.; Coates, N. E.; Moses, D.; Nguyen, T.-Q.; Dante, M.; Heeger, A. J. *Science* **2007**, *317*, 222-225.

(104) Tang, C. W. *Appl. Phys. Lett.* **1986**, *48*, 183-185.

(105) Heremans, P.; Cheyns, D.; Rand, B. P. *Accounts of Chemical Research* **2009**, *42*, 1740-1747.

(106) Coakley, K.; McGehee, M. D. *Chem. Mater.* **2004**, *16*, 4533-4542.

(107) Brabec, C. J.; Sariciftci, N. S.; Hummelen, J. C. *Advanced Functional Materials* **2001**, *11*, 15-26.

(108) Thompson, B. C.; Frechet, J. M. J. *Angewandte Chemie-International Edition* **2008**, *47*, 58-77.

(109) Hummelen, J. C.; Knight, B. W.; Lepeq, F.; Wudl, F.; Yao, J.; Wilkins, C. L. *Journal of Organic Chemistry* **1995**, *60*, 532-538.

(110) Wudl, F. *Journal of Materials Chemistry* **2002**, *12*, 1959-1963.

(111) Roncali, J. *Accounts of Chemical Research* **2009**, *42*, 1719-1730.

(112) Downard, K. *Mass Spectrometry. A foundation course*; The Royal Society of Chemistry, 2004.

(113) Kotsiris, S. G.; Vasil'ev, Y. V.; Streletskii, A. V.; Han, M.; Mark, L. P.; Boltalina, O. V.; Chronakis, N.; Orfanopoulos, M.; Hungerbuhler, H.; Drewello, T. *European Journal of Mass Spectrometry* **2006**, *12*, 397-408.

(114) Ulmer, L.; Mattay, J.; Torres-Garcia, H. G.; Luftmann, H. *Eur. J. Mass Spectrom.* **2000**, *6*, 49-52.

(115) Cristadoro, A.; Rader, H. J.; Mullen, K. *Rapid Comm. Mass Spectrom.* **2008**, *22*, 2463-2470.

(116) Zhou, L. H.; Deng, H. M.; Deng, Q. Y.; Zheng, L. P.; Cao, Y. *Rapid Comm. Mass Spectrom.* **2005**, *19*, 3523-3530.

(117) Brown, T.; Clipston, N. L.; Simjee, N.; Luftmann, H.; Hungerbuhler, H.; Drewello, T. *Int. J. Mass Spectrom. Ion Process.* **2001**, *210*, 249-263.

(118) Brune, D. C. *Rapid Comm. Mass Spectrom.* **1999**, *13*, 384-389.

(119) Streletskii, A. V.; Kouvitchko, I. V.; Esipov, S. E.; Boltalina, O. V. *Rapid Comm. Mass Spectrom.* **2002**, *16*, 99-102.

(120) Vasil'ev, Y. V.; Khvostenko, O. G.; Streletskii, A. V.; Boltalina, O. V.; Kotsiris, S. G.; Drewello, T. *Journal of Physical Chemistry A* **2006**, *110*, 5967-5972.

(121) Zalesny, R.; Loboda, O.; Iliopoulos, K.; Chatzikyriakos, G.; Couris, S.; Rotas, G.; Tagmatarchis, N.; Avramopoulos, A.; Papadopoulos, M. G. *Physical Chemistry Chemical Physics* **2010**, *12*, 373-381.

(122) Vieira, S. M. C.; Kotsiris, S. G.; Drewello, T.; Rego, C. A.; Birkett, P. R. *Fullerenes Nanotubes and Carbon Nanostructures* **2008**, *16*, 404-411.

(123) Kotsiris, S. G.; Vasilev, Y. V.; Streletskii, A. V.; Han, M.; Mark, L. P.; Boltalina, O. V.; Chronakis, N.; Orfanopulos, M.; Hungerbuhler, H.; Drewello, T. *Eur. J. Mass Spectrom.* **2006**, *12*, 397-408.

(124) Bruno, A. *Macromolecules* **2010**, *43*, 10163-10184.

(125) Willoughby, B. G.; Banks, R. E. In *Encyclopedia of Polymer Science and Technology*; Bloor, B. G., Brook, R. J., Flemmings, M. C., Mahajan, S., Cahn, R. W., Eds.; Pergamon: Oxford, 1994, pp 887-895.

(126) Souzy, R.; Ameduri, B.; Boutevin, B. *Progress in Polymer Science* **2003**, *29*, 79-106.

(127) Li, K.; Wu, P.; Han, Z. *Polymer* **2002**, *43*, 4079-4086.

(128) Paz-Pazos, M.; Pugh, C. *J. Polym. Sci., Part A: Polym. Chem.* **2006**, *44*, 3114-3124.

(129) Lin, J. W.; Dudek, L. P.; Majumdar, D. *J. Appl. Polym. Sci.* **1987**, *33*, 657-667.

(130) Luo, J.; Ma, H.; Haller, M.; Jen, A. K.-Y.; Barto, R. B. *Chem. Commun.* **2002**, 888-889.

(131) Hansen, N. M. L.; Jankova, K.; Hvilsted, S. *Eur. Polym. J.* **2007**, *43*, 255-293.

(132) Ma, H.; Chen, B. Q.; Sassa, T.; Dalton, L. R.; Jen, A. K.-Y. *J. Am. Chem. Soc.* **2001**, *123*, 986-.

(133) Latourte, L.; Blais, J. C.; Tabet, J. C.; Cole, R. B. *Anal. Chem.* **1997**, *69*, 2742-2750.

(134) Kostjuk, S. V.; Ortega, E.; Ganachaud, F.; Ameduri, B.; Boutevin, B. *Macromolecules* **2009**, *42*, 612-619.

(135) Ameduri, B.; Ladaviere, C.; Delolme, F.; Boutevin, B. *Macromolecules* **2004**, *37*, 7602-7609.

(136) Lobert, M.; Thijs, H. M. L.; Erdmenger, T.; Eckardt, R.; Ulbricht, C.; Hoogenboom, R.; Schubert, U. S. *Chem. Eur. J.* **2008**, *14*, 10396-10407.

(137) Becer, C. R.; Babiuch, K.; Pilz, D.; Hornig, S.; Heinze, T.; Gottschaldt, M.; Schubert, U. S. *Macromolecules* **2009**, *42*, 2387-2394.

(138) Wesdemiotis, C.; Pingitore, F.; Polce, M. J.; Russell, V. M.; Kim, Y.; Kausch, C. M.; Connors, T. H.; Medsker, R. E.; Thomas, R. R. *Macromolecules* **2006**, *39*, 8369-8378.

(139) Marie, A.; Alves, S.; Fournier, F.; Tabet, J. C. *Anal. Chem.* **2000**, *72*, 5106-5114.

(140) Marie, A.; Alves, S.; Fournier, F.; Tabet, J. C. *Anal. Chem.* **2003**, *75*, 1294-1299.

(141) Gooden, J. K.; Gross, M. L.; Mueller, A.; Stefanescu, A. D.; Wooley, K. L. *J. Am. Chem. Soc.* **1998**, *120*, 10180-10186.

(142) Marie, A.; Fournier, F.; Tabet, J. C.; Ameduri, B.; Walker, J. *Anal. Chem.* **2002**, *74*, 3213-3220.

(143) Romack, T. J.; Danell, A. S.; Cottone, T. M.; Dutta, S. K. *Rapid Comm. Mass Spectrom.* **2008**, *22*, 930-934.

(144) Knochenmuss, R.; Karbach, V.; Wiesli, U.; Breuker, K.; Zenobi, R. *Rapid Comm. Mass Spectrom.* **1998**, *15*, 529-534.

(145) Knochenmuss, R.; Dubois, F.; Dale, M. J.; Zenobi, R. *Rapid Comm. Mass Spectrom.* **1996**, *10*, 871-877.

(146) Jaber, A. J.; Kaufman, J.; Liyanage, R.; Akhmetova, E.; Marney, S.; Wilkins, C. L. *J. Am. Soc. Mass Spectrom.* **2005**, *16*, 1772-1780.

(147) Karas, M.; Bahr, U.; Strupat, K.; Hillenkamp, F. *Anal. Chem.* **1995**, *67*, 675-679.

(148) Rashidezadeh, H.; Guo, B. C. *J. Am. Soc. Mass Spectrom.* **1998**, *9*, 724-730.

(149) Wetzel, S. J.; Guttman, C. M.; Girard, J. E. *Int. J. Mass Spectrom. Ion Process.* **2004**, *238*, 215-225.

(150) Wetzel, S. J.; Guttman, C. M.; Flynn, K. M.; Filliben, J. J. *J. Am. Soc. Mass Spectrom.* **2006**, *17*, 246-252.

(151) Bauer, B. J.; Byrd, H. C. M.; Guttman, C. M. *Rapid Comm. Mass Spectrom.* **2002**, *16*, 1494-1500.

(152) Chavez-Eng, C. Ph.D. Thesis, Drexel University, Philadelphia, PA, 2002.

(153) Chavez-Eng, C.; Owens, K. G. In *Proceedings of 49th ASMS Conference on Mass Spectrometry and Allied Topics*, 2001.

(154) Goldschmidt, R. J.; Owens, K. G.; Hanton, S. D. In *Proceedings of 46th ASMS Conference on Mass Spectrometry and Allied Topics*, 1998, pp 1055.

(155) Goldschmidt, R. J.; Guttman, C. M. *Polymer Preprints* **2000**, *41*, 647-648.

(156) Schriemer, D. C.; Whittal, R. M.; Li, L. *Macromolecules* **1997**, *30*, 1955-1963.

(157) Jakubowski, W.; Kirci-Denizli, B.; Gil, R. R.; Matyjaszewski, K. *Macromol. Chem. Phys.* **2008**, *209*, 32-39.

(158) Lutz, J.-F.; Matyjaszewski, K. *J. Polym. Sci., Part A: Polym. Chem.* **2005**, *43*, 897-910.

(159) Matyjaszewski, K. *Pure Appl. Chem.* **1997**, *A34*, 1785-1801.

(160) Wilczek-Vera, G.; Danis, P. O.; Eisenberg, A. *Macromolecules* **1996**, *29*, 4036-4044.

(161) Wilczek-Vera, G.; Yu, Y.; Waddell, K.; Danis, P. O.; Eisenberg, A. *Rapid Comm. Mass Spectrom.* **1999**, *13*, 764-777.

(162) Donkers, E. H. D.; Willemse, R. X. E.; Klumperman, B. *J. Polym. Sci., Part A: Polym. Chem.* **2005**, *43*, 2536-2545.

(163) Willemse, R. X. E.; Staal, B. B. P.; Donkers, E. H. D.; van Herk, A. M. *Macromolecules* **2004**, *37*, 5717-5723.

(164) Willemse, R. X. E.; van Herk, A. M. *J. Am. Chem. Soc.* **2006**, *128*, 4471-4480.